CHARACTERIZATION OF HAM-1 IN THE ASYMMETRIC DIVISION OF *C. ELEGANS* NEUROBLASTS

by

Amy O. M. Leung
B.Sc., Simon Fraser University, 2004

THESIS SUBMITTED IN PARTIAL FULFILLMENT OF
THE REQUIREMENTS FOR THE DEGREE OF

MASTER OF SCIENCE

In the
Department
of
Molecular Biology and Biochemistry

SIMON FRASER UNIVERSITY

Spring 2007

APPROVAL

Name: **Amy O. M. Leung**

Degree: **Master of Science**

Title of Thesis: **Characterization of HAM-1 in the asymmetric division of *C. elegans* neuroblasts**

Examining Committee:

Chair: **Dr. Christopher Beh**
Assistant Professor of Molecular Biology and Biochemistry

Dr. Nancy Hawkins
Senior Supervisor
Assistant Professor of Molecular Biology and Biochemistry

Dr. Esther Verheyen
Supervisor
Associate Professor of Molecular Biology and Biochemistry

Dr. Nicholas Harden
Supervisor
Associate Professor of Molecular Biology and Biochemistry

Dr. Harald Hutter
Internal Examiner
Associate Professor of Biological Sciences

Date Defended: February 1, 2007

ABSTRACT

HAM-1 (HSN abnormal migration) is a novel protein implicated in asymmetric cell division (ACD) of many *C. elegans* neuroblasts. HAM-1 is localized at cell peripheries and becomes asymmetrically distributed during mitosis. However, little is known about how it regulates ACDs. I have analyzed a series of protein truncations to determine sequences important for HAM-1 function and localization. Results indicate that the C-terminus is essential for function and N-terminal sequences are required for peripheral association. HAM-1 was also observed in the nucleus, a finding not previously reported. Deletion of a predicted nuclear localization signal partially disrupted nuclear targeting and function of the protein. This and other bioinformatics analyses suggest a possible nuclear role for HAM-1. Previous studies have proposed potential interactions between HAM-1 and the Wnt pathway. In this study, mutations in *ham-1* and several Wnt signalling components were shown to produce opposing defects in the lineage generating the PLM neuron.

Keywords: *C. elegans*; asymmetric cell division; HAM-1; Wnt signalling

Subject Terms: cell division; neuronal development; embryogenesis

To my family

ACKNOWLEDGEMENTS

I would like to thank my senior supervisor, Nancy Hawkins, for all her guidance, support and encouragement during the last two years. Nancy is a wonderful mentor and she has been instrumental in my maturation as a scientist. I have yet to meet anyone with more passion and enthusiasm for research.

I am also indebted to Christopher Beh, who has provided a lot of direction and insight for my project. Although Chris was not my official advisor, he certainly guided me as though I were his student. I also greatly appreciate the valuable feedback and suggestions that have been provided by members of my supervisory committee, Esther Verheyen and Nicholas Harden. Furthermore, I am grateful for the generosity of David Baillie – much of my research would not have been possible without the use of his microscopy equipment. I would also like to acknowledge members of the Garriga Lab at UC Berkeley for pioneering the work on HAM-1.

I have been very fortunate to have worked with an exceptional group of colleagues in the Hawkins/Beh Lab. I must thank all my fellow lab mates for their assistance, encouragement and friendship for the past couple of years. They have made this a truly memorable experience.

Finally, I express my deepest gratitude to my beloved family and friends. In particular, I thank my parents and Marie for their incessant patience, encouragement and prayers. I cannot imagine doing this without their support.

TABLE OF CONTENTS

Approval ii

Abstract iii

Dedication iv

Acknowledgements v

Table of Contents vi

List of Figures ix

List of Tables x

Chapter 1: Introduction 1

1.1 Mechanisms of asymmetric cell division 1

1.2 Asymmetric divisions in *Drosophila* neurogenesis 1

1.2.1 *Drosophila* PNS neuroblasts 3

1.2.2 *Drosophila* CNS neuroblasts 5

1.3 Asymmetric divisions in early *C. elegans* embryogenesis 7

1.3.1 *C. elegans* zygote 8

1.3.2 EMS division 9

1.4 Asymmetric divisions in *C. elegans* neuroblasts 12

1.4.1 PHA lineage 12

1.4.2 PHB lineage 14

1.5 HAM-1 14

1.5.1 Identification of *ham-1* 14

1.5.2 Protein expression pattern 15

1.5.3 Models of HAM-1 function 15

1.5.4 Neuronal lineages that require HAM-1 18

1.5.5 Molecular characterization of HAM-1 19

1.6 Preview 20

Chapter 2: Materials and Methods 21

2.1 Strains and alleles 21

2.2 Molecular biology 22

2.2.1 Genotyping *ced-3(n717)* mutants 22

2.2.2 Full-length *ham-1* constructs 23

2.2.3 *ham-1* truncation constructs 25

2.2.4 Myristoylation constructs 25
2.2.5 NLS deletion constructs 27
2.3 Generation of transgenic animals 29
2.3.1 Germline transformation 29
2.3.2 Extrachromosomal array integration 31
2.4 Genetic crosses 31
2.4.1 Strains containing *ham-1* transgenic arrays 31
2.4.2 Strains to examine position of HAM-1 function in the PLM lineage 33
2.4.3 Strains containing *apr-1(zh10)* 34
2.4.4 Strains containing *lin-17(n671)* 35
2.5 Immunofluorescence and microscopy 35
2.6 Bioinformatics analyses 36

Chapter 3: Results 38
3.1 Identification of a winged-helix domain in HAM-1 38
3.2 Truncation analysis of the HAM-1 protein 39
3.2.1 Characterization of exogenous full-length GFP::HAM-1 39
3.2.2 Analysis of HAM-1 C-terminal and N-terminal truncations 50
3.2.3 Investigation of myristoylated HAM-1 proteins 58
3.2.4 Examination of a potential nuclear role of HAM-1 62
3.3 Potential interactions between HAM-1 and the Wnt Pathway 65
3.3.1 Determining the division affected by *ham-1* in the PLM lineage 68
3.3.2 Effects of *apr-1* in the PLM lineage 69
3.3.3 Effects of *lin-17* in the PLM lineage 75

Chapter 4: Discussion 77
4.1 *unc-119p* enables rescue of *ham-1* defects by GFP::HAM-1 77
4.2 *ham-1 3'-UTR* is not required in asymmetric protein localization 78
4.3 Sequences involved in peripheral localization of HAM-1 79
4.4 HAM-1 function is disrupted in N- and C-terminal truncations 81
4.5 Potential role of HAM-1 in the nucleus 83
4.5.1 Visualization of full-length and truncated HAM-1 83
4.5.2 Identification of an NLS sequence 84
4.5.3 Prediction of a putative winged-helix domain 84
4.5.4 Future experiments to investigate the nuclear role of HAM-1 85
4.5.5 Other proteins with cortical and nuclear localization 89
4.6 Possible interactions with the Wnt pathway 90
4.6.1 The PHB lineage 91
4.6.2 The PLM lineage 93
4.7 Summary 94

Appendices **96**
Appendix 1 Backcrossing integrated array 96
Appendix 2 Crossing transgenic arrays into reporter strains 97
Appendix 3 Crossing transgenic arrays into *ham-1* mutants with neuronal reporters 98
Appendix 4 Crossing the ALN reporter into *ham-1* mutants 100
Appendix 5 Crosses to obtain *zdIs5; ced-4* and *zdIs5; ced-4; ham-1* 101
Appendix 6 Crosses to obtain *apr-1 zdIs5 / hT2 zdIs5* 103
Appendix 7 Crosses to obtain *apr-1 zdIs5 / hT2 zdIs5; ham-1* 104
Appendix 8 Crosses to obtain *apr-1 zdIs5 / hT2 zdIs5; ced-3* 105
Appendix 9 Crosses to obtain *lin-17 zdIs5* and *lin-17 zdIs5; dpy-20 unc-30* 106
Appendix 10 Crosses to obtain *lin-17 zdIs5; ham-1* 107

Reference List **108**

LIST OF FIGURES

Figure 1 Intrinsic and extrinsic mechanisms of asymmetric cell division 2
Figure 2 Asymmetric division of the SOP cell 4
Figure 3 Asymmetric division of the CNS neuroblast 6
Figure 4 Asymmetric division of the EMS blastomere 11
Figure 5 Asymmetric divisions in the PHA and PHB lineages 13
Figure 6 HAM-1 expression in wildtype embryos 16
Figure 7 Models of HAM-1 function 17
Figure 8 Generation of myristoylation constructs by PCR 26
Figure 9 Deletion of NLS sequence by the SLIM method 28
Figure 10 HAM-1 sequence homology 40
Figure 11 Full-length *gfp::ham-1* constructs with the *let-858* or *ham-1* 3'-UTR 40
Figure 12 Expression and localization of full-length GFP::HAM-1 fusion proteins 43
Figure 13 PHB neuron visualized by the *gmIs12* reporter 44
Figure 14 PLM neuron visualized by the *zdIs5* reporter 48
Figure 15 Schematic of C-terminal and N-terminal HAM-1 truncations 51
Figure 16 Subcellular localization of C-terminal HAM-1 truncations 53
Figure 17 Subcellular localization of N-terminal HAM-1 truncations 55
Figure 18 Subcellular localization of myristoylated HAM-1 proteins 60
Figure 19 Subcellular localization of HAM-1 proteins with a putative NLS deletion 66
Figure 20 Potential cell fate transformations resulting in PLM loss 70
Figure 21 Potential cell fate transformations resulting in PLM duplication 74
Figure 22 Putative 14-3-3 binding sites in HAM-1 87
Figure 23 Potential cell fate transformations resulting in loss of HSN and PHB 92

LIST OF TABLES

Table 1	Primer sequences	24
Table 2	PCR primers to amplify full-length and truncated *ham-1* cDNA	26
Table 3	Transgenic lines generated	30
Table 4	Rescue of PHB defects by full-length GFP::HAM-1	46
Table 5	Rescue of PLM defects by full-length GFP::HAM-1	49
Table 6	PLM neuron in transgenic animals carrying C-terminal and N-terminal HAM-1 truncations	57
Table 7	PLM defects are not rescued by myristoylated HAM-1 proteins	63
Table 8	Deletion of a putative NLS from full-length HAM-1 reduced rescue of the PLM neuron	67
Table 9	Suppression of PLM loss in *ham-1* mutants by *ced-4*	71
Table 10	PLM defects in *ham-1* and Wnt pathway mutants	73

CHAPTER 1: INTRODUCTION

1.1 Mechanisms of asymmetric cell division

Generation of cellular diversity is a fundamental aspect of metazoan development. A single cell can divide "asymmetrically" to produce two daughter cells that adopt distinct developmental fates (Horvitz and Herskowitz, 1992). Asymmetric cell divisions (ACDs) may occur by intrinsic and/or extrinsic means (Figure 1). Intrinsic mechanisms involve preferential segregation of protein determinants into one of two daughter cells. This often requires unequal distribution of the factors within the dividing mother cell, as well as orientation of the mitotic spindle with respect to the axis of polarity. Daughter cell size may also be regulated through manipulation of the mitotic spindle position. Alternatively, ACDs may depend on intercellular communication. Extrinsic signals may be received by the mother or daughter cells to induce different cell fates. Interactions between the two daughter cells may also result in unequal developmental potential.

1.2 Asymmetric divisions in *Drosophila* neurogenesis

Much of our knowledge about mechanisms underlying ACDs was derived from studies in the fruit fly *Drosophila melanogaster*. During *Drosophila* development, neuroblasts in both the peripheral and central nervous systems (PNS and CNS, respectively) divide asymmetrically to generate neuronal diversity. Many players involved in the regulation of these divisions have now been characterized (reviewed in Betschinger and Knoblich, 2004; Hawkins and Garriga, 1998).

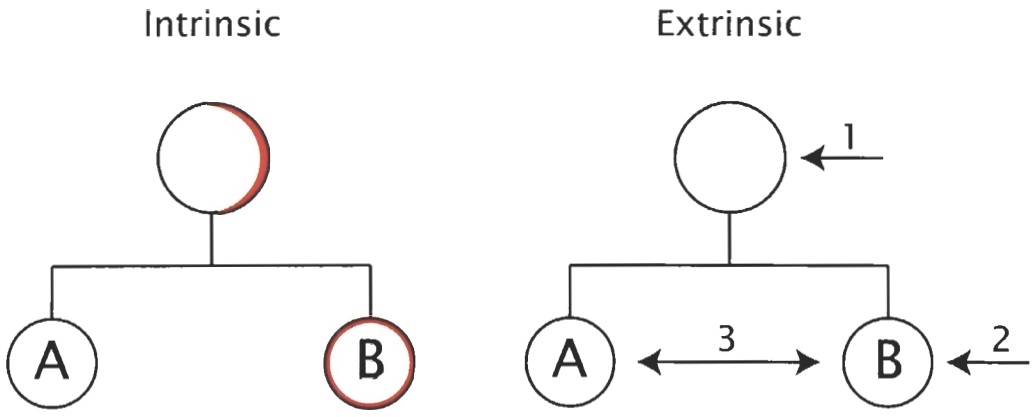

Figure 1 Intrinsic and extrinsic mechanisms of asymmetric cell division

(Left) Intrinsic mechanisms. Factors that regulate developmental fate (red) may be asymmetrically localized within the mother cell and preferentially segregated into one daughter cell. (Right) Extrinsic mechanisms. Signals to the mother cell (1), to one daughter cell (2), or between two daughter cells (3) can result in distinct developmental fates. A combination of intrinsic and extrinsic mechanisms may be used to regulate asymmetric cell divisions.

1.2.1 *Drosophila* PNS neuroblasts

In the adult *Drosophila* PNS, a sensory organ precursor (SOP) undergoes several ACDs, generating four cells that comprise the external sensory organ: a hair cell, a socket cell, a neuron, and a sheath cell. The divisions also give rise to a small glia that subsequently dies and does not incorporate into the mechanosensory organ. Cell fate specification in this lineage involves Notch-mediated signalling. The transmembrane receptor Notch undergoes several proteolytic cleavages upon association with its membrane-bound ligand Delta; this releases an intracellular fragment of Notch, which enters the nucleus to regulate transcription of target genes that specify cell fate (reviewed in Schweisguth, 2004).

Division of the SOP produces two daughter cells (pIIa and pIIb) that express Notch and Delta. Accordingly, both cells are capable of inducing and receiving Notch signals. Cell fate asymmetry is mediated by differential inheritance of Numb, a membrane-associated protein determinant (Figure 2). During the SOP division, Numb is localized at the anterior cell cortex and segregated into the anterior daughter pIIb (Rhyu et al., 1994). Descendants of pIIb ultimately form the internal structures of the sensory organ – neuronal and sheath cells. The posterior daughter pIIa, which does not inherit Numb, divides to form the outer organ structures – hair and socket cells. In *numb* mutants, the SOP division becomes symmetric, producing two pIIa cells. Conversely, overexpression of the protein in both SOP daughters duplicates pIIb. Numb mediates asymmetric fate specification by cell autonomous inhibition of Notch signalling. *Notch* mutants transform the posterior daughter into a second pIIb cell, the opposite phenotype to that observed in *numb* (Guo et al., 1996).

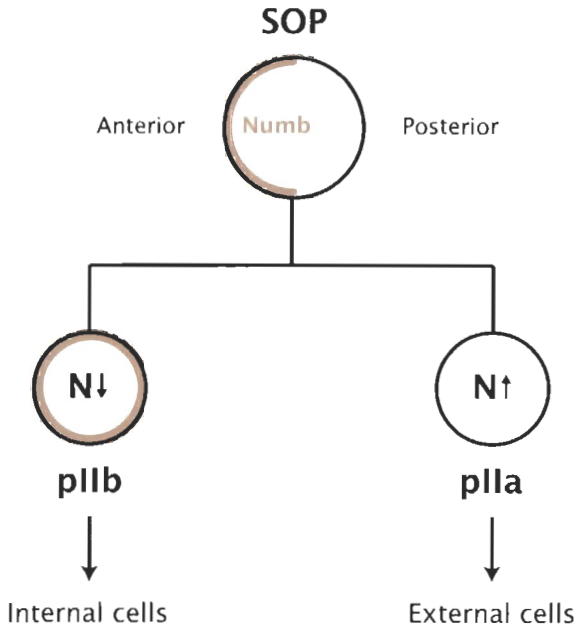

Figure 2 Asymmetric division of the SOP cell

The SOP divides asymmetrically to produce an anterior pIIb cell and a posterior pIIa cell. pIIb gives rise to the internal structures of the sensory organ (neuronal and sheath cells), while pIIa produces the external structures (hair and socket cells). Cell fate asymmetry depends on preferential inheritance of Numb (brown) by pIIb, which results in cell autonomous inhibition of Notch (N) signalling.

Recent studies proposed a mechanism for the downregulation of Notch signals. Numb can physically associate with α-Adaptin, a component of the AP-2 complex involved in endocytosis (Berdnik et al., 2002; Santolini et al., 2000). α-Adaptin segregates preferentially with Numb into the pIIb cell. Because Numb also binds Notch (Guo et al., 1996), it may downregulate signal transduction by inducing receptor internalization. Alternatively, Numb may trigger endocytosis of Sanpodo, another transmembrane protein required for Notch-dependent regulation of sibling cell fates (Dye et al., 1998; Skeath and Doe, 1998). In support of this model, Sanpodo co-localizes with Numb in endosomes of the pIIb cell; conversely, the protein remains at the cortex of pIIa, which does not inherit Numb (Hutterer and Knoblich, 2005).

1.2.2 *Drosophila* CNS neuroblasts

During *Drosophila* CNS development, neuroblasts arise from a monolayer of epithelial cells, known as the ventral neuroectoderm. Upon specification, the CNS progenitors delaminate from this epithelium and undergo successive stem cell-like divisions along the apical-basal axis (Figure 3). Each asymmetric division regenerates a second apical neuroblast and gives rise to a smaller, basal ganglion mother cell (GMC). The GMC then divides further to produce two differentiated neuronal or glial cells (reviewed in Betschinger and Knoblich, 2004; Hawkins and Garriga, 1998).

In the neuroblast division, apical and basal daughter cells adopt distinct developmental fates by unequal inheritance of protein determinants. This process is dependent on Miranda, a coiled-coil protein that physically interacts with Prospero and Staufen (Ikeshima-Kataoka et al., 1997; Schuldt et al., 1998). Prospero is a homeodomain transcription factor involved in specification of the GMC cell fate, while

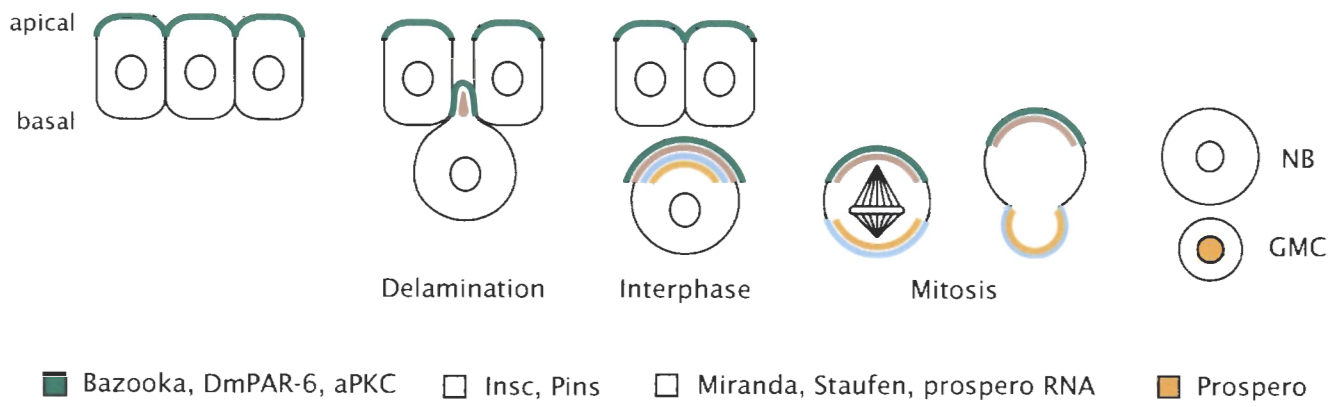

Figure 3 Asymmetric division of the CNS neuroblast

CNS neuroblasts delaminate from the ventral neuroectoderm and divide asymmetrically to produce a larger apical neuroblast (NB) and a smaller basal ganglion mother cell (GMC). Bazooka/DmPAR-6/aPKC recruits Insc and Pins to the apical cortex. These apical proteins are required for segregation of Miranda and Prospero into the basal daughter cell. After division, Prospero dissociates from Miranda and translocates into the nucleus to specify the GMC fate. Adapted from Knoblich (2001), with permission of Macmillan Publishers Ltd: Nature Reviews Molecular Cell Biology.

Staufen is a RNA-binding protein that recruits the *prospero* transcript. This complex of determinants (Miranda, Prospero, Staufen, *prospero* RNA) is detected at the apical cortex of CNS neuroblasts prior to division; during mitosis, it relocates to the basal cortex and is subsequently inherited by the GMC. Finally, Prospero dissociates from Miranda and enters the nucleus to activate GMC-specific genes and to repress neuroblast-specific genes (Doe et al., 1991; Vaessin et al., 1991).

Asymmetric cell division requires prior establishment of apical-basal polarity by an evolutionarily conserved protein complex: Bazooka (PAR-3), DmPAR-6 (PAR-6), and aPKC (PKC-3) (Betschinger and Knoblich, 2004; Kuchinke et al., 1998; Petronczki and Knoblich, 2001; Wodarz et al., 2000). These proteins, known collectively as the PAR-3/6 complex, are concentrated apically within the ventral neuroectoderm (Figure 3). Apical localization is maintained in the neuroblasts as they delaminate from the monolayer. During this process, neuroblasts begin to express Inscuteable (Insc), which associates with PAR-3/6 through direct binding to Bazooka (Kraut et al., 1996; Schober et al., 1999). In turn, Insc recruits Partner of Inscuteable (Pins) to produce a PAR/Insc/Pins crescent at the apical cortex of delaminated cells (Schaefer et al., 2000). Mutations in either *insc* or *pins* result in misorientation of the mitotic spindle; divisions do not occur with respect to the apical-basal axis, and Miranda/Prospero complexes localize randomly at the cell periphery (Kraut et al., 1996; Schaefer et al., 2000).

1.3 Asymmetric divisions in early *C. elegans* embryogenesis

The soil nematode *Caenorhabditis elegans* is also a valuable model organism for the investigation of ACDs. Its complete cell lineage from the single-cell embryo to the

mature adult has been elucidated, and 807 of the 949 nongonadal divisions are known to be asymmetric (Horvitz and Herskowitz, 1992). ACD has been studied most intensely in the early *C. elegans* embryo, beginning with the first division of the zygote.

1.3.1 *C. elegans* zygote

The *C. elegans* zygote (P_0) divides asymmetrically along the anterior-posterior axis to produce two daughter cells of distinct size and fate. The larger anterior blastomere (AB) divides further to generate most of the ectoderm; the smaller posterior blastomere (P_1) mainly gives rise to mesoderm, endoderm and the germline (Sulston et al., 1983). Asymmetric division of the zygote requires polarization by a group of PAR (partitioning-defective) proteins (reviewed in Nance, 2005). Mutations in any of the *par* genes (*par-1* to *par-6*) or *pkc-3* (atypical protein kinase C) leads to abnormalities in daughter cell size, fate and spindle orientation (Kemphues et al., 1988; Morton et al., 2002; Tabuse et al., 1998; Watts et al., 1996). In general, differences between the anterior and posterior blastomeres become less pronounced.

While PAR-4 (a serine/threonine kinase) and PAR-5 (a 14-3-3 protein) are uniformly distributed within the cortex and cytosol, the other PAR proteins exhibit asymmetric localization (Morton et al., 2002; Watts et al., 2000). PKC-3 (aPKC) co-localizes with the PDZ domain proteins PAR-3 (Bazooka) and PAR-6 (DmPAR-6), as observed in the *Drosophila* CNS neuroblasts. This conserved complex is restricted at the anterior cortex of the *C. elegans* zygote (Etemad-Moghadam et al., 1995; Hung and Kemphues, 1999; Tabuse et al., 1998). Conversely, the serine/threonine kinase PAR-1 and the RING-finger protein PAR-2 accumulate at the posterior cell periphery (Boyd et al., 1996; Guo and Kemphues, 1995). PAR proteins are mutually dependent; mutation of

any *par* gene generally affects the distribution of others. Asymmetric localization of the PAR proteins is required for unequal segregation of cell fate determinants and proper positioning of the mitotic spindle (reviewed in Nance, 2005).

1.3.2 EMS division

Although zygote asymmetry depends on intrinsic polarization by the PAR proteins, other ACDs in the early embryo require intercellular communication. During the four-cell stage of embryogenesis, the EMS blastomere is polarized by signals from the neighbouring P_2 cell (Figure 4, reviewed in Korswagen, 2002). EMS normally divides to produce two cells with distinct developmental fates; the anterior daughter (MS) generates mesodermal tissues, while the posterior daughter (E) forms the endoderm. If EMS is cultured in isolation, its division becomes symmetric, forming two MS-like descendants (Goldstein, 1992). This defect can be rescued by co-culturing with P_2. Upon division, an E cell develops from the side of EMS that contacted P_2, while the opposite side gives rise to MS (Goldstein, 1993).

A Wnt/β-catenin pathway is partially responsible for the P_2 polarization signal. Many variations of Wnt signalling are observed in metazoan development; details of these cascades are reviewed elsewhere (Korswagen, 2002; Logan and Nusse, 2004; Strutt, 2003). Essentially, the canonical Wnt pathway regulates gene transcription through stabilization of the effector protein β-catenin. In the absence of Wnt ligands, β-catenin is targeted for degradation by a destruction complex consisting of Axin, APC and GSK-3β. Association of the ligand with Frizzled (Fz) receptors induces a signal via Dishevelled (Dsh) to inhibit this degradation. The stabilized β-catenin translocates into the nucleus

and interacts with TCF/LEF proteins, converting them from transcriptional repressors to activators.

In P_2-EMS signalling, the Wnt/β-catenin pathway regulates transcription by an atypical mechanism; however, it utilizes many components of the canonical cascade described above (Figure 4, reviewed in Korswagen, 2002). Mutations in some of these genes result in the Mom (more mesoderm) phenotype, in which EMS divides symmetrically to produce two MS cells (Rocheleau et al., 1997; Thorpe et al., 1997). Notably, *mom-2* and *mom-5* encodes Wnt and Frizzled proteins, respectively. Unlike the canonical Wnt pathway, however, homologs of the destruction complex SGG-1 (GSK-3β) and APR-1 (APC) positively regulate the P_2 signal. Knockdown of either protein by RNA interference (RNAi) also produces the Mom phenotype (Rocheleau et al., 1997; Schlesinger et al., 1999). In contrast, disruption of *pop-1* results in the formation of two E cells (Lin et al., 1995). POP-1 is a TCF/LEF transcription factor that represses endoderm-specific genes (Calvo et al., 2001). In wildtype embryos, the P_2 signal reduces nuclear levels of POP-1 in the E cell, derepressing the endoderm fate. POP-1 remains elevated in the nucleus of MS, which gives rise to mesodermal tissues (Lin et al., 1995). In addition to Wnt signalling proteins, POP-1 regulation also involves members of the MAPK cascade: MOM-4 (TAK1) and LIT-1 (NLK). In the E daughter cell, MOM-4 activates LIT-1, which interacts with the β-catenin WRM-1. This LIT-1/WRM-1 complex phosphorylates POP-1, resulting in its delocalization from the nucleus (Lo et al., 2004; Rocheleau et al., 1999; Shin et al., 1999). Thus, Wnt and MAPK pathways collaboratively induce the endoderm fate by negative regulation of POP-1.

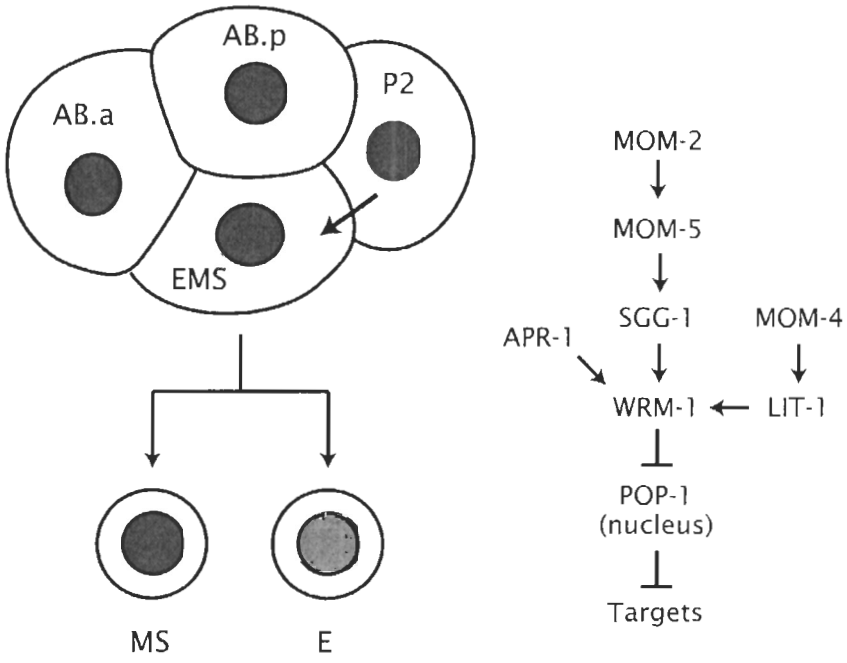

Figure 4 Asymmetric division of the EMS blastomere

At the four-cell stage of embryogenesis, EMS divides asymmetrically to produce the MS and E daughter cells. Cell fate asymmetry requires a Wnt/MAPK signal from the neighbouring P_2 blastomere. This signal results in downregulation of nuclear POP-1 levels in E, which allows the induction of endoderm-specific genes.

1.4 Asymmetric divisions in *C. elegans* neuroblasts

Development of the *C. elegans* nervous system is also highly dependent on ACDs. In the hermaphrodite nematode, all 302 neurons are generated from asymmetric neuroblast divisions (Sulston et al., 1983). Unfortunately, little is known about mechanisms that mediate ACDs in *C. elegans* neurogenesis. Our lab studies these processes using two lineages that give rise to the phasmid sensory neurons, PHA and PHB.

Phasmids are bilateral chemosensory structures located on both sides of the tail (Hall and Russell, 1991; Hilliard et al., 2002). Each phasmid organ is comprised of two ciliated neurons (PHA and PHB) and two accessory cells (phasmid socket and sheath cells). Ciliated endings of the phasmid neurons protrude through the sheath cell to sense the external environment. Although PHA and PHB have common function and spatial position within the animal, they are derived from distinct embryonic lineages (Sulston et al., 1983). The asymmetric divisions within these lineages are also regulated by different means.

1.4.1 PHA lineage

In the PHA lineage, a neuroblast (ABpl/rpppa) divides asymmetrically at 175 minutes after the first zygote cleavage (Figure 5A). The anterior daughter undergoes further divisions to produce PHA and four additional neurons (LUA, PVC, DA6, DA9). Conversely, the posterior daughter generates a phasmid sheath cell (Phsh), a hypodermal cell (hyp8 or hyp9), and a cell that undergoes apoptosis (X). Recent studies have proposed an involvement of Wnt signalling in the regulation of this ACD (Hawkins et al., 2005). Upon mutation of a Dishevelled homolog, *dsh-2*, the posterior daughter is thought

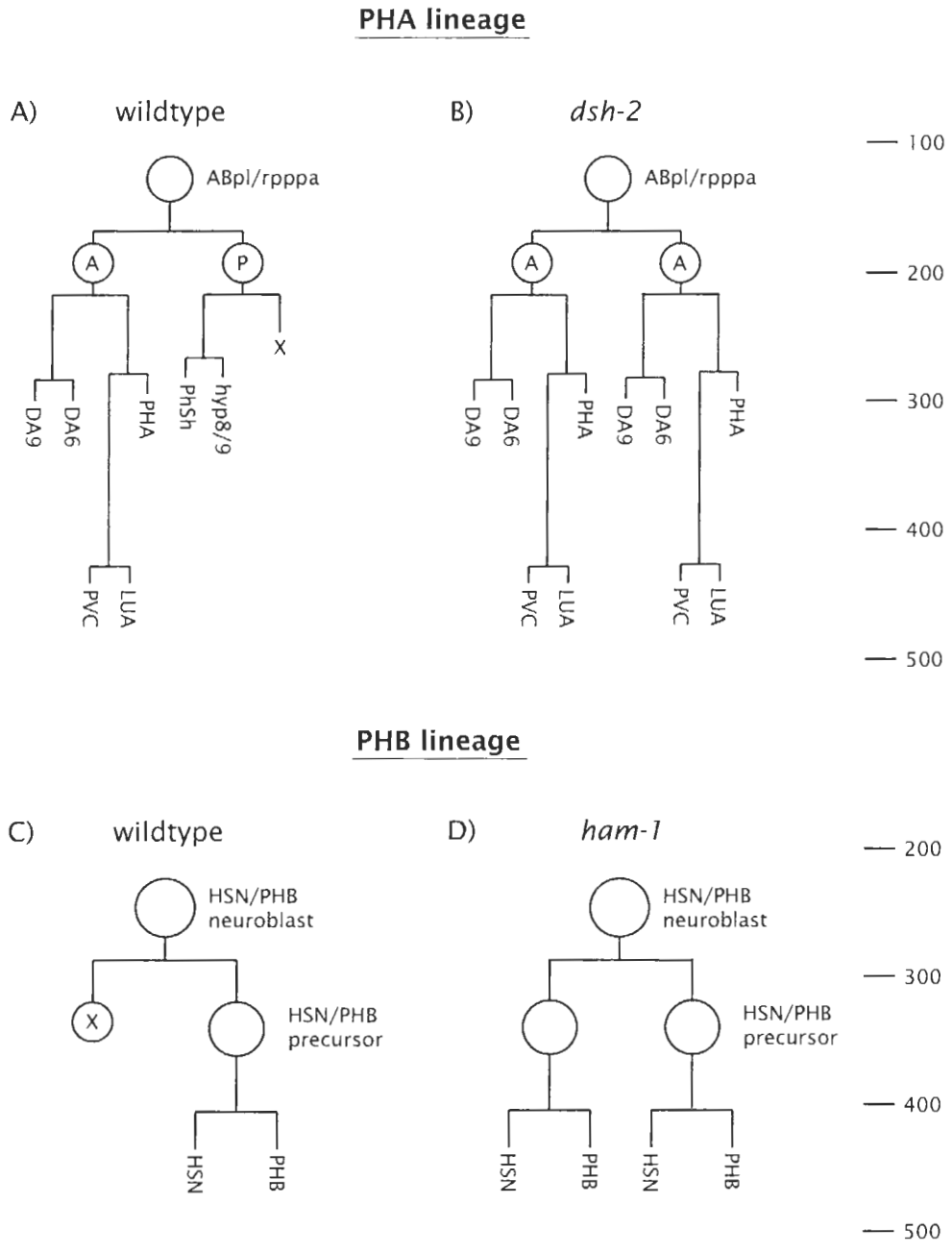

Figure 5 Asymmetric divisions in the PHA and PHB lineages

(A and B) PHA lineage. (A) In wildtype embryos, ABpl/rpppa divides asymmetrically at 175 minutes after the first zygote cleavage. The anterior daughter produces five neurons, including PHA. The posterior daughter gives rise to non-neuronal cells. (B) In *dsh-2* mutants, the posterior daughter adopts an anterior-like fate, resulting in the duplication of neuronal descendants.

(C and D) PHB lineage. (C) In wildtype embryos, the HSN/PHB neuroblast divides asymmetrically at 270 minutes of embryogenesis. The smaller anterior cell undergoes apoptosis, while the larger posterior daughter gives rise to HSN and PHB neurons. (D) In *ham-1* mutants, the neuroblast divides symmetrically to produce two posterior-like cells.

to adopt the sister cell fate (Figure 5B). Specifically, descendents of the posterior cell are lost (Phsh, hyp8/9, X), while neurons derived from the anterior daughter are duplicated (PHA, PVC). Similarly, disruption of the Frizzled receptor MOM-5 also produces extra PHA neurons. These results implicate a Wnt-dependent mechanism for the asymmetric neuroblast division.

1.4.2 PHB lineage

In the PHB lineage, the HSN/PHB neuroblast (ABpl/rapppap) undergoes asymmetric division at 270 minutes of embryogenesis (Figure 5C). The smaller anterior daughter is destined for apoptosis, while the larger posterior daughter becomes the HSN/PHB precursor. Subsequent division of the latter cell generates the HSN motor neuron and the PHB phasmid sensory neuron. Loss of DSH-2 function does not disrupt the PHB lineage (Hawkins et al., 2005). Instead, this asymmetric neuroblast division depends on a novel protein, HAM-1 (Frank et al., 2005; Guenther and Garriga, 1996). In *ham-1* mutants, the anterior apoptotic daughter often adopts the sister cell fate, resulting in duplication of HSN and PHB neurons (Figure 5D). Occasional loss of these neurons is also observed.

1.5 HAM-1

1.5.1 Identification of *ham-1*

ham-1 (HSN abnormal migration) encodes a novel protein of 414 amino acids (Frank et al., 2005; Guenther and Garriga, 1996). It was originally identified in a genetic screen (Desai et al., 1988) for mutants affecting the development of hermaphrodite-specific neurons (HSNs). These motor neurons innervate egg-laying muscles in the vulva.

In wildtype animals, HSNs are born in the tail of the embryo and migrate anteriorly to positions near the gonadal primordium. Mutations in *ham-1* produce extra HSN neurons with abnormalities in cell migration. The resultant animals are viable but exhibit minor defects in egg laying.

1.5.2 Protein expression pattern

Endogenous HAM-1 expression is detected in many cells during embryogenesis (Figure 6), from the onset of gastrulation (100 minutes) to the 1.5-fold stage (430 minutes). HAM-1 is typically observed in a ring-shaped pattern around cell peripheries. Intriguingly, the protein becomes asymmetrically localized during mitosis. In the PHB lineage, HAM-1 is restricted at the posterior border of the dividing HSN/PHB neuroblast and preferentially segregated into the neuronal precursor cell.

1.5.3 Models of HAM-1 function

Mutations in *ham-1* often induce the anterior daughter of the HSN/PHB neuroblast to adopt a posterior-like fate; thus, cell fate transformation occurs in the daughter that does not normally inherit the protein. These results indicate that HAM-1 does not function as a cell fate determinant (Guenther and Garriga, 1996). Conversely, HAM-1 may tether neuronal determinants at the posterior cortex of the mitotic neuroblast, ensuring specific inheritance by the HSN/PHB precursor cell (Figure 7A). In *ham-1* mutants, these factors may be incorporated into the anterior daughter, ultimately leading to the duplication of HSN and PHB. Interestingly, the resultant neurons often exhibit developmental defects: HSN may fail to complete cell migration, while the PHB sensory cilia do not protrude into the environment (Guenther and Garriga, 1996). Such

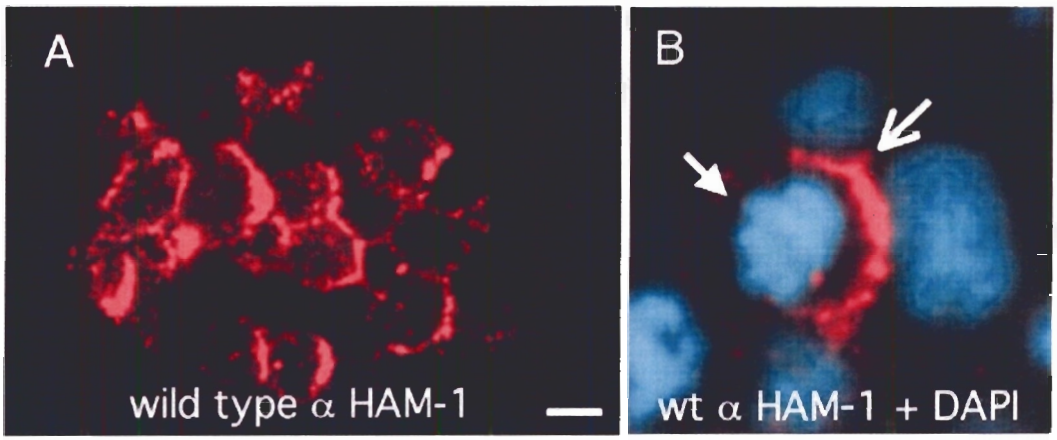

Figure 6 HAM-1 expression in wildtype embryos

Wildtype embryos stained with anti-HAM-1 antibodies (red) and DAPI (blue). (A) HAM-1 expression is detected at the cortex of many cells during embryogenesis. (B) Asymmetric HAM-1 localization (open arrow) is often observed in cells that are mitotic, as indicated by condensed chromosomes (closed arrow). Reprinted from Frank et al. (2005), with permission from Elsevier.

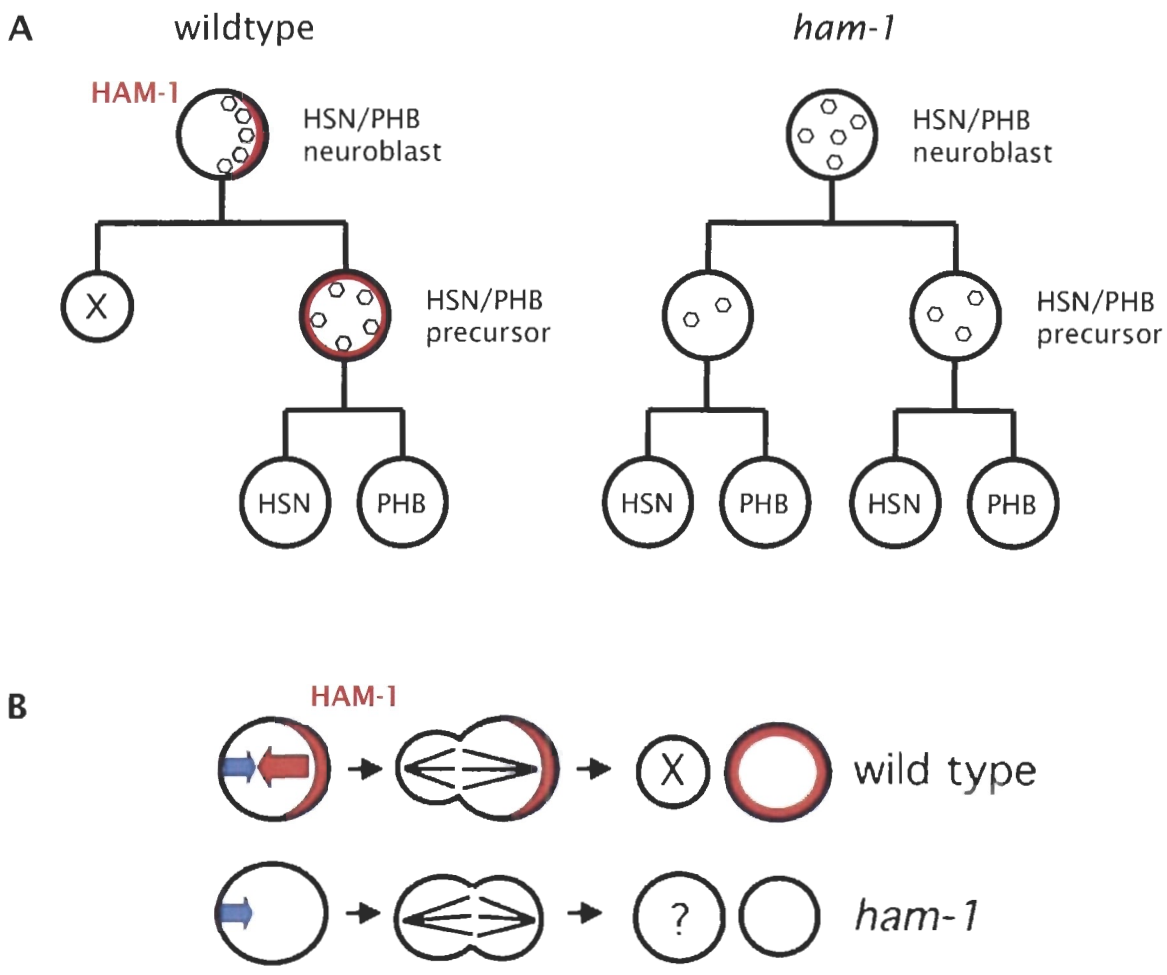

Figure 7 Models of HAM-1 function

Two non-mutually exclusive models for HAM-1 function. (A) HAM-1 (red) may tether cell fate determinants and preferentially segregate them into the posterior HSN/PHB precursor cell. Loss of HAM-1 results in distribution of these factors between both daughter cells and duplication of the posterior cell fate. (B) HAM-1 is responsible for positioning of the mitotic spindle. In wildtype embryos, the cleavage plane is biased anteriorly, producing a smaller anterior daughter and larger posterior daughter. In *ham-1* mutants, the cell size asymmetry is often reversed. The larger anterior cell sometimes bypasses apoptosis and adopts a posterior cell fate. This may be a secondary consequence of cleavage plane displacement (for example, more cell fate determinants may be inherited by the anterior daughter cell). Panel B is reprinted from Frank et al. (2005), with permission from Elsevier.

abnormalities may be expected if the absence of HAM-1 results in dilution of cell fate determinants between two sister cells. Although the proposed tether function is consistent with the *ham-1* mutant defects, direct evidence for this model has not thus far been obtained.

Recent studies revealed a role for HAM-1 in positioning of the cleavage plane (Frank et al., 2005). In the wildtype HSN/PHB neuroblast division, the mitotic spindle is biased anteriorly, producing a smaller anterior daughter and a larger posterior daughter. Mutations in *ham-1* often reverse this size asymmetry (Figure 7B). Thus, the cell fate defects may be a secondary consequence, resulting from posterior displacement of the cleavage plane. In the absence of HAM-1 function, the anterior daughter may inherit more neuronal determinants from the mother cell, allowing it to bypass apoptosis and produce extra neurons. However, duplication of HSN and PHB is not completely penetrant in *ham-1* mutants. Notably, when a cell death does occur in this lineage, it is typically observed in the anterior daughter even if it is larger than the posterior cell (Frank et al., 2005). Thus, while position of the mitotic spindle may contribute to differential inheritance of molecular determinants, cell size alone is not sufficient to dictate developmental fates.

1.5.4 Neuronal lineages that require HAM-1

Aside from the HSN/PHB defects, *ham-1* mutants also disrupt the generation of other neurons: PLM, RID, ADE, ADL, I2, AVA, RIM, and RME (Frank et al., 2005; Guenther and Garriga, 1996). Interestingly, all of the affected lineages include ACDs that generate apoptotic cells during the time of HAM-1 expression. Although *ham-1* alleles do not perturb every division that fulfills this criterion (NSM and PVQ lineage),

lineages that do not produce cell deaths are, thus far, shown to be unaffected. Currently, it is unclear why HAM-1 functions specifically in divisions that give rise to apoptotic daughter cells.

1.5.5 Molecular characterization of HAM-1

HAM-1 is a novel protein with limited sequence homology. According to the most recent publication, the 414-amino acid sequence does not contain any recognizable domains (Frank et al., 2005). Its closest homolog is an unknown protein in *C. briggsae*, which shares 76% sequence identity with HAM-1. An N-terminal portion of the protein (residues 15-170) appears to be conserved. It is approximately 30% identical to *Drosophila* Knockout (Ko), as well as several human and mouse sequences of unknown function. *ko* is a Kruppel target gene required for innervation of certain larval muscles (Hartmann et al., 1997). However, the protein has not been further characterized; thus, this homology gives little insight into potential mechanisms of HAM-1 function.

Several important regions of HAM-1 were revealed by analysis of mutant alleles (Frank et al., 2005). *ham-1(n1811)* encodes the missense protein, HAM-1(G47D), which is primarily delocalized within the cytoplasm. This result suggests the importance of residue 47 in protein cortical association. A second allele, *ham-1(gm214)*, produces a 21-amino acid deletion at residues 369-389. The resultant protein is non-functional, even though it retains proper localization at the cell periphery; thus, this C-terminal region may be required for HAM-1 activity.

1.6 Preview

To identify the localization and function domains of HAM-1, we performed a serial deletion analysis. The C-terminal third of the protein appeared to be dispensable for cortical association, while truncations from the N-terminus resulted in cytoplasmic distribution. Consistent with previous analysis of *ham-1(gm214)*, we found that HAM-1 activity was dependent on C-terminal sequences. However, N-terminal deletions also failed to exhibit HAM-1 activity, which may be an indirect consequence of protein delocalization.

Unexpectedly, full-length and truncated HAM-1 proteins were also detected in the nucleus. This observation was not reported in previous studies. Through a combination of bioinformatics analysis and experimental validation, we identified a nuclear localization signal (NLS) that was partially responsible for this protein distribution. Deletion of this sequence moderately reduced protein activity, suggesting that nuclear targeting may be biologically significant. Furthermore, we identified a putative DNA binding domain within the conserved N-terminal region of HAM-1. These results support a potential nuclear role of HAM-1 in the regulation of ACDs.

CHAPTER 2: MATERIALS AND METHODS

2.1 Strains and alleles

Methods for growth and culture of *C. elegans* were previously described (Brenner, 1974). Strains were maintained at 20°C on Nematode Growth Media (NGM) agar, with *Escherichia coli* OP50 as the food source. The wildtype strain used in this study was N2 Bristol. Other mutant alleles and cell-specific reporters are listed below:

LG I: *apr-1(zh10)* (Hoier et al., 2000), *lin-17(n671)* (Sawa et al., 1996), *zdIs5[mec-4::gfp]* (Clark and Chiu, 2003)

LG II: *ncIs1[eat-20::gfp pRF4]* (Shibata et al., 2000)

LG III: *ced-4(n1162)* (Ellis and Horvitz, 1986), *dpy-17(e164)* (Brenner, 1974), *gmIs12[srb-6::gfp]* (Troemel et al., 1995)

LG IV: *ced-3(n717)* (Ellis and Horvitz, 1986), *dpy-20(e1282ts)* (Hosono et al., 1982), *ham-1(gm279)* (Frank et al., 2005), *unc-30(e191)* (Brenner, 1974)

LG V: *him-5(e1490)* (Broverman and Meneely, 1994)

hT2[qIs48] (I; III) was used as a translocation balancer for *apr-1*(McKim et al., 1993). The extrachromosomal and integrated arrays generated in this study are described in Section 2.3 (Generation of transgenic animals).

2.2 Molecular biology

2.2.1 Genotyping *ced-3(n717)* mutants

The *ced-3(n717)* mutation was detected by a PCR-digest method as previously described (Lee, 2005). This allele exhibits a single nucleotide deletion that disrupts a recognition site for the Fnu4H I restriction enzyme (GCAGC to GCGC). Thus, to distinguish between wildtype (N2) and *ced-3(n717)* strains, we PCR amplified a fragment from the *ced-3* locus and performed an Fnu4H I digest.

To isolate genomic DNA, eight adult hermaphrodites were placed in 16 µL of worm lysis solution (60 µg/mL proteinase K, 10mM Tris pH 8.2, 50 mM KCl, 2.5mM $MgCl_2$, 0.5% Tween 20, 0.05% gelatine) in a PCR microfuge tube. After a quick centrifugation step (2 minutes at 13,000 rpm), the mixture was frozen at -80°C for 15 minutes. Once thawed, the microfuge tube was incubated (in the PCR machine) for 1 hour at 60°C to release genomic DNA, followed by 15 minutes at 95°C to heat-inactive proteinase K.

We amplified the *ced-3* gene fragment using the primers n717-F and n717-R (Table 1). 2.5 µL of the worm lysate was used as template in a PCR reaction. The resulting N2 and *ced-3(n717)* amplicons were 319 bp and 318 bp in length, respectively. Upon digestion with Fnu4HI, the wildtype PCR product generated two sub-fragments (121 and 198 bp). Conversely, the *ced-3(n717)* product was not cleaved. Since *ced-3* heterozygotes produce both wildtype and mutant amplicons, three fragments were observed upon Fnu4HI digestion (121, 198, 318 bp).

2.2.2 Full-length *ham-1* constructs

We generated two full-length constructs that express GFP::HAM-1 from the *unc-119* pan-neural promoter (Maduro and Pilgrim, 1995). pNH144 *[unc-119p-gfp::ham-1-let-858-3'UTR]* utilizes a standard *C. elegans* 3'-UTR from the *let-858* gene, while pNH146 *[unc-119p-gfp::ham-1-ham-1-3'UTR]* contains the *ham-1* 3'-UTR.

To create these constructs, we amplified *unc-119* promoter sequences from the pBY103 plasmid (a gift from M. Maduro). The PCR primers unc119-1 and unc119-2 contain XbaI and KpnI restriction sites, respectively (Table 1). These enzymes were used to clone the *unc-119p* sequence into a promoter-less GFP vector, pPD118.15 (A. Fire, personal communication); the resulting intermediate construct was named pAL13. pNH144 was formed by insertion of full-length *ham-1* cDNA into the EcoRI site of pAL13, which is located downstream of *gfp* coding sequences. We amplified this cDNA from the PH1 plasmid (provided by G. Garriga), using primers hm69 and hm70. As shown in Table 1, both oligonucleotides contain the EcoRI recognition sequence.

pNH144 contains the *let-858* 3'-UTR present in the pPD118.15 vector. To generate a second construct with the *ham-1* 3'-UTR, this region was amplified from a plasmid containing *ham-1* genomic sequences, p3F9B (a gift from G. Garriga). We used the primers hm71 and hm72, which contain NheI and NarI restriction sites, respectively (Table 1). These two enzymes were used to replace the *let-858* 3'-UTR in pNH144 with the corresponding *ham-1* sequences, generating pNH146. Both pNH144 and pNH146 were confirmed by sequencing prior to germline transformation.

Table 1 Primer sequences

Primer	F/R [a]	Sequence (5' to 3') [b]	Site [c]	Use [d]
5'MyrGFP	F	tcagACCGGTAGAAAAAA*ATGgggagtagtaaaagt*AGTAAAGGAG [e]	AgeI	myr
3'MyrGFP	R	GTCTGCTAGTTGAACGCTTCC	N/A	myr
hm60	F	gtacgaattcATGACCTACTTAGCCGTTGTGC	EcoRI	hmC
hm70	R	gactgaattcCTACAAATTGGAGATCAGGACGC	EcoRI	hmC
hm71	F	catcgctagcGCGTCCTGATCTCCAATTTGTAG	NheI	hmU
hm72	R	gactggcgccGTAGCACGCTCTGGATATTCC	NarI	hmU
hm73	R	gactgaattcTCTCCGAATCACTGATACTGCC	EcoRI	hmC
hm74	R	gactgaattcaGGTAGGCAACATAGCAGCTGG	EcoRI	hmC
hm75	R	gactgaattcCTGACACAAAGTAGTGATCTGCC	EcoRI	hmC
hm76	R	gactgaattcaGAGCACGGTTAGTTGTGAGGC	EcoRI	hmC
hm77	F	gtacgaattcTGGAATCGAGAACTCACTTCGG	EcoRI	hmC
hm78	F	gtacgaattcCTCAATCGTCAGGGACTTGCC	EcoRI	hmC
hm79	F	gtacgaattcGAGCATGTGATAGAGCCTGCG	EcoRI	hmC
hm80	F	gtacgaattcCCAGTTGATATGCCAGAGACC	EcoRI	hmC
hm84	F	ATGGCTTCACCACTCCGAAG	N/A	NLS
hm85	F	*ATATGCCAGAGACCCGA*ATGGCTTCACCACTCCGAAG [f]	N/A	NLS
hm86	R	CAACTGGATAGTACTTGAGACATTC	N/A	NLS
hm87	R	*TCGGGTCTCTGGCATAT*CAACTGGATAGTACTTGAGACATTC [f]	N/A	NLS
n717-F	F	TCGGATTGGT TTGAAAGTGG	N/A	ced
n717-R	R	ACAGACGGCTTGAATGAACC	N/A	ced
unc119-1	F	catgtctagaAAGCTTCAGTAAAAGAAGTAGAATTTTATAG	XbaI	unc
unc119-2	R	cgatggtaccCCGTGGAGATCTTATCGATAATGG	KpnI	unc

[a] Forward or reverse primer
[b] Sequences that are complementary to the template are capitalized
[c] Restriction enzyme recognition sites are underlined
[d] Oligonucleotides were designed for several main purposes:
myr – addition of myristoylation sequence
hmC – amplification of *ham-1* cDNA sequences
hmU – amplification of *ham-1* 3'-UTR
NLS – deletion of putative HAM-1 NLS
ced – genotyping *ced-3(n717)*
unc – amplification of *unc-119p* sequences
[e] Italicized sequence of 5'MyrGFP encode the human c-Src myristoylation sequence
[f] Italicized oligonucleotides of hm85 and hm87 are reverse complementary sequences corresponding to the region just upstream of the NLS

2.2.3 *ham-1* truncation constructs

To identify sequences responsible for localization and function of HAM-1, we created a series of deletion constructs: Trunc1 to Trunc4 remove *ham-1* coding sequences from the N-terminus, while Trunc5 to Trunc8 delete C-terminal regions. Partial *ham-1* cDNA sequences were amplified from PH1. The primers used for each PCR reaction are listed in Table 2. We incorporated an EcoRI recognition sequence into both the forward and reverse primers (Table 1). This allowed insertion of the various *ham-1* fragments into the EcoRI site of pAL13, producing the complete truncation constructs. All plasmids were subsequently confirmed by DNA sequencing.

2.2.4 Myristoylation constructs

To target various full-length and truncated GFP::HAM-1 proteins to the cell periphery, a myristoylation signal from human c-Src (MGSSKS) was fused to the N-terminus of GFP (Gitai et al., 2003). Myristoylation constructs were prepared in our lab by M. Wu.

An N-terminal region of *gfp* was amplified from pNH144 using the 5'MyrGFP and 3'MyrGFP primers. Sequences of these oligonucleotides are shown in Table 1. The forward primer 5'MyrGFP contains two segments that are complementary to pNH144 (Figure 8). The first segment spans an AgeI restriction site located just upstream of *gfp*; the second segment extends into the N-terminal *gfp* coding sequences. Between these two regions, we inserted codons corresponding to MGSSKS, such that the myristoylation signal would be fused translationally to the N-terminus of GFP. The reverse primer 3'MyrGFP is complementary to downstream *gfp* coding sequences (Figure 8). Although a restriction site was not incorporated into this primer, the *gfp* region amplified by

Table 2 PCR primers to amplify full-length and truncated *ham-1* cDNA

Description	Plasmid Name	Forward Primer [a]	Reverse Primer [a]	cDNA region (bp)
Full-length	pNH144	hm69	hm70	1-1245
Trunc1	pNH150	hm69	hm73	1-1093
Trunc2	pNH151	hm69	hm74	1-804
Trunc3	pNH152	hm69	hm75	1-505
Trunc4	pNH153	hm69	hm76	1-198
Trunc5	pNH154	hm77	hm70	94-1245
Trunc6	pNH155	hm78	hm70	340-1245
Trunc7	pNH156	hm79	hm70	628-1245
Trunc8	pNH157	Hm80	hm70	937-1245

[a] oligonucleotides sequences are shown in Table 1

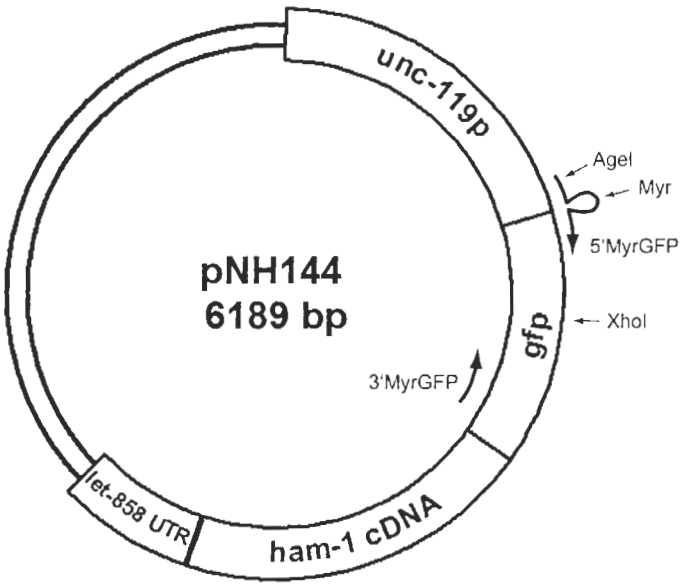

Figure 8 Generation of myristoylation constructs by PCR

An N-terminal region of *gfp* was amplified from pNH144, using the primers 5'MyrGFP (forward) and 3'MyrGFP (reverse). Sequences encoding the myristoylation signal were incorporated into the forward primer. The full-length myristoylated construct was created by replacing the AgeI/XhoI fragment of pNH144 with the corresponding fragment of the PCR amplicon.

5'MyrGFP and 3'MyrGFP contains an internal XhoI recognition sequence. To make the full-length myristoylation construct, we replaced the AgeI/XhoI fragment of pNH144 with the corresponding fragment of the PCR product. Similarly, we also modified plasmids pNH154 to pNH156 to create myristoylated forms of Trunc5 to Trunc7. All myristoylation constructs were sequenced prior to injection.

2.2.5 NLS deletion constructs

To analyse the involvement of a putative NLS (PTRRRAR, residues 321-327) in the localization and function of HAM-1, we deleted this sequence from Trunc7 and the full-length protein, respectively. Trunc7ΔNLS and FLΔNLS constructs were created by a site-directed mutagenesis approach known as SLIM (site-directed, ligase-independent mutagenesis). Details of the protocol are found in the original publication (Chiu et al., 2004). We used two minor modifications as previously described (Esmail, 2006): 1) Two PCR reactions were set-up, with primer pairs $F_T + R_S$ and $F_S + R_T$, respectively. 2) Mutagenesis products were transformed into electrocompetent DH5α cells instead of chemically competent cells.

To generate the FLΔNLS construct, we performed two inverse PCR reactions on the template pNH144 (Figure 9). The first amplification used the primers hm85 (F_T) and hm86 (R_S), while the second reaction used hm84 (F_S) and hm87 (R_T). Sequences of these oligonucleotides are shown in Table 1; hm85 and hm87 contain a tail that corresponds to the region directly upstream of the NLS (Figure 9). After amplification, PCR mixtures were pooled and incubated with DpnI, which cleaves the methylated template. The remaining DNA duplexes were then denatured and re-annealed to allow formation of hybrid products. Heteroduplexes with one strand from each PCR reaction exhibit

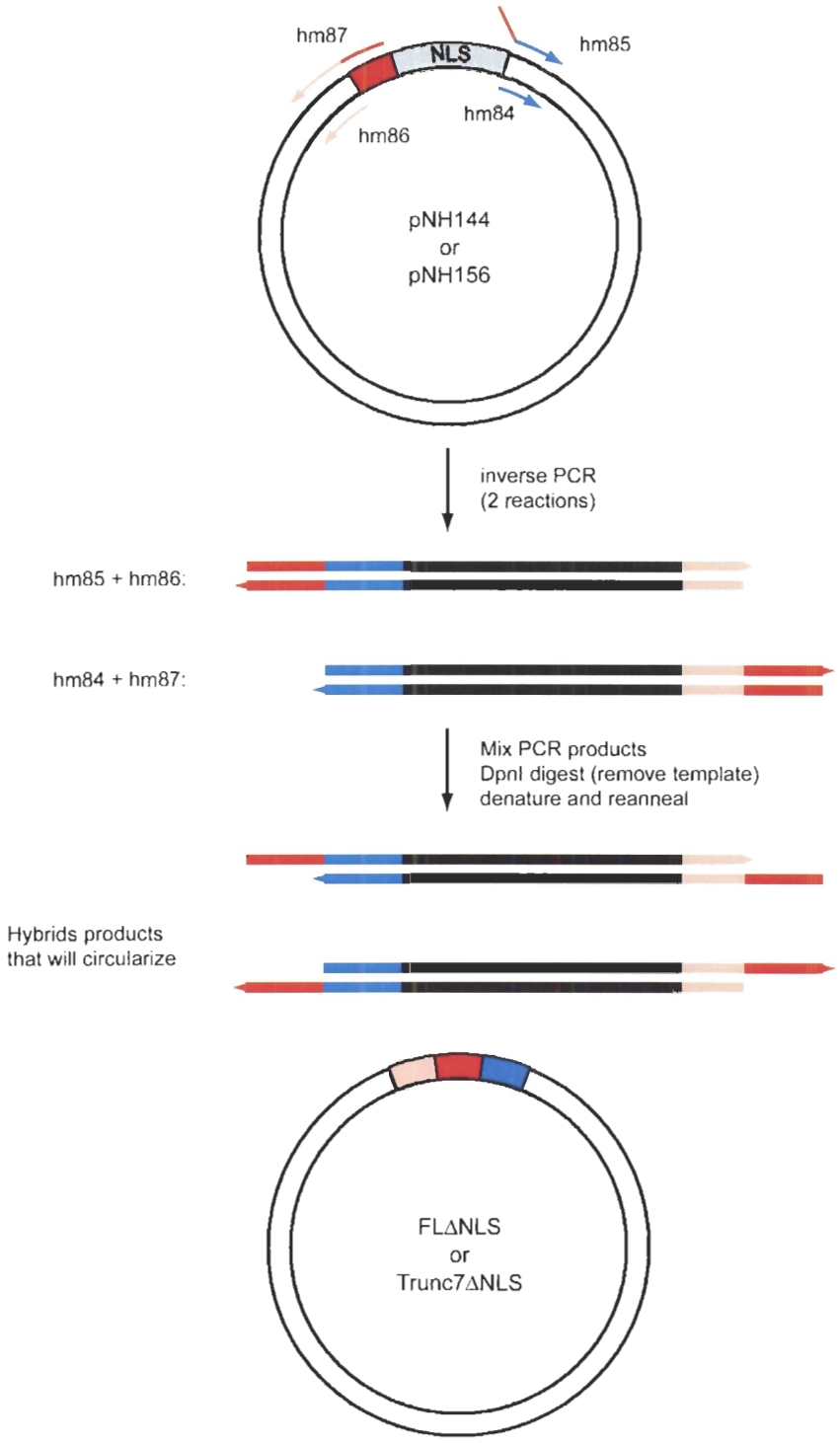

Figure 9 Deletion of NLS sequence by the SLIM method

Two inverse PCR reactions were performed, using primers hm85 + hm86 or hm84 + hm87. The reaction mixtures were mixed and digested with DpnI to remove the template plasmid. Denaturation and re-annealing allowed formation of heteroduplexes, which spontaneously circularized. These products lack the NLS coding sequence.

compatible overhangs that resulted in spontaneous circularization. These circular products lack the NLS coding sequence (Figure 9), as confirmed by DNA sequencing.

For the generation of Trunc7ΔNLS, analogous procedures were followed, using pNH156 as the template for initial inverse PCR reactions.

2.3 Generation of transgenic animals

2.3.1 Germline transformation

To isolate plasmid DNA for injection, we used various commercial purification columns (QIAprep Spin Miniprep Kit or GenElute Plasmid Miniprep Kit). The column eluate was further purified by a polyethylene glycol (PEG) precipitation. Briefly, 100 μL of plasmid DNA was mixed with 400 μL of TE and 200 μL of PEG solution (30% PEG-8000, 1.6 M NaCl). Following an overnight incubation at 4°C, DNA was sedimented by centrifugation (13,000 rpm, 20 minutes, 4°C). The resulting pellet was resuspended in 200 μL of TE and extracted by phenol-chloroform according to standard procedures (Sambrook et al., 1989). Plasmid concentrations were determined by UV spectrophotometry (absorbance at 260 nm).

Transgenic animals were generated by microinjection, as previously described (Mello et al., 1991). Each construct was co-injected with one of two fluorescent markers: *unc-122p::gfp*, which expresses in coelomocytes, or *dpy-30p::dsRed* (Cordes et al., 2006), which is detected throughout the body. Exogenous DNA forms large extrachromosomal concatemers that are inherited mosaically by a fraction of the offspring. Details of each injection, along with the respective transgenic arrays, are illustrated in Table 3.

Table 3 Transgenic lines generated

ham-1 construct [a]	Co-injection marker [b]	Injected strain	Transgenic Arrays
unc-119p-gfp::ham-1-let-858-3'UTR	*unc-122p::gfp*	wildtype (N2)	*hkEx41-44*
unc-119p-gfp::ham-1-ham-1-3'UTR	*unc-122p::gfp*	wildtype (N2)	*hkEx45-49*
unc-119p-gfp::Trunc1-let-858-3'UTR	*dpy-30p::dsRed*	*zdIs5[mec-4::gfp]*	*hkEx66-69*
unc-119p-gfp::Trunc2-let-858-3'UTR	*dpy-30p::dsRed*	*zdIs5[mec-4::gfp]*	*hkEx87-90*
unc-119p-gfp::Trunc3-let-858-3'UTR	*dpy-30p::dsRed*	*zdIs5[mec-4::gfp]*	*hkEx91-95*
unc-119p-gfp::Trunc4-let-858-3'UTR	*dpy-30p::dsRed*	*zdIs5[mec-4::gfp]*	*hkEx97-102*
unc-119p-gfp::Trunc5-let-858-3'UTR	*dpy-30p::dsRed*	*zdIs5[mec-4::gfp]*	*hkEx104-107*
unc-119p-gfp::Trunc6-let-858-3'UTR	*dpy-30p::dsRed*	*zdIs5[mec-4::gfp]*	*hkEx108-112*
unc-119p-gfp::Trunc7-let-858-3'UTR	*dpy-30p::dsRed*	*zdIs5[mec-4::gfp]*	*hkEx115-118*
unc-119p-gfp::Trunc8-let-858-3'UTR	*dpy-30p::dsRed*	*zdIs5[mec-4::gfp]*	*hkEx119-121*
unc-119p-myr::gfp::ham-1-let-858-3'UTR	*dpy-30p::dsRed*	*zdIs5[mec-4::gfp]*	*hkEx136-139*
unc-119p-myr::gfp::Trunc5-let-858-3'UTR	*dpy-30p::dsRed*	*zdIs5[mec-4::gfp]*	*hkEx140-143,158*
unc-119p-myr::gfp::Trunc6-let-858-3'UTR	*dpy-30p::dsRed*	*zdIs5[mec-4::gfp]*	*hkEx144-146,155-157*
unc-119p-myr::gfp::Trunc7-let-858-3'UTR	*dpy-30p::dsRed*	*zdIs5[mec-4::gfp]*	*hkEx159-163*
unc-119p-gfp::ham-1ΔNLS-let-858-3'UTR	*dpy-30p::dsRed*	*zdIs5[mec-4::gfp]*	*hkEx153-154*
unc-119p-gfp::Trunc7ΔNLS-let-858-3'UTR	*dpy-30p::dsRed*	*zdIs5[mec-4::gfp]*	*hkEx147-150*

[a] *ham-1* constructs were injected at 50 ng/μL

[b] *unc-122p::gfp* was injected at 20 ng/μL while *dpy-30p::dsRed* was injected at 40 ng/μL

2.3.2 Extrachromosomal array integration

Because extrachromosomal arrays exhibit mitotic instability, the transgenic animals are often mosaic (Evans, 2006). These arrays can be stably incorporated into chromosomes by X-ray irradiation. We integrated *hkEx42[unc-119p-gfp::ham-1-let-858-3'UTR]* in the N2 background according to a protocol provided by D. Baillie. Details of this procedure have been previously published (Lee, 2005). Briefly, transgenic hermaphrodites of the L4 to young adult stage were exposed to 1500 rads X-ray. The P0 animals were cloned onto large plates and allowed to lay eggs for 24 hours before removed. Transgenic worms in the F2 generation were cloned, and their progeny were screened for stable transmission of the array (all F3 animals express the co-injection marker). By this strategy, we obtained a single integrated transgenic line, *hkIs39[unc-119p-gfp::ham-1-let-858-3'UTR]*. Since X-ray irradiation can result in other background mutations, the transgenic animals were backcrossed six times with the wildtype strain to remove potential lesions (Appendix 1).

2.4 Genetic crosses

2.4.1 Strains containing *ham-1* transgenic arrays

Transgenic arrays carrying full-length *ham-1* constructs were crossed into cell-specific GFP reporter strains. *gmIs12[srb-6::gfp]* is expressed in the PHA and PHB phasmid neurons (Troemel et al., 1995), while *zdIs5[mec-4::gfp]* is specific for the PLM neuron in the L1 hermaphrodite tail (Clark and Chiu, 2003). The general crossing scheme (Appendix 2) illustrates the introduction of extrachromosomal arrays into GFP reporter strains. Similar genetic crosses were used for the integrated concatemer, *hkIs39*,

with an extra final step to homozygose the array. This mating scheme was only used for full-length *ham-1* constructs, which were injected into N2 hermaphrodites. The remaining *ham-1* constructs (truncation, myristoylation or NLS deletion) were injected into *zdIs5[mec-4::gfp]* animals, which allowed direct examination of the PLM neuron (Table 3).

Function of the exogenous HAM-1 products was assessed by their ability to rescue neuronal defects in *ham-1* mutants. Strains containing *ham-1(gm279)*, neuronal reporters, and transgenic arrays expressing these constructs were created by a generic strategy (Appendix 3). Normally, homozygous *ham-1* mutants exhibit an abnormal tail phenotype, which can be used to follow the allele during genetic crosses (Roh, 2004). However, since the presence of transgenic arrays may rescue these defects, *ham-1* was tracked by an alternative method. *dpy-20(e1282ts)* and *unc-30(e191)* are two recessive visible mutations that map to the left and right of the *ham-1* locus, respectively. The *dpy-20(e1282ts)* and *unc-30(e191)* recombinant (provided by G. Garriga) was used *in trans* to counter-select for *ham-1(gm279)*.

Counter-selection is illustrated in the following example, where *ham-1* homozygous progeny are isolated from *ham-1 / dpy-20 unc-30* heterozygotes. This parental strain gives rise to two main F1 phenotypes: animals that are Dpy and Unc, or those that look wildtype (recombination may produce progeny that are only Dpy or only Unc, which should not be used). The first phenotypic class is indicative of *dpy-20 unc-30* homozygous mutants. The remaining animals may be of two genotypes: *ham-1 / ham-1* or *ham-1 / dpy-20 unc-30*. These possibilities can be distinguished by examination of the F2 progeny; the heterozygote would segregate animals that are Dpy and Unc, while the

ham-1 homozygote would not. Thus, by selecting for the absence of these two markers, we could identify *ham-1* mutants.

2.4.2 Strains to examine position of HAM-1 function in the PLM lineage

Loss of HAM-1 function disrupts the production of the PLM neuron (Frank et al., 2005; Guenther and Garriga, 1996). To determine whether the sister neuron (ALN) is also affected, the integrated reporter *ncIs1[eat-20::gfp pRF4]* (Shibata et al., 2000) was crossed into a *ham-1(gm279)* null mutant background (Appendix 4). As described in the previous section, *dpy-20(e1282ts) unc-30(e191)* was used *in trans* to track *ham-1(gm279)* throughout these genetic crosses. Because GFP fluorescence from the ALN reporter is very faint, *ncIs1[eat-20::gfp pRF4]* was followed by the dominant rolling phenotype (Rol) conferred by *pRF4*.

ham-1 mutants often affect divisions that give rise to apoptotic daughter cells (Frank et al., 2005). Two of such divisions are observed in the PLM lineage. To determine whether PLM neuronal loss could be rescued by inhibition of cell death, the *ced-4(n1162)* mutation was used (Ellis and Horvitz, 1986). We generated two strains: *zdIs5[mec-4::gfp]; ced-4(n1162)* and *zdIs5[mec-4::gfp]; ced-4(n1162); ham-1(gm279)*. The mating scheme is shown in Appendix 5. To follow the *ced-4(n1162)* allele during these crosses, we used the counter-selection marker *dpy-17(e164)* (Brenner, 1974), which maps close to the right of *ced-4*. Presence of the cell death mutant was confirmed by examination of live embryos, which did not contain any apoptotic bodies.

2.4.3 Strains containing *apr-1(zh10)*

To investigate APR-1 function in the PLM lineage, *zdIs5[mec-4::gfp]* was introduced into the *apr-1(zh10)* null mutant (Hoier et al., 2000). Since *apr-1(zh10)* results in zygotic embryonic/larval lethality, this allele was maintained by the translocation balancer *hT2[qIs48] (I;III)* (McKim et al., 1993). Presence of this balancer results in pharyngeal GFP expression, and *hT2* homozygotes are inviable. The strain *apr-1(zh10) / hT2[qIs48]* was previously created in our lab (Roh, 2004). Because *apr-1* and the integrated PLM reporter are both on LG I, recombination was required to generate *apr-1(zh10) zdIs5[mec-4::gfp] / hT2[qIs48] zdIs5[mec-4::gfp]* (Appendix 6).

To examine PLM defects in *apr-1* and *ham-1* double mutants, we created an additional strain: *apr-1(zh10) zdIs5[mec-4::gfp] / hT2[qIs48] zdIs5[mec-4::gfp]; ham-1(gm279)*. The complete crossing scheme is illustrated in Appendix 7. Basically, *ham-1(gm279)* was introduced into *apr-1(zh10) zdIs5[mec-4::gfp] / hT2[qIs48] zdIs5[mec-4::gfp]* by mating with *ham-1(gm279); him-5(e1490)* males (provided by G. Garriga). The *him-5* allele results in high levels of X chromosome nondisjunction, which generates male progeny (Broverman and Meneely, 1994). As we did not select for this mutant, it was lost in the genetic crosses. Presence of *ham-1* was followed by the abnormal tail phenotype.

apr-1(zh10) zdIs5[mec-4::gfp] / hT2[qIs48] zdIs5[mec-4::gfp]; ced-3(n717) was generated to examine PLM defects in *apr-1; ced-3* double mutants. Appendix 8 shows the mating scheme used to obtain this strain (performed by N. Hawkins). In general, *ced-3(n717)* was introduced into *apr-1(zh10) zdIs5[mec-4::gfp] / hT2[qIs48] zdIs5[mec-4::gfp]* by crossing with *ced-3(n717); him-5(e1490)* males (provided by G. Garriga). As

described above, we did not select for the *him-5* allele; thus, it was lost throughout the crosses. Presence of *ced-3(n717)* was confirmed by a PCR-digest method described in Section 2.2.1 (Genotyping *ced-3(n717)* mutants).

2.4.4 Strains containing *lin-17(n671)*

Several strains were created to investigate potential genetic interactions between *lin-17* and *ham-1* in the PLM lineage. First, effects of the *lin-17* single mutant was examined with *lin-17(n671) zdIs5[mec-4::gfp]*. Secondly, to introduce the *ham-1* allele, we used a second strain that contained the *dpy-20 unc-30* counter-selection markers: *lin-17(n671) zdIs5[mec-4::gfp]; dpy-20(e1282ts) unc-30(e191)*. As shown in Appendix 9, these two lines were isolated from a single set of genetic crosses (performed by N. Hawkins). Recombination between *lin-17* and *zdIs5* was required, as they were both located on LG I. Homozygous *lin-17* animals were identified by the occasional production of an extra pseudo-vulva (Sternberg, 2005), known as the Bivul phenotype.

To examine PLM defects in the *lin-17; ham-1* double mutant, we generated *lin-17(n671) zdIs5[mec-4::gfp]; ham-1(gm279)*. The mating scheme is illustrated in Appendix 10. Basically, *lin-17(n671) zdIs5[mec-4::gfp]; dpy-20(e1282ts) unc-30(e191)* was crossed with *ham-1(gm279); him-5(e1490)* males to introduce the *ham-1* mutation. Once again, the *him-5* allele was subsequently lost.

2.5 Immunofluorescence and microscopy

To investigate subcellular localization of exogenous GFP::HAM-1 fusion proteins, we fixed and stained transgenic embryos according to a modified Ruvkun protocol. Details of this procedure were previously described (Finney and Ruvkun, 1990; Hawkins

et al., 2005). We labelled embryos with chicken anti-GFP primary antibodies (Upstate Technologies, 1:200), followed by goat anti-chicken secondary antibodies conjugated to Alexa Fluor 488 (Molecular Probes, 1:2000). DAPI (4',6-diamidino-2-phenylindole) was also added at 1 μg/mL to visualize the nuclei.

Prior to examination, samples were mounted on a 2% agarose pad. Immunostained embryos were immersed in DABCO antifade solution (0.1 g/mL DABCO in 1x PBS and 90% glycerine) to reduce photobleaching. Live embryos were placed in M9 buffer (22 mM KH_2PO_4, 42mM Na_2HPO_4, 86 mM NaCl, 1 mM $MgSO_4$). For inspection of cell-specific GFP markers, live larvae were immobilized in 100 mM NaN_3. All samples were visualized on a Leica DMRA2 upright microscope equipped with epifluorescence and differential interference contrast optics. Images were collected by a Hamamatsu ORCA-285 digital camera and Openlab software (Improvision). Adobe Photoshop and Illustrator (Adobe Systems) were used to prepare images for publication.

2.6 Bioinformatics analyses

To identify HAM-1 sequence homology, we executed BLASTP searches against the NCBI non-redundant (nr) protein database, using default parameters (Altschul et al., 1997). Multiple sequence alignments were created by ClustalW (Thompson et al., 1994). Formatting and annotation of aligned sequences were performed with ESPript 2.2 (Gouet et al., 1999). To detect potential protein domains, HAM-1 was used as query against InterPro databases (Mulder et al., 2005). Nuclear localization signals were predicted by PSORTII (Horton and Nakai, 1997). ELM analyses (the Eukaryotic Linear Motif server, Puntervoll et al., 2003) identified short linear patterns that represent potential functional sites in HAM-1.

BLAST	http://www.ncbi.nlm.nih.gov/BLAST
ClustalW	http://www.ebi.ac.uk/clustalw/
ESPript	http://espript.ibcp.fr
InterProScan	http://www.ebi.ac.uk/InterProScan/
PSORT	http://psort.ims.u-tokyo.ac.jp/
ELM	http://elm.eu.org/

CHAPTER 3: RESULTS

HAM-1 is a novel protein implicated in the ACD of many neuroblasts during embryogenesis. Although several preliminary models have been proposed for the involvement of HAM-1 in these divisions, the true mechanism of its function remains obscure. Furthermore, HAM-1 lacks sequence similarity to known proteins involved in ACDs, which could have provided mechanistic insights from other characterized systems.

3.1 Identification of a winged-helix domain in HAM-1

Previous investigations identified an N-terminal stretch of HAM-1 with similarity to *Drosophila* Knockout and several other unknown sequences (Frank et al., 2005). Unfortunately, these poorly characterized molecules could not enhance our understanding of HAM-1 function. Since protein databases undergo continual expansion, we performed periodic BLAST searches throughout the course of this study to uncover new sequence homologies.

Recently, the N-terminal HAM-1 region was found to be homologous to a novel member of the winged-helix protein family, STOX1 (33% identity, Figure 10). *STOX1* was identified in humans as a locus involved in preeclampsia – a pregnancy-associated condition characterized by hypertension and proteinuria (van Dijk et al., 2005). Endogenous protein expression is detected in various cells of the early placenta, residing in either the nucleus or cytoplasm. Although the molecular function of STOX1 has not

been elucidated, the authors discovered a putative winged-helix domain within the sequence region homologous to HAM-1.

To determine if HAM-1 also encodes this motif, we performed a protein domain search using InterProScan (Mulder et al., 2005). Excitingly, a winged-helix module (accession IPR011991) was predicted between amino acids 94 to 180 (Figure 10). These domains often mediate DNA binding (Aravind et al., 2005), which is consistent with the nuclear distribution of STOX1. Although HAM-1 was previously detected at the cell cortex (Frank et al., 2005; Guenther and Garriga, 1996), additional support for its potential nuclear function is provided in this study.

3.2 Truncation analysis of the HAM-1 protein

Aside from the above bioinformatics approach, we also identified important HAM-1 sequences by serial deletion analysis. N-terminal and C-terminal truncations of HAM-1 were expressed in transgenic animals. Subcellular localization of each protein was examined by immunofluorescence, while function was assessed by their ability to rescue neuronal defects in *ham-1* mutants.

3.2.1 Characterization of exogenous full-length GFP::HAM-1

Prior to truncation analysis, the proper localization and function of exogenous full-length GFP::HAM-1 must be confirmed. HAM-1 was fused translationally with GFP to allow detection of the fusion protein with anti-GFP antibodies. Because C-terminal HAM-1 fusions were previously shown to be non-functional (C. Guenther, unpublished results), we added GFP sequences onto the N-terminus of HAM-1 (Figure 11). This fusion protein was placed under the control of a heterologous promoter as the *ham-1*

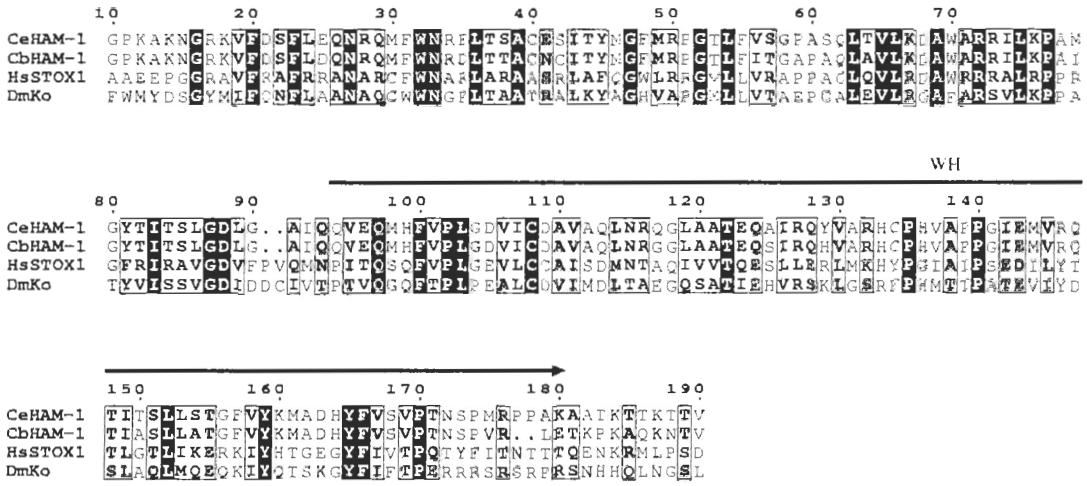

Figure 10 HAM-1 sequence homology

A partial multiple sequence alignment between *C. elegans* HAM-1 (CeHAM-1, accession CAA98132), its *C. briggsae* homolog (CbHAM-1, accession CAE67925), human STOX1 (HsSTOX1, accession NP_689922) and *Drosophila* Knockout (DmKo, accession AAB62567). The numbering on the alignment corresponds to position in the CeHAM-1 sequence. Identical residues are shaded in black, similar residues are shown in boxes. The predicted winged-helix (WH) domain in HAM-1 spans amino acids 94-180.

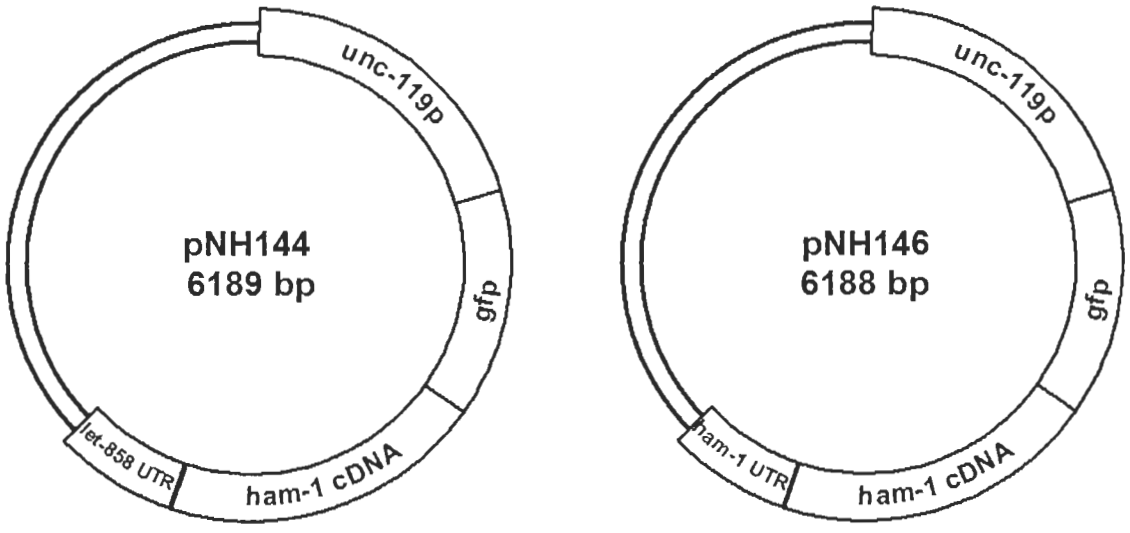

Figure 11 Full-length *gfp::ham-1* constructs with the *let-858* or *ham-1* 3'-UTR

gfp was fused to the N-terminus of *ham-1* cDNA and expressed under the *unc-119p* promoter. Two constructs were designed with different 3'-UTRs (*let-858* or *ham-1*). See Materials and Methods for details of construction.

promoter sequence has not been identified; prior experiments that expressed reporter genes with a 3.3 kb fragment upstream of the *ham-1* transcription start site failed to produce the appropriate expression patterns (N. Hawkins, unpublished results). Consequently, we used the *unc-119* promoter to regulate transcription of our *gfp::ham-1* constructs. UNC-119 expression begins at the 60-cell stage of embryogenesis and is observed in numerous neuronal lineages (Maduro and Pilgrim, 1995), including many cells that also exhibit HAM-1 staining (N. Hawkins, unpublished results).

We generated two full-length *ham-1* constructs that differed in the 3'-untranslated regions (UTR), as shown in Figure 11. One plasmid (pNH144) utilizes the *let-858* 3'-UTR, a standard 3'-UTR found in *C. elegans* cloning vectors, while the second construct (pNH146) contains the corresponding sequences from the *ham-1* locus. The latter plasmid was designed in consideration that the *ham-1* 3'-UTR may be important for proper localization or function of the protein. As reviewed by Bashirullah et al. (1998), the localization of some proteins requires prior recruitment of the mRNA by elements within the 3'-UTR.

The full-length constructs were injected independently at 50 ng/µl into the syncytial gonad of wildtype (N2) hermaphrodites. The exogenous DNA can form high-copy extrachromosomal concatemers that are transmitted through both meiotic and mitotic divisions (Stinchcomb et al., 1985). We obtained multiple transgenic lines of each *gfp::ham-1* construct for subsequent localization and function analyses (shown in Table 3).

3.2.1.1 *let-858* 3'-UTR enables expression and localization of GFP::HAM-1

To examine the expression and subcellular localization of the exogenous full-length HAM-1 proteins, transgenic embryos were isolated and immunostained with anti-GFP antibodies. We also treated embryos with the DNA fluorochrome DAPI for visualization of the nuclei. As shown in Figure 12, the GFP::HAM-1 fusion proteins were properly detected at the cell cortex. Asymmetric localization was also observed in a subset of transgenic embryos (Figure 12A,B). This is consistent with the immunostaining pattern of endogenous HAM-1, which shows that peripheral distribution of the protein can become asymmetric in mitotic cells (Guenther and Garriga, 1996). Since similar staining patterns were observed for transgenic embryos expressing either full-length construct, the *ham-1* 3'-UTR is not likely required for proper subcellular distribution of the protein. Aside from the typical peripheral localization of HAM-1, we occasionally detected a low level of GFP staining in the nucleus (Figure 12C). This faint signal was only present in a subset of the cells in some transgenic embryos.

3.2.1.2 Rescue of neuronal defects in *ham-1* mutants by GFP::HAM-1

To determine whether the GFP::HAM-1 fusion proteins were functional, we assayed the ability of these transgenic arrays to rescue neuronal defects observed in *ham-1* mutants. Previous studies have shown that the lack of HAM-1 activity results in aberrant numbers of PHB, a phasmid sensory neuron (Guenther and Garriga, 1996). This neuron can be visualized with *gmIs12[srb-6::gfp]*, an integrated reporter that expresses GFP in both the PHA and PHB phasmid neurons (Figure 13). Because HAM-1 function is not required in the PHA lineage, any deviation in the number of GFP-expressing cells is attributed to PHB defects (Frank et al., 2005).

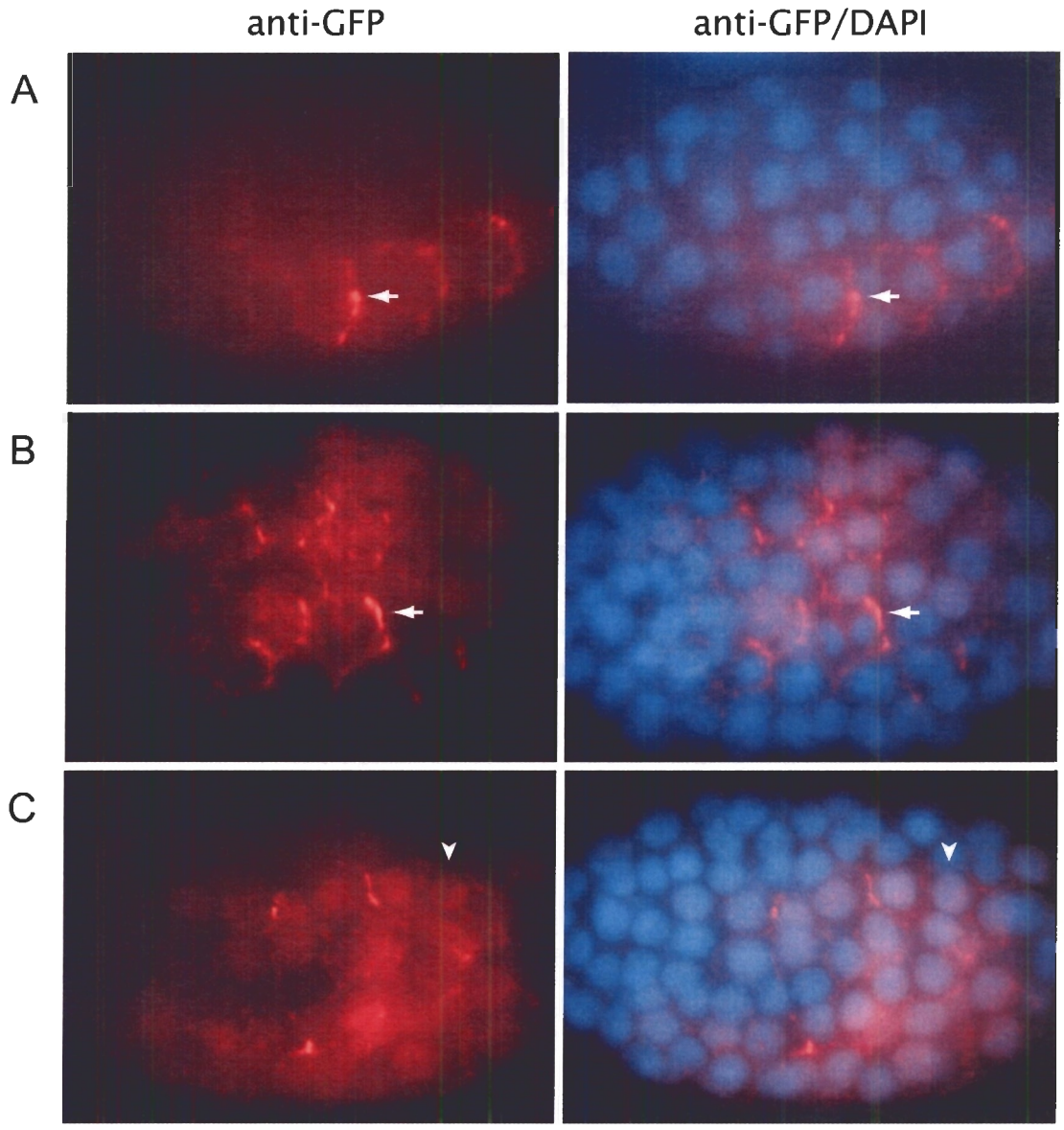

Figure 12 Expression and localization of full-length GFP::HAM-1 fusion proteins

Fluorescence images of transgenic embryos stained with anti-GFP antibodies (red) and DAPI (blue). (A, B) Full-length GFP::HAM-1 can exhibit asymmetric localization (arrow) at the cell cortex regardless of the 3'-UTR. (A) Transgenic embryo carrying *hkEx42[unc-119p-gfp::ham-1-let-858-3'UTR]*. (B) Transgenic embryo carrying *hkEx46[unc-119p-gfp::ham-1-ham-1-3'UTR]*. (C) Occasionally, weak nuclear staining is also observed (arrowhead). This embryo is contains the full-length array *hkEx42*. Embryos with *hkEx46* also exhibit low levels of nuclear staining (data not shown).

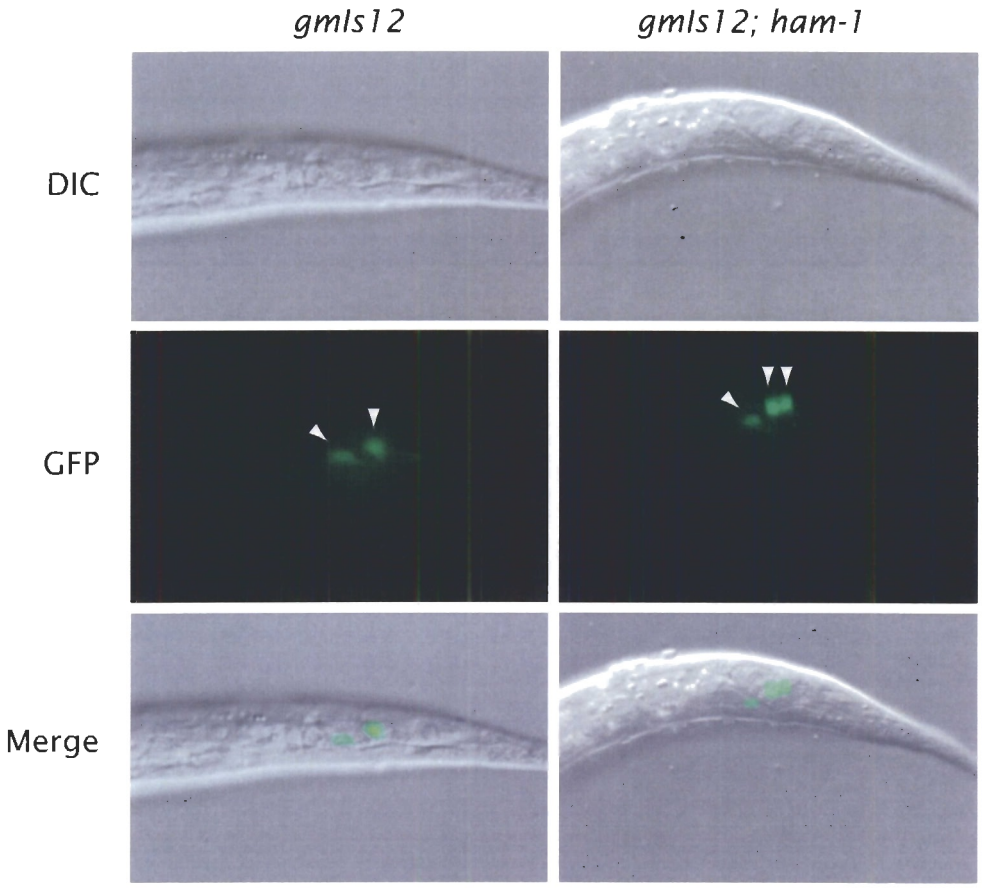

Figure 13 PHB neuron visualized by the *gmIs12* reporter

The integrated *gmIs12[srb-6::gfp]* reporter is expressed in both the PHA and PHB neurons. (Left) Two GFP-expressing cells are observed on each side of wildtype animals. (Right) In *ham-1* mutants, duplication of PHB often results in three GFP-expressing cells.

In the first larval (L1) stage of *ham-1(gm279)* null mutants, we observed approximately 20% duplication and 7% loss of the PHB neuron (Table 4). Extrachromosomal arrays carrying *gfp::ham-1* with the *let-858* 3'-UTR (*hkEx42* and *hkEx43*) produced a moderate rescue of the PHB duplications down to 10% or 6%, indicating that the constructs were functional. Unexpectedly, we also observed an increase in the percentage of neuronal loss from 7% up to 20% or 13%, respectively. In contrast, transgenic animals expressing *gfp::ham-1* with the *ham-1* 3'-UTR did not exhibit rescue of the PHB defects (Table 4). This may reflect differences in the mRNA stability or translatability conferred by the distinct 3'-UTRs (reviewed in Kuersten and Goodwin, 2003). Nonetheless, our results demonstrate that a construct containing the *let-858* 3'-UTR is functional.

Although the functionality of exogenous GFP::HAM-1 has been confirmed, we did not observe a clear, substantial rescue of the PHB duplications. This is partly due to the low penetrance of neuronal defects (20%) observed in the *ham-1* null mutant; incomplete rescue by the full-length construct only produced minor reductions in the levels of PHB duplication. Conversely, partial rescue should be more evident for neurons that are frequently disrupted by the loss of HAM-1 function. Furthermore, the ability of the full-length construct to rescue may vary according to the lineage assayed, as transgene expression was driven by a heterologous promoter. Thus, we sought to identify a more suitable lineage for subsequent truncation analysis, based on two criteria: (1) the high penetrance of neuronal defects in *ham-1(gm279)*, and (2) a significant rescue of the defect by expression of exogenous full-length HAM-1.

Table 4 Rescue of PHB defects by full-length GFP::HAM-1

	# phasmid neurons / side			
Genotype	**1**	**2**	**3**	**N**
gmIs12 [a]	0%	100%	0%	160
gmIs12; ham-1(gm279)	7%	73%	20%	136
gmIs12; hkEx42 [b]	2%	98%	0%	124
gmIs12; ham-1(gm279); hkEx42	20%	70%	10%	134
gmIs12; hkEx43 [b]	1%	97%	1%	138
gmIs12; ham-1(gm279); hkEx43	13%	82%	6%	110
gmIs12;hkEx46 [c]	0%	100%	0%	112
gmIs12; ham-1(gm279); hkEx46	9%	65%	26%	130
gmIs12; hkEx49 [c]	2%	97%	1%	114
gmIs12; ham-1(gm279); hkEx49	12%	61%	27%	124

[a] *gmIs12 = [srb-6::gfp]*
[b] *hkEx42, hkEx43 = [unc-119p-gfp::ham-1-let-858-3'UTR]*
[c] *hkEx46, hkEx49 = [unc-119p-gfp::ham-1-ham-1-3'UTR]*

Loss of HAM-1 function frequently disrupts the lineage that generates the PLM mechanosensory neuron (Frank et al., 2005; Guenther and Garriga, 1996). Previous studies investigating these defects in *ham-1* mutants visualized PLM with antibodies against UNC-86, a transcription factor involved in neural development. However, this protein is expressed in 47 cells of the L1 hermaphrodite (Finney and Ruvkun, 1990), complicating the identification of PLM. Alternatively, this cell can be examined with the integrated GFP reporter *zdIs5[mec-4::gfp]*, which is expressed in the six touch receptor neurons (ALML/R, PLML/R, AVM and PVM) (Clark and Chiu, 2003). At the L1 stage, PLM is the only GFP-expressing cell in the tail (Figure 14).

As shown in Table 5, *ham-1(gm279)* null mutants exhibited an 81% loss of the PLM neuron. In the presence of extrachromosomal arrays carrying *gfp::ham-1* with the *let-858* 3'-UTR (*hkEx42* and *hkEx43*), these defects were reduced to 21% and 39%, respectively. A mild increase in PLM duplication was observed, possibly due to overexpression of the protein by extrachromosomal concatemers. In this lineage, the full-length construct containing the *ham-1* 3'-UTR (*hkEx46* and *hkEx49*) was also able to rescue neuronal defects, albeit less dramatically, to 64% and 57% loss, respectively.

The incomplete rescue of the PLM neuron may be attributed to the mosaicism of extrachromosomal array expression. To determine the maximal rescue attainable by the exogenous full-length HAM-1 protein, *hkEx42* was stably integrated into the genome by X-ray irradiation. A single integrated array was obtained, which reduced PLM loss to 5% in a *ham-1(gm279)* background (Table 5, *hkIs39*). Expression of *hkIs39* also produced a 24% duplication of this neuron in the presence or absence of endogenous HAM-1.

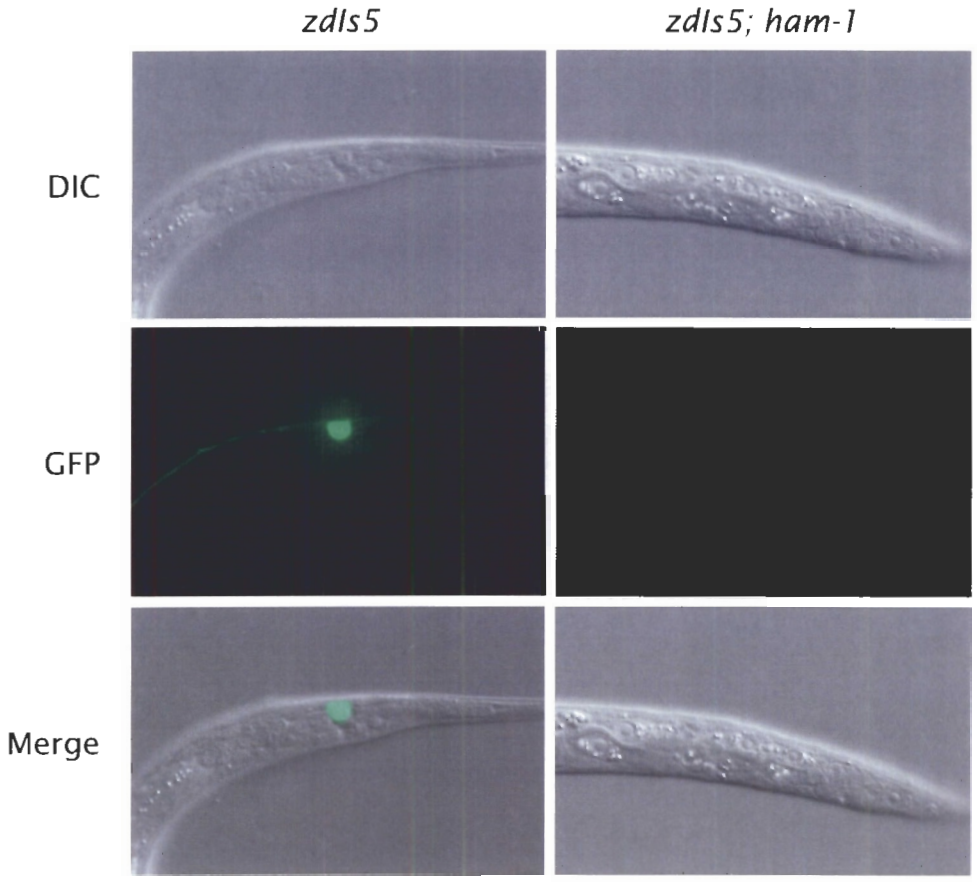

Figure 14 PLM neuron visualized by the *zdIs5* reporter

The integrated *zdIs5[mec-4::gfp]* reporter is expressed in the PLM neuron. (Left) A single GFP-expressing cell is observed on each side of wildtype animals. (Right) *ham-1* mutants exhibit a highly penetrant loss of this neuron.

Table 5 Rescue of PLM defects by full-length GFP::HAM-1

	# PLM neurons / side			
Strains	**0**	**1**	**2**	**N**
zdIs5 [a]	0%	100%	0%	200
zdIs5; ham-1(gm279)	81%	18%	1%	140
zdIs5; hkEx42 [b]	3%	91%	7%	222
zdIs5; ham-1(gm279); hkEx42	21%	70%	9%	106
zdIs5; hkEx43 [b]	2%	88%	10%	310
zdIs5; ham-1(gm279); hkEx43	39%	56%	5%	126
zdIs5; hkIs39 [c]	1%	74%	24%	148
zdIs5; ham-1(gm279); hkIs39	5%	71%	24%	132
zdIs5; hkEx46 [d]	7%	93%	0%	244
zdIs5; ham-1(gm279); hkEx46	64%	35%	1%	138
zdIs5; hkEx49 [d]	4%	95%	1%	316
zdIs5; ham-1(gm279); hkEx49	57%	42%	1%	138

[a] *zdIs5 = [mec-4::gfp]*
[b] *hkEx42, hkEx43 = [unc-119p-gfp::ham-1-let-858-3'UTR]*
[c] *hkIs39* = integrated *hkEx42*
[d] *hkEx46, hkEx49 = [unc-119p-gfp::ham-1-ham-1-3'UTR]*

Results of the above experiments revealed several important details. First, we showed that the *unc-119* promoter enables expression in the appropriate cells to rescue PHB and PLM defects in *ham-1* mutants. Furthermore, the function of our full-length constructs does not depend on the *ham-1* 3'-UTR. In fact, the *let-858* 3'-UTR produced better rescue in both lineages, and thus was used in the subsequent truncation studies. Finally, because the highly penetrant loss of PLM neurons were readily rescued by GFP::HAM-1, this lineage was ideal for functional analysis of additional *ham-1* constructs.

3.2.2 Analysis of HAM-1 C-terminal and N-terminal truncations

With confirmation of proper localization and function for the exogenous full-length HAM-1 fusions, we created a set of serial deletions to identify important sequence regions of this novel protein. Eight truncations were designed to span the HAM-1 sequence, including four C-terminal and four N-terminal deletions (Figure 15). Each truncation construct was made by replacement of the full-length *ham-1* cDNA in pNH144 *[unc-119p-gfp::ham-1-let-858-3'-UTR]* with the corresponding partial *ham-1* coding regions. Since the function of these truncated proteins were to be assessed in the PLM lineage, we injected the plasmid DNA directly into hermaphrodites carrying the integrated GFP reporter *zdIs5[mec-4::gfp]*. Multiple transgenic lines were obtained from the injection of each construct at 50 ng/µl (Table 3). Unless otherwise stated, a single representative array was chosen for further analysis.

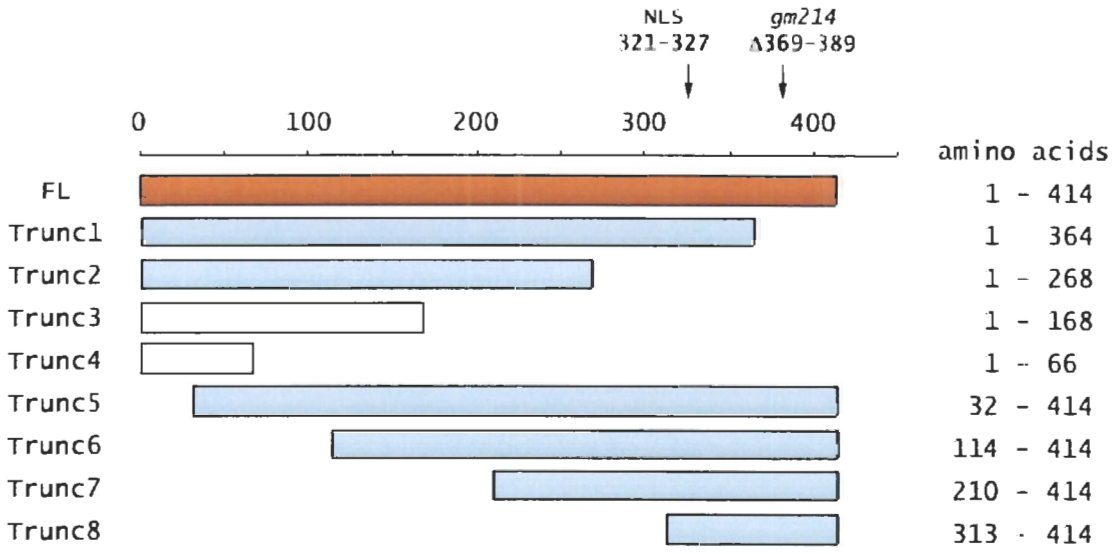

Figure 15 Schematic of C-terminal and N-terminal HAM-1 truncations

Eight HAM-1 truncations were designed to remove coding regions from the C-terminus (Trunc1-4) and the N-terminus (Trunc5-8). A putative NLS (PTRRRAR) sequence resides at amino acids 321-327. The *ham-1(gm214)* allele encodes a non-functional protein with a short deletion near the C-terminus (Δ369-389).

3.2.2.1 Subcellular localization of HAM-1 truncations

To identify sequences required for the localization of HAM-1, the subcellular distribution of each truncated protein was examined in transgenic embryos using anti-GFP antibodies. Because a prior yeast-two-hybrid assay revealed the potential of HAM-1 to homodimerize (N. Hawkins, unpublished results), truncated proteins that lacked localization domains may retain wildtype distribution patterns due to interactions with endogenous HAM-1. Consequently, we examined the localization of each truncation in both the *zdIs5[mec-4::gfp]* and *zdIs5[mec-4::gfp]; ham-1(gm279)* backgrounds. Qualitatively, we did not detect differences in any of the GFP staining patterns in the absence of endogenous HAM-1.

3.2.2.1.1 Peripheral localization

Visualization of the GFP::HAM-1 truncations revealed that the C-terminus is dispensable for asymmetric cortical localization of the protein. As shown in Figure 16A, a truncation lacking 50 C-terminal residues (Trunc1, amino acids 1-364) retained asymmetric distribution at the cell periphery (arrow). Cortical localization was also observed in Trunc2 (amino acids 1-268); however, protein asymmetry was less evident and rarely detected (Figure 16B). Future studies are required to further quantitate this observation. The removal of an additional 100 amino acids from the C-terminus (Trunc3, amino acids 1-168) resulted in diffused cellular staining (Figure 16C), indicating that a region between residues 168 and 268 is essential for localization to the cell periphery. Finally, in the shortest C-terminal truncation (Trunc4, amino acids 1-66), we observed bright GFP puncta (Figure 16D). This may be caused by a tendency of Trunc4 to form protein aggregates.

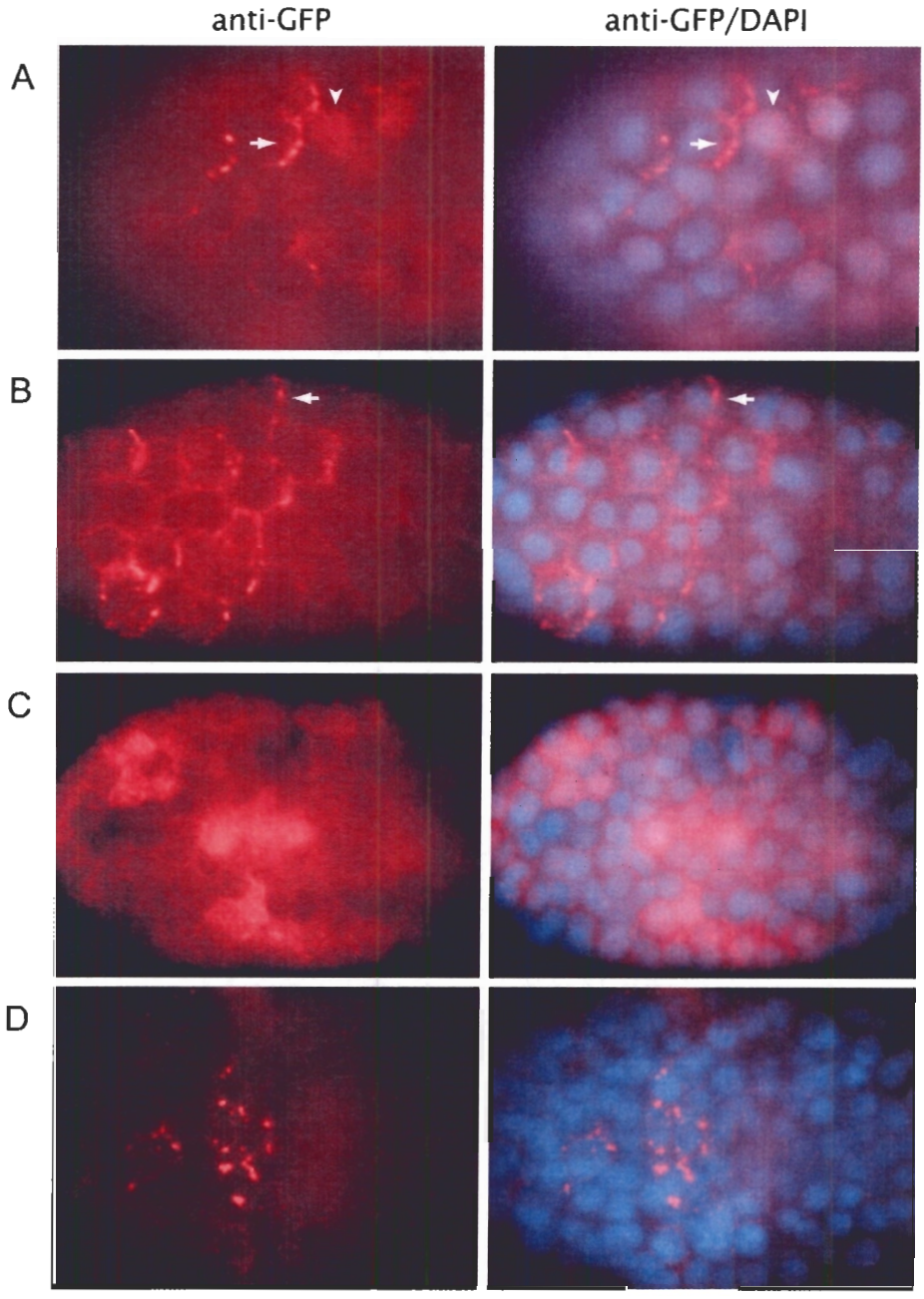

Figure 16 Subcellular localization of C-terminal HAM-1 truncations

Fluorescence images of transgenic embryos stained with anti-GFP antibodies (red) and DAPI (blue). (A) GFP::Trunc1 is localized at the cell cortex. Asymmetric distribution can be observed in some cells (arrow). Occasionally, GFP staining is detected in a subset of the nuclei (arrowhead). (B) GFP::Trunc2 is associated with the cell cortex; however, asymmetric localization (arrow) appears to be rare. Further quantification is required. (C) GFP::Trunc3 is delocalized from the cell periphery. (D) GFP::Trunc4 is detected in bright puncta. Transgenic embryos shown in this figure also express endogenous HAM-1. Staining in the *ham-1(gm279)* background produces similar results.

Examination of subsequent truncations showed that the N-terminus was essential for peripheral localization. A deletion of the first 31 residues (Trunc5, amino acids 32-414) resulted in complete delocalization of the protein (Figure 17A). Unexpectedly, a second truncation lacking additional N-terminal sequences (Trunc6, amino acids 114-414) exhibited minor cortical staining (Figure 17B, arrow). Due to the inherent variability between different extrachromosomal arrays (Evans, 2006), the reproducibility of this observation must be determined by analysis of other transgenic lines that have been obtained for these two constructs (Table 3). Interestingly, Trunc7 (amino acids 210-414) was detected almost exclusively in the nucleus (Figure 17C). Because varying levels of nuclear staining have been noted in both full-length HAM-1 and a number of truncated proteins, it will be discussed in detail below. Finally, reminiscent of Trunc4 localization, the shortest N-terminal truncation (Trunc8, amino acids 313-414) was detected in puncta (Figure 17D).

3.2.2.1.2 Nuclear localization

Previous investigations of endogenous HAM-1 staining reported protein localization at the cell cortex (Frank et al., 2005; Guenther and Garriga, 1996). However, visualization of our full-length and truncated GFP::HAM-1 products revealed potential nuclear targeting of HAM-1. As shown previously in Figure 12C, a low level of nuclear staining was occasionally observed in transgenic embryos expressing full-length GFP::HAM-1. This localization pattern was also observed in the first C-terminal truncation, Trunc1 (Figure 16A, arrowhead). The removal of additional residues in Trunc2 resulted in the elimination of this signal. Additional transgenic lines expressing this construct can be analyzed to confirm this observation (Table 3).

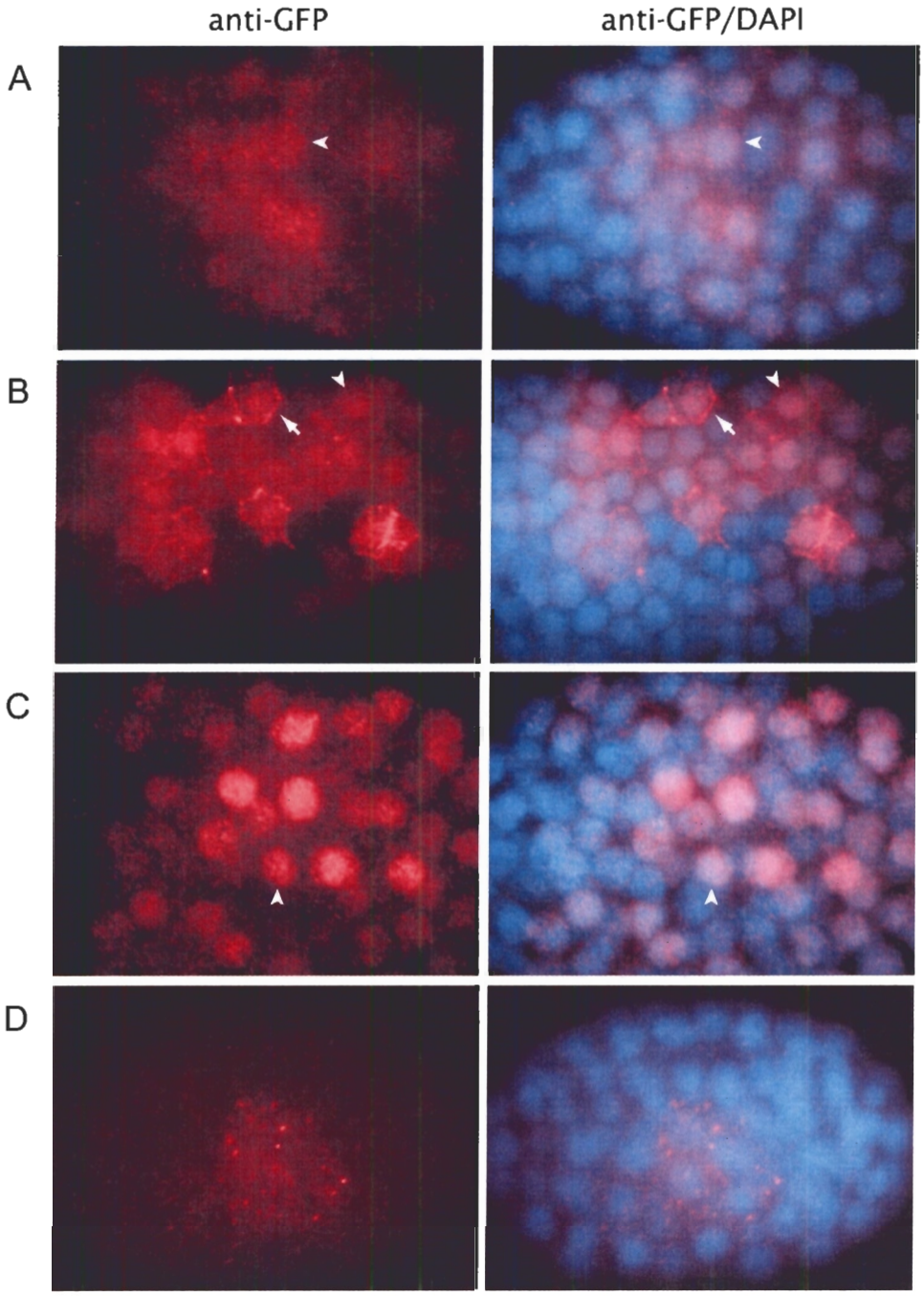

Figure 17 Subcellular localization of N-terminal HAM-1 truncations

Fluorescence images of transgenic embryos stained with anti-GFP antibodies (red) and DAPI (blue). (A) GFP::Trunc5 is delocalized within the cytoplasm. Minor enhancement in the nucleus is occasionally observed (arrowhead). (B) GFP::Trunc6 exhibits weak localization at the cell periphery (arrow), in the nucleus (arrowhead) and within the cytoplasm. (C) GFP::Trunc7 is almost exclusively nuclear. (D) GFP::Trunc4 is detected in puncta. Transgenic embryos shown in this figure also express endogenous HAM-1. Staining in the *ham-1(gm279)* background produces similar results.

N-terminal HAM-1 deletions also exhibited nuclear localization. Although visualization of Trunc5 primarily produced diffused cellular staining, a weak enhancement in the nucleus was sometimes observed (Figure 17A). This was also evident in the immunostaining of Trunc6, which showed a mixture of peripheral, cytoplasmic and nuclear signals (Figure 17B). Nuclear localization became predominant in Trunc7, as mentioned above, generating almost a complete overlap of GFP and DAPI staining patterns (Figure 17C).

3.2.2.2 HAM-1 truncations fail to rescue PLM defects in *ham-1* mutants

To investigate the function of our eight C-terminal and N-terminal protein truncations, we assessed the ability of these extrachromosomal arrays to rescue PLM defects in the *ham-1(gm279)* background. As shown in Table 6, arrays carrying the C-terminal truncations (*hkEx69, hkEx88, hkEx94,* and *hkEx101*) were unable to rescue the 81% loss of PLM neurons observed in *ham-1* mutants. This is consistent with previous investigations of the *ham-1(gm214)* allele, an in-frame deletion of 21 amino acids in the C-terminal region (Δ369-389). *ham-1(gm214)* expression produces a protein product with proper peripheral localization; however, it displays similar neuronal defects as *ham-1(gm279)* and is predicted to be non-functional (Frank et al., 2005). The four C-terminal truncations lacked this 21 amino acid region (Figure 15), and accordingly did not allow for rescue of the PLM neuron.

N-terminal HAM-1 truncations also failed to produce substantial rescue of the PLM neuron (Table 6, *hkEx107*, *hkEx109*, *hkEx117*, and *hkEx121*). A minor reduction of neuronal loss from 81% to 73% was observed in the presence of Trunc6 (*hkEx109*). Although this result was not statistically significant ($p > 0.05$, Chi-Square test), it

Table 6 **PLM neuron in transgenic animals carrying C-terminal and N-terminal HAM-1 truncations**

	# PLM neurons / side			
Strains	**0**	**1**	**2**	**N**
zdIs5 [a]	0%	100%	0%	200
zdIs5; ham-1(gm279)	81%	18%	1%	140
zdIs5; hkEx69 [b]	4%	96%	0%	140
zdIs5; ham-1(gm279); hkEx69	83%	16%	1%	134
zdIs5; hkEx88 [c]	1%	99%	0%	110
zdIs5; ham-1(gm279); hkEx88	83%	17%	0%	114
zdIs5; hkEx94 [d]	0%	99%	1%	110
zdIs5; ham-1(gm279); hkEx94	80%	21%	0%	132
zdIs5; hkEx101 [e]	0%	98%	2%	120
zdIs5; ham-1(gm279); hkEx101	91%	9%	0%	184
zdIs5; hkEx107 [f]	0%	100%	0%	118
zdIs5; ham-1(gm279); hkEx107	79%	21%	0%	110
zdIs5; hkEx109 [g]	5%	95%	0%	116
zdIs5; ham-1(gm279); hkEx109	73%	25%	1%	142
zdIs5; hkEx111 [g]	14%	86%	0%	122
zdIs5; ham-1(gm279); hkEx111	87%	13%	0%	108
zdIs5; hkEx112 [g]	3%	97%	0%	154
zdIs5; ham-1(gm279); hkEx112	83%	16%	1%	120
zdIs5; hkEx117 [h]	2%	97%	1%	110
zdIs5; ham-1(gm279); hkEx117	77%	21%	2%	106
zdIs5; hkEx121 [i]	0%	100%	0%	100
zdIs5; ham-1(gm279); hkEx121	88%	12%	9%	126

[a] *zdIs5[mec-4::gfp]*
[b] *hkEx69 = [unc-119p-gfp::Trunc1-let-858-3'UTR]*
[c] *hkEx88 = [unc-119p-gfp::Trunc2-let-858-3'UTR]*
[d] *hkEx94 = [unc-119p-gfp::Trunc3-let-858-3'UTR]*
[e] *hkEx101 = [unc-119p-gfp::Trunc4-let-858-3'UTR]*
[f] *hkEx107 = [unc-119p-gfp::Trunc5-let-858-3'UTR]*
[g] *hkEx109, hkEx111, hkEx112 = [unc-119p-gfp::Trunc6-let-858-3'UTR]*
[h] *hkEx117 = [unc-119p-gfp::Trunc7-let-858-3'UTR]*
[i] *hkEx121 = [unc-119p-gfp::Trunc8-let-858-3'UTR]*

correlated with slight peripheral localization of the protein, as previously observed (Figure 17B). We examined two additional arrays carrying this construct, *hkEx111* and *hkEx112*, which did not result in a reduction of the PLM defects (Table 6). However, embryo staining has not been performed to examine peripheral localization of Trunc6 in these transgenic lines.

3.2.3 Investigation of myristoylated HAM-1 proteins

The failure of the N-terminal truncations to rescue *ham-1* defects may be a secondary consequence of delocalization from the cell cortex. Accordingly, some truncations may still possess functional sequences even though they were unable to reduce PLM loss. To address this issue, we attempted to target truncated HAM-1 proteins to the plasma membrane by the addition of an N-myristoylation signal. This sequence promotes the covalent attachment of myristate (a 14-carbon fatty acid) to the N-terminal glycine of the substrate protein. The modification enables protein-membrane interactions through its insertion into the lipid bilayer (reviewed in Resh, 1999).

The myristoylation signal from human c-Src, MGSSKS, has been used in previous experiments to promote membrane association of other proteins (Gitai et al., 2003). We fused the corresponding coding sequences to the N-terminus of *gfp* to generate *myr::gfp::ham-1* constructs. The lipidation signal was added to three N-terminal truncations (Trunc5-7) and to full-length HAM-1 as a control. As mentioned above, transgenic lines were obtained by the injection of each construct into *zdIs5[mec-4::gfp]* hermaphrodites (Table 3).

3.2.3.1 Myristoylation partially targets delocalized HAM-1 truncations to cell periphery

We first examined transgenic embryos for localization of the myristoylated full-length protein using anti-GFP antibodies. Although a moderate level of cytosolic staining was detected, MYR::GFP::HAM-1 was also clearly localized at the cell periphery (Figure 18A). This fusion product was observed as crescents in both the wildtype and *ham-1(gm279)* backgrounds, confirming that myristoylation did not affect asymmetric distribution of the full-length protein. Intriguingly, weak nuclear localization was also seen in some embryos (Figure 18B); thus, lipid modification was unable to outcompete the signal(s) targeting HAM-1 to the nucleus.

Myristoylation of Trunc5 partially directed the delocalized protein back to the cell cortex (Figure 18C). However, as demonstrated by the substantial amount of diffused staining that remained, this membrane anchor was not highly efficient. Similar results were obtained for the myristoylated Trunc6 product (Figure 18D). Although the addition of a lipid moiety qualitatively increased the proportion of peripheral staining (compare with Figure 17B), we continued to detect a moderate level of cytoplasmic distribution. Myristoylation also failed to abolish the nuclear targeting of this N-terminal deletion. Finally, the predominance of nuclear localization was demonstrated in myristoylated Trunc7, which remained almost exclusively in the nucleus despite membrane targeting by the lipid moiety (Figure 18E).

3.2.3.2 Myristoylation impedes HAM-1 function

Although the myristoylation sequence only resulted in partial peripheral localization of the HAM-1 truncations, we assayed the ability of these extrachromosomal arrays to rescue PLM defects in *ham-1(gm279)* mutants. As a control, we first examined

Figure 18 Subcellular localization of myristoylated HAM-1 proteins

Fluorescence images of transgenic embryos stained with anti-GFP antibodies (red) and DAPI (blue). (A, B) Transgenic embryos expressing full-length MYR::GFP::HAM-1. (A) The myristoylated protein can still localize asymmetrically at the cell cortex (arrow). Similar results are observed in the *ham-1(gm279)* background (data not shown). (B) A moderate level of cytoplasmic staining is observed along with cortical localization. In some embryos, GFP is also weakly detected in the nucleus (arrowhead). (C) MYR::GFP::Trunc5 exhibits cytoplasmic and peripheral distribution. (D) Myristoylated GFP::Trunc6 is localized to the periphery (arrow), in the nucleus (arrowhead) and within the cytoplasm. (E) MYR::GFP::Trunc7 is primarily detected in the nucleus. Transgenic embryos shown in this figure also express endogenous HAM-1.

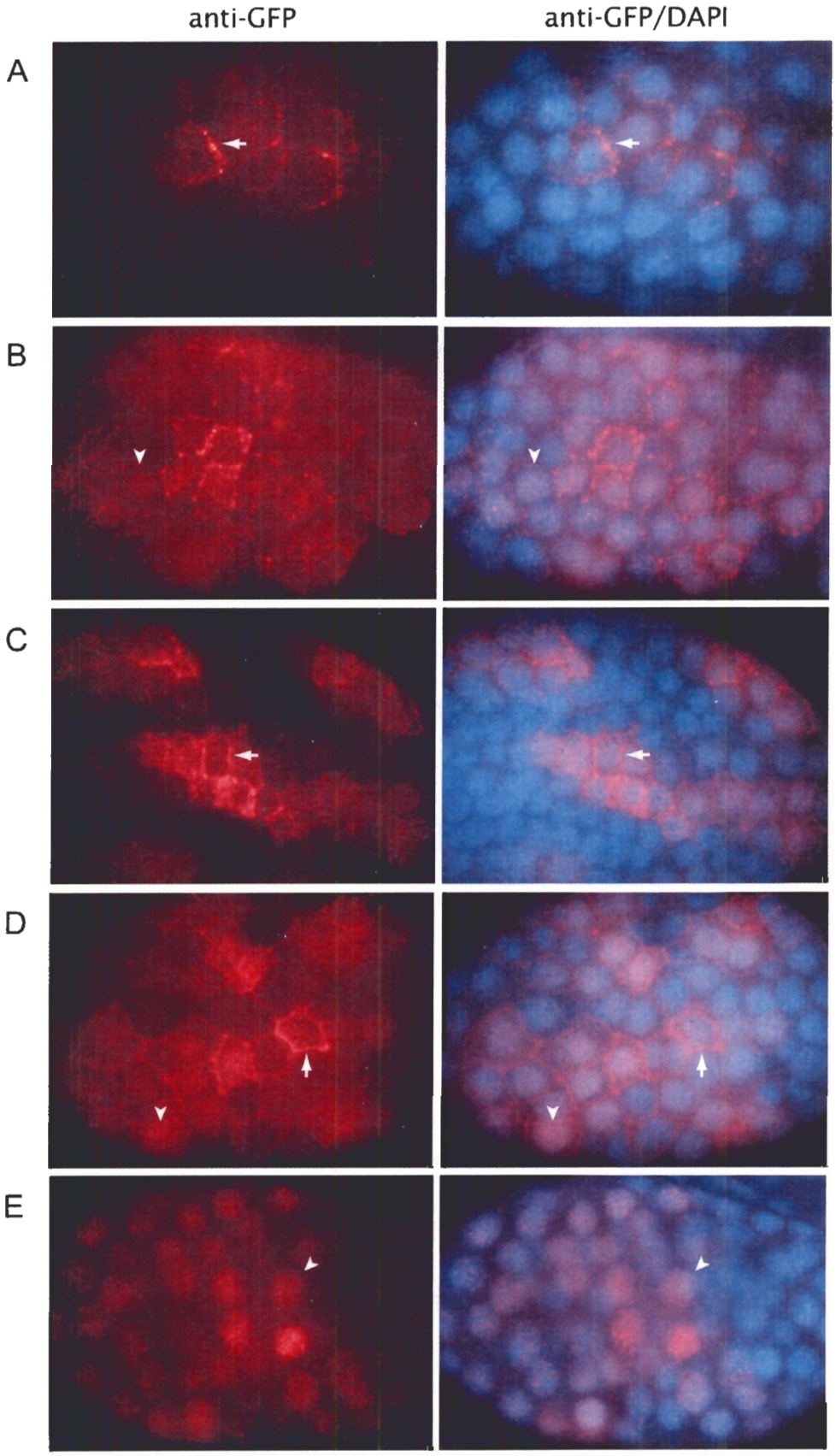
anti-GFP
anti-GFP/DAPI
A
B
C
D
E

the PLM neuron in transgenic L1 animals expressing myristoylated full-length HAM-1. Unexpectedly, three independent arrays carrying this construct (*hkEx136*, *hkEx137*, and *hkEx138*) consistently gave poor rescue of the *ham-1* defects, exhibiting 62-69% PLM loss (Table 7). Comparison with the non-lipidated protein, which reduced neuronal defects to 21% or 39% (Table 5, *hkEx42 and hkEx43*), suggests that addition of myristate impeded the function of HAM-1. As predicted from these results, myristoylation of Trunc5 and Trunc6 did not produce rescue of the PLM loss in *ham-1* mutants (Table 7, *hkEx141* and *hkEx146*). Since localization of Trunc7 was not altered by the lipid modification, we omitted this protein from the functional analysis.

3.2.4 Examination of a potential nuclear role of HAM-1

Several lines of indirect evidence have suggested a potential role of HAM-1 in the nucleus. As mentioned previously, sequence homology revealed the presence of a putative winged-helix motif, which often mediates DNA binding (Aravind et al., 2005). Moreover, products of different *ham-1* constructs have been detected in the nucleus at various intensities (full-length, Trunc1, 5-7). Although full-length GFP::HAM-1 was only weakly detected in some nuclei, Trunc7 staining was almost exclusively nuclear.

To determine whether a nuclear localization signal (NLS) is responsible for the observed HAM-1distribution, we analyzed the protein sequence with PSORTII, a computational tool that predicts protein-sorting signals in the amino acid sequence (Horton and Nakai, 1997). A putative NLS was identified in the C-terminal portion of HAM-1 at amino acids 321-327 (PTRRRAR). Due to the wide diversity of NLS motifs, however, *in silico* prediction methods are often limited in accuracy and coverage (Cokol et al., 2000). Thus, putative localization sequences must be experimentally verified.

Table 7 PLM defects are not rescued by myristoylated HAM-1 proteins

	# PLM neurons / side			
Strains	**0**	**1**	**2**	**N**
zdIs5 [a]	0%	100%	0%	200
zdIs5; ham-1(gm279)	81%	18%	1%	140
zdIs5; hkEx136 [b]	5%	94%	1%	106
zdIs5; ham-1(gm279); hkEx136	69%	31%	0%	106
zdIs5; hkEx137 [b]	1%	96%	4%	138
zdIs5; ham-1(gm279); hkEx137	67%	32%	1%	152
zdIs5; hkEx138 [b]	1%	99%	0%	106
zdIs5; ham-1(gm279); hkEx138	62%	39%	0%	122
zdIs5; hkEx141 [c]	11%	88%	2%	168
zdIs5; ham-1(gm279); hkEx141	83%	17%	0%	156
zdIs5; hkEx146 [d]	11%	89%	0%	108
zdIs5; ham-1(gm279); hkEx146	81%	19%	0%	144

[a] *zdIs5[mec-4::gfp]*
[b] *hkEx136, hkEx137, hkEx138 = [unc-119p-myr::gfp::ham-1-let-858-3'UTR]*
[c] *hkEx141 = [unc-119p-myr::gfp::Trunc5-let-858-3'UTR]*
[d] *hkEx146 = [unc-119p-myr::gfp::Trunc6-let-858-3'UTR]*

The role of PTRRRAR in nuclear targeting is partially supported by prior visualization of the HAM-1 truncations. As mentioned above, nuclear localization was observed in the first C-terminal truncation (Trunc1), but eliminated by removal of additional residues in Trunc2. Interestingly, the putative NLS sequence resides within this region, as shown in Figure 15. For additional validation of this targeting signal, we asked whether nuclear localization of Trunc7 would be disrupted upon deletion of these seven amino acids (Trunc7ΔNLS). Furthermore, we investigated the physiological relevance of nuclear targeting by functional analysis of full-length HAM-1 protein with this deletion (FLΔNLS).

3.2.4.1 PTRRRAR is partially responsible for nuclear localization of a HAM-1 truncation

A construct expressing Trunc7ΔNLS was injected into *zdIs5[mec-4::gfp]* hermaphrodites to generate transgenic animals (Table 3). Visualization of the exogenous product with anti-GFP antibodies revealed that the putative NLS sequence (PTRRRAR) was partially responsible for recruitment into the nucleus. In general, deletion of these seven residues resulted in delocalization of Trunc7 to the cytoplasm. However, some embryos retained variable levels of nuclear staining in a subset of the cells (Figure 19A). These results suggest that additional sequences may be involved in targeting HAM-1 to the nucleus.

3.2.4.2 Nuclear localization may be required for full functionality of the HAM-1 protein

Although the deletion of amino acids 321 to 327 did not completely abolish the nuclear localization of Trunc7, we examined whether it would be sufficient to disrupt the function of full-length HAM-1. Transgenic arrays expressing FLΔNLS were generated

(Table 3) and introduced into *zdIs5[mec-4::gfp]; ham-1(gm279)* animals. In the presence of two independent arrays, the 81% loss of PLM was reduced to 69% and 50%, respectively (Table 8, *hkEx153* and *hkEx154*). This rescue was evidently weaker than that observed for full-length GFP::HAM-1, which exhibited only 21% and 39% neuronal loss (Table 5, *hkEx42 and hkEx43*). Interestingly, expression of *hkEx154* in the wildtype background produced 17% loss of the PLM neuron, surpassing the dominant effects observed for any other extrachromosomal *ham-1* construct.

While deletion of the NLS should not impede HAM-1 function by affecting the peripheral protein distribution, we analyzed transgenic embryos with anti-GFP antibodies for verification. As shown in Figure 19B, FLΔNLS retained asymmetric localization at the cell cortex. Furthermore, examination of these embryos did not reveal weak nuclear staining that we previously observed for full-length GFP::HAM-1 (Figure 12C). Perhaps partial obstruction of nuclear targeting by the NLS deletion reduced signal levels below the limits of detection. Ultimately, results of these function and localization studies provide additional support for a nuclear role of HAM-1.

3.3 Potential interactions between HAM-1 and the Wnt Pathway

As a second approach to elucidate the mechanisms of HAM-1 function, we investigated its potential interactions with the Wnt pathway. Several preliminary studies have suggested that HAM-1 may interact with Wnt signalling components. Two homologs of the Dishevelled protein, DSH-1 and MIG-5, were isolated in a yeast-two-hybrid screen for HAM-1 binding partners (N. Hawkins, unpublished results). To examine the biological relevance of this physical association, DSH-1 and MIG-5 levels were knocked down individually, or in combination, by RNAi. The resulting animals did

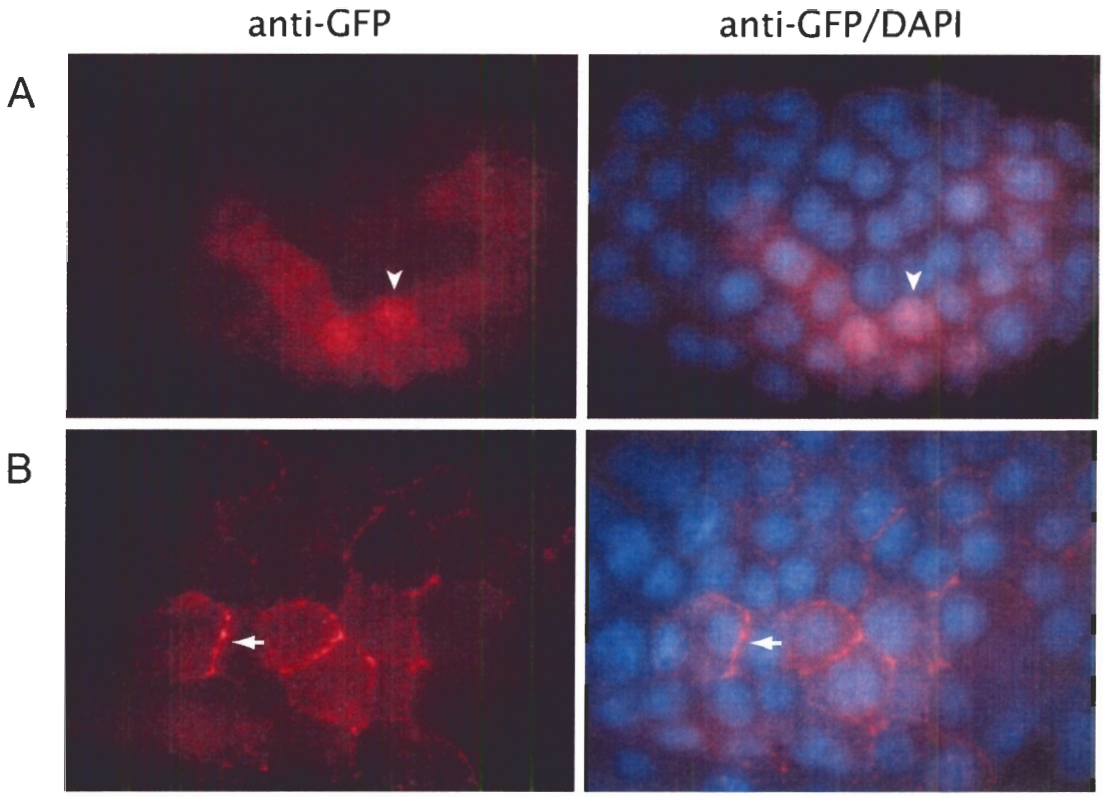

Figure 19 Subcellular localization of HAM-1 proteins with a putative NLS deletion

Fluorescence images of transgenic embryos stained with anti-GFP antibodies (red) and DAPI (blue). Embryos shown in this figure also express endogenous HAM-1. (A) GFP::Trunc7ΔNLS is primarily delocalized within the cytoplasm. Varying levels of nuclear staining is occasionally observed in some cells (arrowhead). (B) GFP::FLΔNLS is detected at the cell cortex. The protein can exhibit asymmetric localization (arrow). Staining in the *ham-1(gm279)* background produces similar results (data not shown)

Table 8 **Deletion of a putative NLS from full-length HAM-1 reduced rescue of the PLM neuron**

	# PLM neurons / side			
Strains	**0**	**1**	**2**	**N**
zdIs5 [a]	0%	100%	0%	200
zdIs5; ham-1(gm279)	81%	18%	1%	140
zdIs5; hkEx153 [b]	5%	94%	1%	156
zdIs5; ham-1(gm279); hkEx153	69%	31%	0%	120
zdIs5; hkEx154 [b]	17%	81%	2%	190
zdIs5; ham-1(gm279); hkEx154	50%	49%	1%	130

[a] *zdIs5 = [mec-4::gfp]*
[b] *hkEx153, hkEx154 = [unc-119p-gfp::ham-1ΔNLS-let-858-3'UTR]*

not exhibit defects in the PHB lineage (N. Hawkins, unpublished results), which is known to be disrupted by the loss of HAM-1 function. However, mutations in other components of the Wnt pathway, *apr-1* (APC) and *pop-1* (TCF/LEF), resulted in 30% and 8% PHB loss, respectively (Roh, 2004). In contrast, *ham-1* mutants produced extra PHB neurons by a cell fate transformation (Figure 5D). If HAM-1 interacts with this pathway for general regulation of asymmetric divisions, then other HAM-1-dependent lineages may also show sensitivity to Wnt signaling mutations. Thus, we probed for evidence of this relationship using the PLM neuron.

3.3.1 Determining the division affected by *ham-1* in the PLM lineage

Unfortunately, details of the PLM lineage defects have not been well characterized in *ham-1* alleles. In particular, the precise division disrupted by lack of HAM-1 activity remains ambiguous. Thus, before investigating the involvement of Wnt signals in PLM production, we attempted to determine where HAM-1 functions in this lineage. As shown in Figure 20, the loss of PLM neurons in *ham-1* mutants may be attributed to cell fate transformations at various divisions. For example, defects in division 3 may induce PLM to adopt the fate of its sister cell, resulting in a duplication of the ALN neuron (Figure 20B). To investigate this possibility, ALN was visualized by an integrated GFP reporter, *ncIs1[eat-20::gfp]* (Shibata et al., 2000). Due to weak GFP expression at the L1 stage, our analyses were performed on late larval animals. In the wildtype control, a single neuron was consistently detected on each side of the tail (100%, N=110). Conversely, *ham-1(gm279)* mutants exhibited frequent neuronal loss (67% loss, N=116). These results contradict the predictions of a cell fate transformation at the final

division; however, they are consistent with potential transformations at division 1 or 2 (Figure 20C,D).

An apoptotic cell is generated from both upstream divisions of the wildtype PLM lineage (divisions 1 and 2). Disruption of either division may produce neuronal loss by inappropriately triggering death of the non-apoptotic daughter cell (Figure 20C,D). Such defects are potentially rescued by inhibition of programmed cell death. During the development of wildtype hermaphrodites, 131 cells are fated to die. Each cell death can be prevented by disrupting one of two essential pro-apoptotic genes, *ced-3* (Caspase-3) or *ced-4* (Apaf-1) (Liu and Hengartner, 1999). Introduction of the PLM marker into *ced-4(n1162)* mutants revealed a 23% neuronal duplication in the absence of apoptosis (Table 9). Remarkably, the 81% PLM loss observed for *ham-1(gm279)* was strongly suppressed in a double mutant with *ced-4(n1162)*. These results support the model whereby HAM-1 acts at asymmetric division 1 or 2 to ensure that a single daughter cell undergoes programmed cell death. In the future, lineage analysis can be performed to determine whether the additional cell corpse appears after division 1 (300 minutes) or division 2 (395 minutes).

3.3.2 Effects of *apr-1* in the PLM lineage

As mentioned previously, mutations in *apr-1* and *ham-1* generated opposing defects in the PHB lineage. To investigate APR-1 function in the PLM lineage, *zdIs5[mec-4::gfp]* was introduced into the *apr-1(zh10)* null mutant. Because this allele of *apr-1* results in zygotic embryonic/larval lethality (Hoier et al., 2000), it was maintained with the translocation balancer *hT2[qIs48] (I;III)* (McKim et al., 1993). We

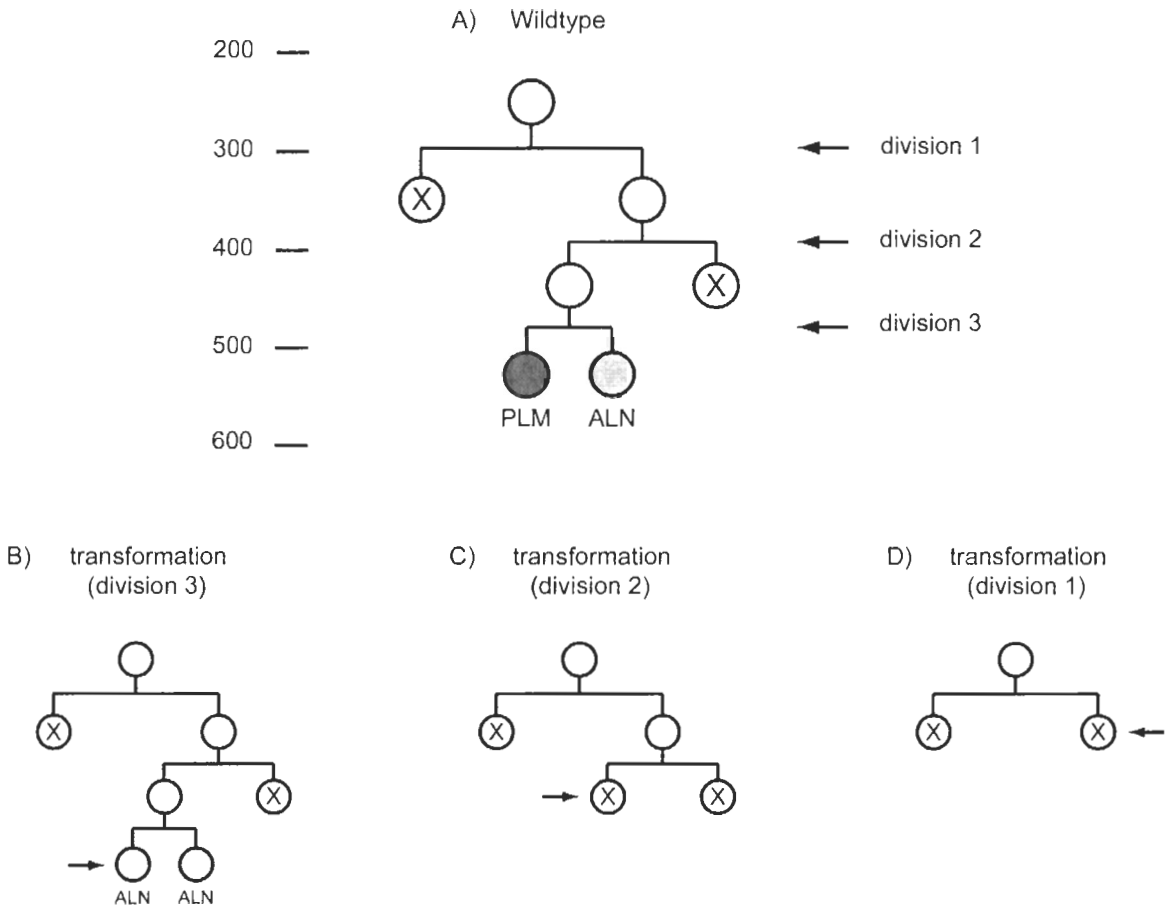

Figure 20 Potential cell fate transformations resulting in PLM loss

(A) Wildtype PLM lineage. Time scale is shown in minutes from first cleavage of the zygote. Division 1 occurs at 300 minutes to produce an anterior daughter that undergoes apoptosis and a posterior neuroblast. The posterior daughter divides again at 395 minutes (division 2), forming the PLM/ALN precursor and a posterior apoptotic cell. Division 3 occurs at 480 minutes to generate the PLM and ALN neurons. (B to D) Potential cell fate transformations that can result in PLM loss observed in *ham-1* mutants.

Table 9 Suppression of PLM loss in *ham-1* mutants by *ced-4*

	# PLM neurons / side			
Strains	**0**	**1**	**2**	**N**
zdIs5 [a]	0%	100%	0%	200
zdIs5; ham-1(gm279)	81%	18%	1%	140
zdIs5; ced-4(n1162)	0%	77%	23%	124
zdIs5; ced-4(n1162); ham-1(gm279)	10%	83%	7%	166

[a] *zdIs5 = [mec-4::gfp]*

examined PLM defects in *apr-1(zh10) [m+z-]* progeny that survived to the L1 stage. As shown in Table 10, the loss of APR-1 function generated 34% PLM duplication, 3% of which exhibited more than two neurons. Since 81% loss was observed for the *ham-1(gm279)* allele, *apr-1* and *ham-1* mutants also demonstrated opposing phenotypes in the PLM lineage. Analysis of the double mutant revealed a reduction in the neuronal loss, from 81% down to 26%. In contrast, the PLM duplication observed in *apr-1(zh10)* was not suppressed by loss of HAM-1 activity.

To determine whether APR-1 and HAM-1 function at the same division in the PLM lineage, we examined genetic interactions between *apr-1* and *ced-3* mutants. As described above, *ham-1* alleles may generate PLM loss by cell fate transformations at division 1 or 2 (Figure 20C,D). If the loss of APR-1 produces extra PLM neurons by a reciprocal transformation (Figure 21C,D), then the penetrance of these defects may be enhanced by inhibiting cell death. A similar situation had been observed in the PHB lineage, as neuronal duplications nearly attained complete penetrance when *ham-1* mutants were introduced into a *ced-3* background (Guenther and Garriga, 1996). These results indicate that cell fate transformations were often undetected due to a competing signal for cell death.

Prevention of apoptosis by the *ced-3(n717)* allele generated 6% PLM duplications in *apr-1(zh10)/hT2[qIs48]* heterozygotes (Table 10). Because the lack of zygotic APR-1 resulted in 34% duplication, the absence of genetic interactions would predict a 40% PLM defect in *apr-1; ced-3* double mutants. A comparable frequency was experimentally observed, suggesting that additional PLM precursor cells have not been masked by cell death. Unfortunately, this negative result does not preclude APR-1

Table 10 PLM defects in *ham-1* and Wnt pathway mutants

	# PLM neurons / side				
Strains	**0**	**1**	**2**	**3**	**N**
zdIs5 [a]	0%	100%	0%	0%	200
zdIs5; ham-1(gm279)	81%	18%	1%	0%	140
apr-1(zh10)/hT2 [b] *zdIs5*	0%	100%	0%	0%	124
apr-1(zh10) zdIs5	1%	65%	31%	3%	128
apr-1(zh10)/hT2 zdIs5; ham-1(gm279)	66%	33%	1%	0%	246
apr-1(zh10) zdIs5; ham-1(gm279)	26%	30%	34%	9% [c]	224
apr-1(zh10)/hT2 zdIs5; ced-3(n717)	0%	95%	5%	1%	128
apr-1(zh10) zdIs5; ced-3(n717)	1%	55%	40%	5%	124
lin-17(n671) zdIs5	0%	80%	19%	1%	138
lin-17(n671) zdIs5; ham-1(gm279)	79%	16%	5%	0%	122

[a] *zdIs5 = [mec-4::gfp]*
[b] balancer *hT2[qIs48] (I;III)*
[c] Two incidences of 4 PLM neurons per side were observed

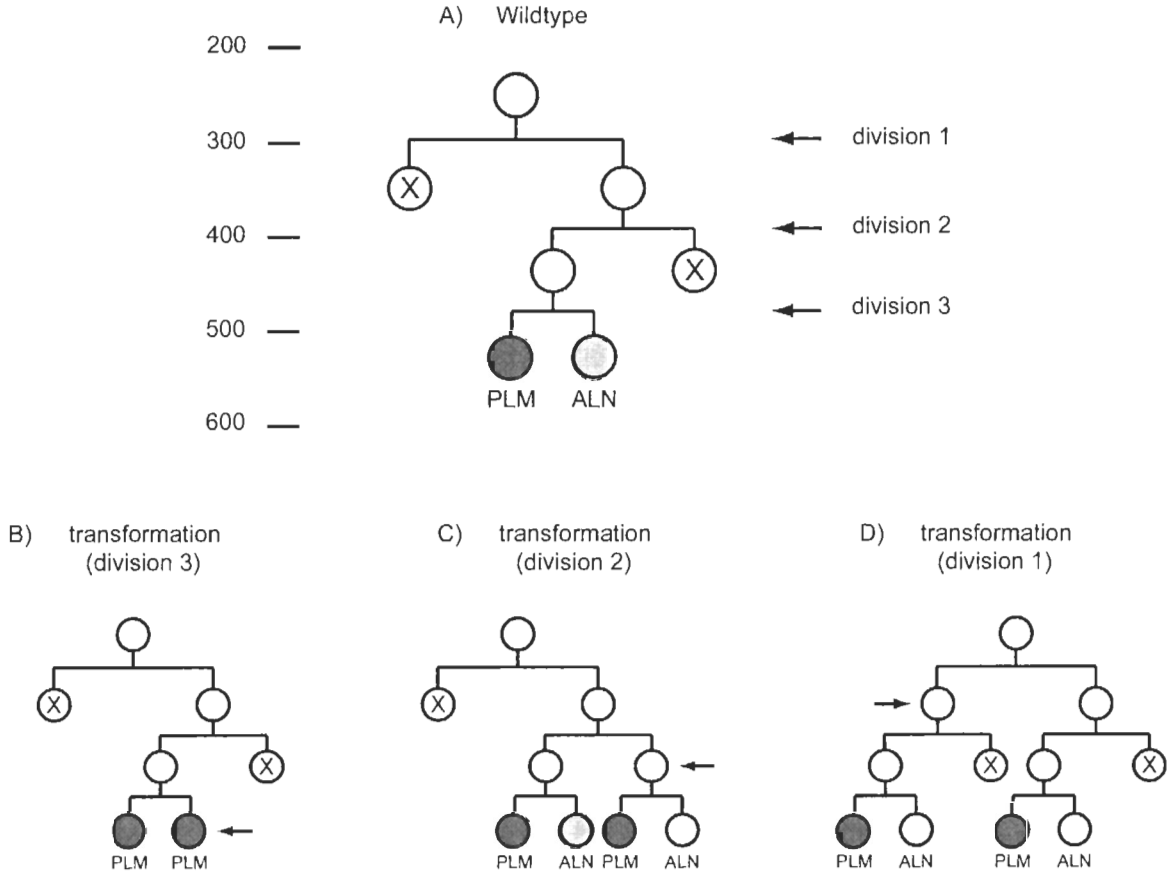

Figure 21 Potential cell fate transformations resulting in PLM duplication

(A) Wildtype PLM lineage. Time scale is shown in minutes from first cleavage of the zygote. Division 1 occurs at 300 minutes to produce an anterior daughter that undergoes apoptosis and a posterior neuroblast. The posterior daughter divides again at 395 minutes (division 2), forming the PLM/ALN precursor and a posterior apoptotic cell. Division 3 occurs at 480 minutes to generate the PLM and ALN neurons. (B to D) Potential cell fate transformations that can result in PLM duplication observed in *apr-1* or *lin-17* mutants.

function at division 1 or 2. Future examination of the ALN neuron may help elucidate the role of APR-1 in this lineage.

3.3.3 Effects of *lin-17* in the PLM lineage

To further investigate potential interactions between HAM-1 and the Wnt pathway, we probed for PLM defects in *lin-17* mutants. This gene encodes a *C. elegans* homolog of the Wnt receptor protein Frizzled. Examination of the *lin-17(n671)* null allele (Sawa et al., 1996) revealed the presence of extra PLM neurons at a 20% frequency (Table 10). Our results are consistent with a recent publication that also reported the neuronal duplication (Hilliard and Bargmann, 2006). Furthermore, the authors observed a loss of the sister cell ALN, suggesting that the absence of LIN-17 function may induce a cell fate transformation at the final division of this lineage (division 3, Figure 21B).

In contrast with previous *apr-1* results, the *lin-17* allele did not suppress PLM loss in *ham-1* mutants. As shown in Table 10, *lin-17(n671); ham-1(gm279)* exhibited 80% loss and 5% duplication of this neuron. These observations may be explained by the additive effects of each single mutant, producing cell fate transformations at different points in the PLM lineage.

As discussed above, lack of HAM-1 function may disrupt division 1 or 2 to induce 81% death of the non-apoptotic cell and the consequent loss of PLM (Figure 20C,D). In these animals, the effects of *lin-17* are concealed since division 3 does not occur. The remaining 19% of the population retain the PLM/ALN precursor cell. In the absence of LIN-17 activity, division of this cell generates an extra PLM neuron at 20% frequency. In the total population, this amounts to approximately 4% PLM duplication.

The neuronal defects observed in the *lin-17; ham-1* double mutant (80% loss and 5% duplication) are compatible with these theoretical predictions; thus, HAM-1 and LIN-17 appear to function independently at distinct divisions of this lineage.

CHAPTER 4: DISCUSSION

HAM-1 is a novel asymmetrically localized protein involved in many neuroblast divisions during *C. elegans* embryogenesis. In this study, we have taken two main approaches to investigate the mechanisms of HAM-1 activity. A serial truncation analysis was first performed to identify localization and function domains of this novel protein. Furthermore, we investigated potential interactions between HAM-1 and members of the Wnt signalling pathway.

4.1 *unc-119p* enables rescue of *ham-1* defects by GFP::HAM-1

Ideally, expression of full-length and truncated GFP::HAM-1 proteins would be driven by the endogenous *ham-1* promoter. However, prior experiments to identify these regulatory sequences have been unsuccessful (N. Hawkins, unpublished results). To circumvent this problem, we used a heterologous promoter, *unc-119p*. As previously mentioned, HAM-1 expression is first detected at the onset of gastrulation (28-cell stage), and persists in many neuronal lineages throughout embryogenesis (Guenther and Garriga, 1996). Likewise, UNC-119 is expressed pan-neuronally beginning at the 60-cell stage (Maduro and Pilgrim, 1995). Our studies confirmed that full-length GFP::HAM-1 under the control of *unc-119p* can partially rescue PHB and PLM neuronal defects in *ham-1* mutants. The rescuing ability was especially evident in the PLM lineage, which was chosen for subsequent functional analysis of the HAM-1 truncations.

Although the levels of PHB duplication and PLM loss were reduced by the expression of GFP::HAM-1, we also observed a moderate enhancement of the opposing phenotype. Particularly, the integrated array *hkIs39* produced extra PLM neurons at a 24% frequency. This may be attributed to overexpression of the full-length construct by the DNA concatemers. For example, in the *Drosophila* peripheral nervous system, a wildtype level of Numb is essential for asymmetric division of the sensory organ precursor (SOP) to produce pIIa and pIIb. Loss of *numb* function results in a symmetric division that generates two pIIa cells, whereas heat shock-induced overexpression of the protein results in the reciprocal transformation (Rhyu et al., 1994). An alternative explanation for the observed PLM duplication is the use of a heterologous promoter; *unc-119p* may ectopically express the full-length construct in cells that do not normally exhibit HAM-1 function. Nonetheless, this promoter was adequate for the purposes of our functional analyses, as it allowed strong rescue of the PLM neuronal loss by exogenous full-length HAM-1.

4.2 *ham-1 3'-UTR* is not required in asymmetric protein localization

Asymmetric protein distribution often involves prior localization of the mRNA by its 3'-UTR elements (reviewed in Bassell et al., 1999; Shav-Tal and Singer, 2005). During *Xenopus* development, the transforming growth factor-β (TGFβ) protein Vg1 is involved in endoderm and mesoderm formation (Joseph and Melton, 1998). The maternally supplied Vg1 mRNA is tightly restricted to the vegetal cortex of the oocyte (Melton, 1987). Studies revealed that the localization and translational control of this transcript are both mediated by regions of the 3'-UTR (Mowry and Melton, 1992; Wilhelm et al., 2000). Similarly, axis formation in *Drosophila* is also highly dependent

on asymmetric RNA regulation. For example, the Bicoid protein exhibits an anterior-to-posterior gradient in the embryo. This distribution pattern requires prior recruitment of the transcript to the anterior pole (Ferrandon et al., 1994; St Johnston et al., 1989). In contrast, the Nanos protein forms a posterior-to-anterior gradient, which primarily involves localized mRNA translation (Bergsten and Gavis, 1999). Both of these processes also require cis-acting elements in the 3'-UTR.

Conversely, asymmetric distribution of HAM-1 is likely not dependent on local accumulation or translation of the mRNA. Visualization of GFP::HAM-1 revealed asymmetric cortical localization regardless of whether the *let-858* or *ham-1* 3'-UTR was used. However, these results do not necessarily preclude a non-uniform distribution of the transcript in wildtype embryos. In the *Drosophila* central nervous system, neuroblasts divide along the apical-basal axis to regenerate a neuroblast and produce a ganglion mother cell (GMC). The transcription factor Prospero and its mRNA are targeted to the basal cortex during mitosis and segregate into the GMC (Hirata et al., 1995; Li et al., 1997). Transcript localization was shown to be a redundant mechanism, as GMC development was not affected by disruption of this process (Broadus et al., 1998). To determine whether *ham-1* mRNA is also unevenly distributed, *in situ* hybridization studies can be performed. However, our results indicate that transcript localization is not a prerequisite for asymmetric accumulation of HAM-1.

4.3 Sequences involved in peripheral localization of HAM-1

To determine the protein sequences responsible for wildtype HAM-1 distribution, we analyzed a series of N-terminal and C-terminal truncations. Asymmetric peripheral localization was only evident for Trunc1, containing amino acids 1-364. Removal of

additional sequences from the C-terminus (Trunc2, amino acids 1-268) qualitatively disrupted protein asymmetry, despite the persistence of cortical association. These results suggest that a region between residues 269-364 may be involved in asymmetric localization. To confirm this observation, future studies should examine additional transgenic lines that express Trunc2 (Table 3). Furthermore, the asymmetric distribution of this truncation should be quantitatively compared with full-length HAM-1. Endogenous HAM-1 crescents are mainly observed in cells that are undergoing division (Guenther and Garriga, 1996). Protein asymmetry could be quantitated specifically in mitotic cells by co-staining with markers such as anti-phospho-histone H3 antibodies.

Previous investigation of the missense allele *ham-1(n1811)* revealed the importance of amino acid 47 for cortical association. The mutant HAM-1(G47D) protein was primarily delocalized throughout the cytoplasm (Frank et al., 2005; Guenther and Garriga, 1996). From our deletion analysis, Trunc2 (amino acids 1-268) was the smallest protein fragment that was sufficient for localization to the periphery. Deletion of the first 31 N-terminal residues resulted in diffused cytoplasmic staining (Trunc5, amino acids 32-414). Further truncation from the C-terminus in Trunc3 (amino acids 1-168) also delocalized the protein. These observations suggest the existence of a large localization domain encompassing almost two-thirds of the entire protein. Interestingly, Trunc3 removed a C-terminal portion of the winged-helix domain (amino acids 94-180). Future studies can investigate whether a construct that extends from the N-terminus to the end of this domain would be sufficient for peripheral localization. Alternatively, sequences necessary for cortical association may be present in two distinct regions, residing at the

N-terminus and near the middle of the protein (between Trunc2 and Trunc3), respectively. Analysis of internal deletions will be required to further define the localization domains.

4.4 HAM-1 function is disrupted in N- and C-terminal truncations

To identify the functional regions of HAM-1, we examined the ability of each truncation to rescue PLM lineage defects in *ham-1* mutants. Unfortunately, the loss of PLM neurons was not evidently reduced by any of the eight deletion constructs. The lack of rescue by the C-terminal truncations had been predicted from several prior observations. A mutant protein encoded by *ham-1(gm214)* contains a 21 amino acid deletion (Δ369-389) that eliminates HAM-1 function (Frank et al., 2005). This protein region was also absent from each C-terminal truncation (Figure 15). Moreover, the importance of the C-terminus was demonstrated by a previous study examining HAM-1::GFP fusion proteins. GFP coding sequences were inserted before the translational stop codon of a *ham-1* genomic construct. Due to the placement of GFP, the resultant chimeric protein lacked the final four amino acids of HAM-1. This fusion product was also shown to be non-functional, suggesting these residues may be essential for protein activity (C. Guenther, unpublished results). Alternatively, function may be disrupted by an indirect mechanism; for example, HAM-1 protein folding may be affected by fusion of GFP sequences to its C-terminus.

Interestingly, the four final amino acids of HAM-1 (ISNL) comprise a putative binding site for PDZ domains (predicted by ELM, the Eukaryotic Linear Motif server). These domains are highly prevalent protein interaction modules that have been conserved throughout evolution. As reviewed by van Ham and Hendriks (2003), PDZ proteins exhibit important roles in the scaffolding and targeting of their associated partners. Since

the C-terminal truncation Trunc1 (amino acids 1-364) retained wildtype crescent staining patterns, the PDZ recognition sequence is not required for asymmetric localization to the cell cortex. However, this motif may mediate protein interactions that are essential for HAM-1 activity. To further investigate the importance of PDZ binding, future experiments can alter this recognition sequence by site-directed mutagenesis.

Functional analysis of the N-terminal truncations also revealed an inability to rescue. To determine whether this was a secondary consequence of cortical delocalization, we targeted truncations to the plasma membrane by a myristoylation sequence. Although the modification partially recruited proteins to the cell periphery, a considerable level of delocalized staining was still observed. Indeed, myristoylated proteins often exhibit weak and reversible membrane associations; these interactions can be stabilized by the presence of a basic amino acid patch or a second lipid moiety (Resh, 1999).

More effective methods of membrane anchoring were not pursued, however, as full-length GFP::HAM-1 function was unexpectedly disrupted by myristoylation. We do not expect the lipidation signal to affect protein structure since it was added to the N-terminus of GFP. Plausibly, this post-translational modification altered the subcellular localization pattern of GFP::HAM-1. By embryo staining, we established that myristate did not prevent asymmetric distribution of the full-length protein. However, if HAM-1 normally exhibits dynamic redistribution and dissociates from the cell cortex, then the weak membrane anchor would be expected to hinder its activity. Although this is consistent with a potential role of HAM-1 in the nucleus (discussed below), we did not observe impaired nuclear targeting of the myristoylated proteins. Nonetheless, because

our studies were not quantitative, the functional defects may be caused by an undetected reduction of nuclear protein levels. Alternatively, insertion of the myristoyl moiety into the lipid bilayer may incorrectly orient HAM-1 at the cell cortex, thus preventing its interactions with other proteins.

4.5 Potential role of HAM-1 in the nucleus

4.5.1 Visualization of full-length and truncated HAM-1

Several of our observations revealed a potential nuclear role of HAM-1. Most importantly, we detected HAM-1 protein in the nucleus, which has not been observed in previous studies. Although this localization was weak and sporadic for full-length GFP::HAM-1, other truncations revealed various levels of nuclear staining. In particular, Trunc7 was almost completely targeted to the nucleus.

Previous visualization of endogenous HAM-1 may not have revealed this localization for several reasons. Perhaps HAM-1 is not targeted to the nucleus in wildtype embryos, and our observations were simply artifacts of overexpression. Conceivably, a high level of GFP::HAM-1 may enhance passive diffusion through the nuclear pores, enabling subsequent accumulation of the protein in the nucleus by an unidentified mechanism. Alternatively, because full-length HAM-1 was controlled by a heterologous promoter, nuclear localization may have been observed in cells that do not normally express the endogenous protein. However, we detected Trunc7 in the nucleus of all expressing cells, which does not support this hypothesis. A more intriguing possibility is that HAM-1 truly exhibits a nuclear function. In wildtype embryos, protein levels in the nucleus may be tightly regulated and fall below the limits of detection;

overexpression of the full-length protein in our experiments revealed this localization. Interestingly, Trunc7 was almost exclusively nuclear, suggesting that it may lack regulatory sequences that prevent accumulation of HAM-1 in the nucleus.

4.5.2 Identification of an NLS sequence

Consistent with active nuclear localization of HAM-1, an NLS signal (PTRRRAR) was predicted by PSORTII analysis. We confirmed this *in silico* prediction by deleting the sequence from Trunc7. The resulting protein exhibited decreased localization to the nucleus, suggesting that PTRRRAR may cooperate with other sequences for nuclear targeting of HAM-1. To explore the functional requirement of this localization, we created a similar mutation in the full-length protein (FLΔNLS). Although HAM-1 activity was not completely abolished, FLΔNLS exhibited a weaker ability to rescue PLM lineage defects. The incomplete reduction of protein function may be attributed to the low levels of nuclear localization that persist despite the absence of the NLS sequence.

4.5.3 Prediction of a putative winged-helix domain

Additional support for a nuclear role of HAM-1 originates from sequence homology analysis. Comparison of the HAM-1 sequence to protein domain databases by InterProScan (Mulder et al., 2005) identified a putative winged-helix motif near the N-terminus (amino acids 94-180). A winged-helix is a variant of the helix-turn-helix domain that often mediates DNA binding. It is present in numerous proteins involved in transcriptional regulation, DNA replication and repair (reviewed in Aravind et al., 2005). Occasionally, these motifs are adapted for RNA or protein associations; however, such functions are only exhibited in a small subset of the protein family. Future experiments

can investigate the ability of HAM-1 to bind DNA, using methods such as chromatin immunoprecipitation.

4.5.4 Future experiments to investigate the nuclear role of HAM-1

4.5.4.1 Nuclear localization signals

As discussed above, the residual rescuing ability of FLΔNLS may be due to incomplete delocalization from the nucleus. Accordingly, future investigations should examine the protein function upon abolishment of nuclear targeting. NLS sequences are typically enriched in basic amino acids (Hicks and Raikhel, 1995). Aside from PTRRRAR, a second basic segment (RRR) is located at position 288-290. Numerous bipartite NLS motifs have been identified, containing two short stretches of basic residues interrupted by a spacer region. In general, 10-12 amino acids are present in this intervening sequence (Hicks and Raikhel, 1995). However, previous studies reported an atypical linker that was 29 residues in length (Moore et al., 1998). In HAM-1, the two basic clusters are separated by 30 amino acids. Mutation of the second basic segment in Trunc7ΔNLS could determine its contribution to nuclear localization. If the resulting protein is fully delocalized, this modification can be performed in the context of FLΔNLS to determine if the rescuing ability would be completely eliminated.

Although the lack of rescue may be attributed to nuclear delocalization, the mutations may also disrupt protein activity by other mechanisms. For example, the modifications may affect the overall protein structure, or specific interaction sites for other molecules. To account for these possibilities, a bona fide NLS from the SV40 large T antigen (Kalderon et al., 1984) can be added onto the mutated protein to determine if nuclear localization and function can be concurrently restored. However, as discussed

previously, HAM-1 levels in the nucleus might be tightly regulated. The addition of a strong NLS may induce excessive nuclear targeting. Thus, optimization of the DNA concentration injected may be required to produce rescue of the PLM neuron. Conversely, an SV40 NLS can be added onto functional full-length HAM-1 to deliberately induce nuclear accumulation. Resulting penetrant defects in HAM-1 dependent lineages may also be indicative of protein activity in the nucleus.

4.5.4.2 14-3-3 proteins

Cytoplasmic-nuclear shuttling can be modulated by 14-3-3 proteins (Muslin and Xing, 2000). This highly conserved protein family interacts with components involved in numerous cellular processes (van Heusden, 2005). The associations are mediated through phosphoserine/threonine consensus motifs, and result in the regulation of target proteins by various mechanisms (Bridges and Moorhead, 2005). A common consequence of 14-3-3 binding is the physical occlusion of signal sequences. The FOXO transcription factors contain a non-classical NLS that coincides with the C-terminus of the DNA binding (winged-helix) domain. A 14-3-3 recognition sequence within this NLS is involved in protein delocalization from the nucleus (Van Der Heide et al., 2004). Interestingly, a second binding site is located upstream of the winged-helix module, which enables 14-3-3 to associate with FOXO proteins as stable dimers. This interaction prevents DNA binding, presumably by sequestration of the winged-helix domain (Obsil et al., 2003).

The HAM-1 sequence contains three putative 14-3-3 binding sites (predicted by ELM analysis, Figure 22). The first motif is detected in the winged-helix module, at

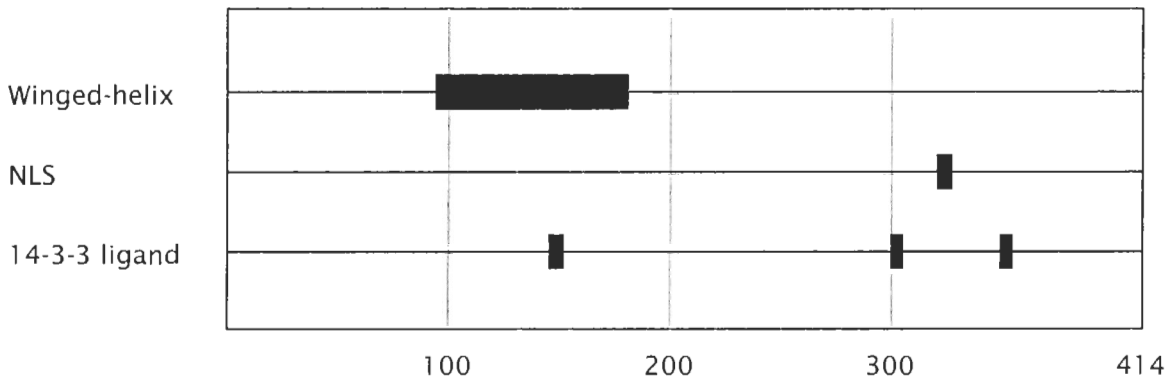

Figure 22 Putative 14-3-3 binding sites in HAM-1

Three putative 14-3-3 binding sites were predicted in the HAM-1 sequence by ELM analysis: RQTITSL (residues 146-152); KLLSSS (residues 300-305); HTDSNE (residues 350-355). The first motif resides within the putative winged-helix domain (residues 94-180), while the remaining sites flank the NLS sequence (PTRRRAR – residues 321-327).

amino acids 146-152. The remaining sequences are within a C-terminal region of the protein, at positions 300-305 and 350-355, respectively. The locations of each motif suggest their potential involvement in cytoplasmic-nuclear shuttling of HAM-1. As discussed previously, Trunc5 and Trunc6 resulted in cortical delocalization. However, the proteins were primarily distributed within the cytoplasm, suggesting that loss of peripheral association does not inevitably lead to nuclear accumulation. In contrast, a high level of Trunc7 was detected in the nucleus. The first 14-3-3 binding site resides between the endpoints of Trunc6 and Trunc7; thus, it may be responsible for modulating the nuclear levels of HAM-1. The two C-terminal motifs flank the NLS sequence (PTRRRAR, amino acids 321-327). Accordingly, they may mediate interactions with 14-3-3 dimers to mask the localization signal. However, both of these binding sites were retained in Trunc7, which was almost completely nuclear. Thus, this C-terminal region is either not sufficient for association with 14-3-3 dimers, or the resulting interaction does not obstruct nuclear targeting.

Future studies can investigate the involvement of 14-3-3 proteins in HAM-1 subcellular distribution. The three consensus sequences can be disrupted individually, or in combination, by site-directed mutagenesis. These modifications are ideally performed on Trunc5 or Trunc6, as they are no longer restricted at the cell cortex. A resultant increase in nuclear protein levels would suggest that HAM-1 undergoes cytoplasmic-nuclear translocation, mediated by 14-3-3 interactions.

Alternatively, the role of each *C. elegans* 14-3-3 protein can be directly examined. Previous investigations identified two isoforms, FTT-1/PAR-5 and FTT-2, which share 90% sequence similarity (Wang and Shakes, 1997). FTT-1/PAR-5 is required for

asymmetric division of the zygote. Disruption of its activity by mutation or RNAi results in mislocalization of the other PAR proteins (Morton et al., 2002). Interestingly, FTT-1/PAR-5 is also involved in regulation of nuclear POP-1 levels in the EMS daughter cells. Wnt/MAPK signalling induces phosphorylation of POP-1 in the E blastomere, this promotes its interaction with the 14-3-3 protein, ultimately leading to delocalization from the nucleus (Lo et al., 2004). Similarly, FTT-2 was recently implicated in the *daf-2*/insulin-like signalling pathway. In response to the DAF-2 signal, FTT-2 negatively regulates the transcription factor DAF-16 (FOXO) by its retention in the cytoplasm (Li et al., 2006; Lin et al., 2001). To determine if these 14-3-3 isoforms also prevent nuclear accumulation of HAM-1, the distribution Trunc5 and Trunc6 can be examined upon reduction of FTT levels by RNAi. Moreover, future studies can examine whether knockdown of 14-3-3 isoforms also disrupts neuronal lineages dependent on HAM-1.

4.5.5 Other proteins with cortical and nuclear localization

Our studies indicate that HAM-1 may exhibit both cortical and nuclear localization. Interestingly, similar distribution patterns have been reported for several other proteins. As mentioned above, Prospero is restricted to the basal cortex of mitotic *Drosophila* CNS neuroblasts; this localization is mediated by the adaptor protein Miranda. Both components are segregated into the GMC daughter cell, where Prospero subsequently dissociates from Miranda and translocates into the nucleus (Ikeshima-Kataoka et al., 1997; Spana and Doe, 1995). Specification of the GMC fate requires Prospero-dependent induction and repression of various target genes (Doe et al., 1991; Vaessin et al., 1991).

Unlike Prospero, endogenous HAM-1 has not been detected in the nucleus (Guenther and Garriga, 1996). Notch exemplifies a protein that is typically detected at the cell periphery, yet performs a nuclear function. The Notch family of single-pass transmembrane receptors regulate many cell fate decisions during development (Artavanis-Tsakonas et al., 1999). Interactions with membrane-bound ligands (Delta and Jagged/Serrate proteins) induce a sequence of proteolytic cleavages that release the intracellular domain of Notch. This fragment enters the nucleus, where it interacts with the DNA-binding protein CSL (CBF1/Suppressor of Hairless/Lag-1) to activate transcription of target genes (reviewed in Weinmaster, 2000). Although the nuclear role of Notch is now well established, it was slow to gain acceptance because endogenous protein levels in the nucleus were below the limits of detection (Struhl and Adachi, 1998). However, nuclear staining could be observed when a high concentration of Notch DNA was transfected into mammalian cells (Schroeter et al., 1998). Similarly, our studies revealed nuclear localization of HAM-1 upon overexpression.

4.6 Possible interactions with the Wnt pathway

As a second approach to investigate HAM-1 function, we explored its potential associations with the Wnt pathway. The first indication of this interaction originated from a yeast-two-hybrid screen that revealed DSH-1 and MIG-5 as binding partners of HAM-1 (N. Hawkins, unpublished results). Although knockdown of these proteins by RNAi did not produce PHB neuronal defects (N. Hawkins, unpublished results), this lineage was disrupted by mutations in other components of the Wnt pathway (Roh, 2004). Our studies demonstrate a requirement for Wnt signalling genes in a second HAM-1-dependent lineage, one that generates the PLM neuron. The preliminary data supporting

potential interactions between HAM-1 and the Wnt pathway in these neuronal lineages are presented below.

4.6.1 The PHB lineage

In the PHB lineage, absence of HAM-1 function primarily results in the duplication of HSN and PHB neurons (Guenther and Garriga, 1996). This is attributed to asymmetric division defects of the HSN/PHB neuroblast. The anterior daughter, which typically undergoes apoptosis, adopts the fate of its sister cell – the HSN/PHB precursor (Figure 5D). In contrast, mutations in two Wnt signalling components, *apr-1* (APC) and *pop-1* (TCF/LEF), produced a loss of the PHB neuron (Roh, 2004). *apr-1* was found to be epistatic to *ham-1* as the double mutant primarily exhibited PHB neuronal loss (Roh, 2004).

To further investigate the opposing phenotypes of *apr-1* and *ham-1*, other lineally related cells have been examined. Disruption of APR-1 function also produced a loss of HSN, suggesting defective formation of the HSN/PHB precursor (Roh, 2004). This may be caused by a cell fate transformation opposite to that observed in *ham-1* mutants, where the posterior daughter of the HSN/PHB neuroblast adopts the anterior apoptotic fate (Figure 23B). Alternatively, division defects could occur earlier in the PHB lineage, such that the HSN/PHB neuroblast is transformed into its sister cell – the PVQ neuroblast (Figure 23C). However, contrary to predictions of the latter model, *apr-1* alleles did not exhibit extra PVQ neurons (N. Hawkins, unpublished results). To confirm whether *apr-1* and *ham-1* mutants produce reciprocal cell fate transformations, embryos lacking APR-1 activity can be examined for the extra cell corpse by Nomarski microscopy.

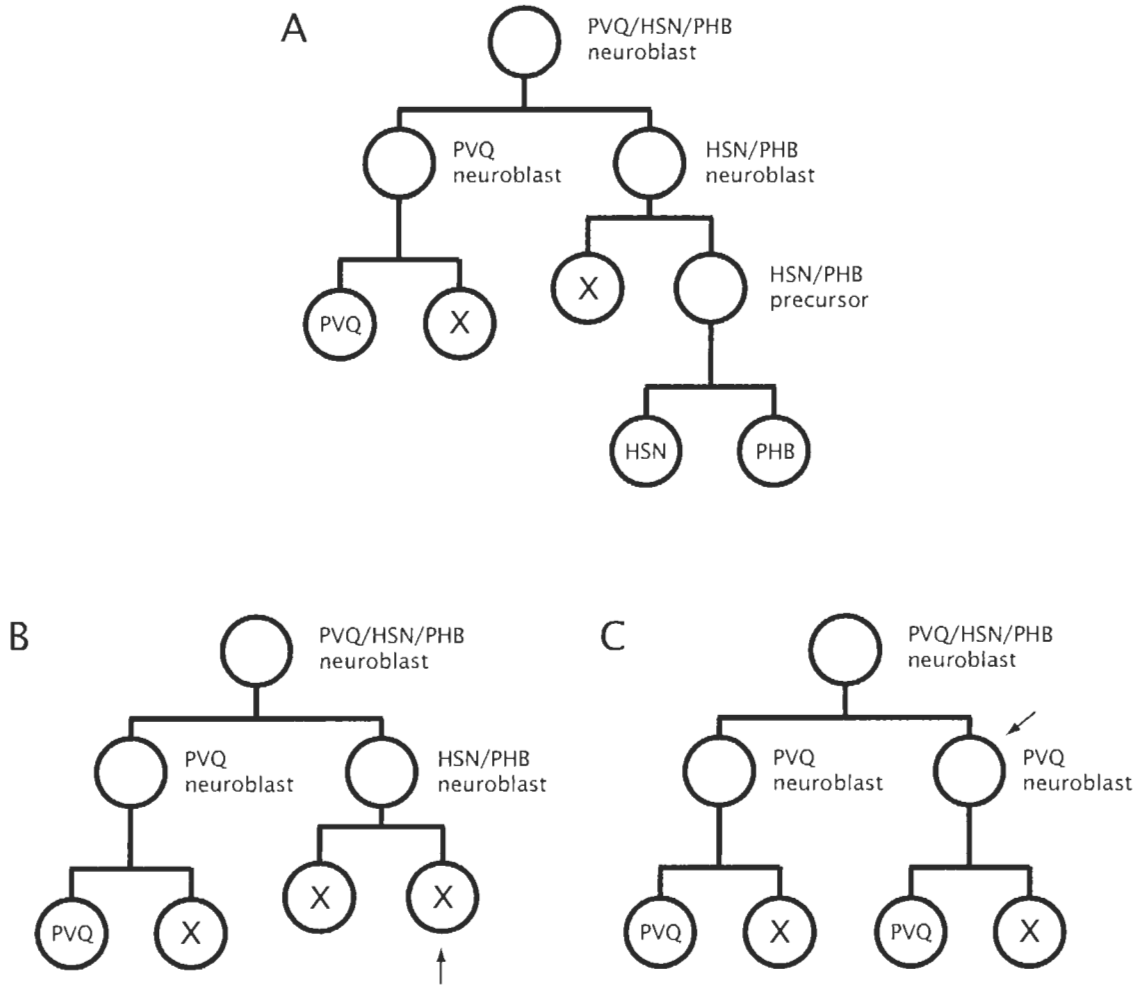

Figure 23 Potential cell fate transformations resulting in loss of HSN and PHB

(A) In wildtype embryos, the PVQ/HSN/PHB neuroblast divides asymmetrically to produce the PVQ neuroblast and the HSN/PHB neuroblast. The latter cell divides further to generate an apoptotic anterior daughter and the posterior HSN/PHB precursor. (B, C) The loss of the HSN and PHB neurons in *apr-1* mutants may result from several possible cell fate transformations. (B) The posterior daughter of the HSN/PHB neuroblast may adopt the anterior apoptotic fate. This is the opposite transformation to that observed in *ham-1* mutants. (C) Defects may also occur at a higher point in the lineage, such that the HSN/PHB neuroblast is transformed into a second PVQ neuroblast.

4.6.2 The PLM lineage

Our studies indicate that *apr-1* and *ham-1* alleles also exhibit opposing phenotypes in the PLM lineage. To determine if these mutants disrupted the same cell division, we first investigated the position of HAM-1 function in this lineage. *ham-1(gm279)* animals exhibited a loss of PLM and ALN neurons. This may be caused by cell fate transformations at divisions 1 or 2, inducing the ectopic cell death of a precursor cell (Figure 20C,D). Consistent with this model, PLM neuronal loss was suppressed by the inhibition of apoptosis in *ced-4* mutants. However, distinction between HAM-1 function at division 1 and 2 will require further lineage analysis. Both transformations predict a duplication of the apoptotic fate; thus, an extra cell corpse should be observed soon after the defective division. Accordingly, the time of ectopic cell death in *ham-1* mutants will clearly establish the point at which the lineage is disrupted.

In contrast to the Ham-1 phenotype, loss of APR-1 activity resulted in the duplication of PLM neurons. This may also be caused by cell fate transformations at divisions 1 or 2, in the opposite direction to that observed in *ham-1* mutants. Specifically, the apoptotic daughter adopts the fate of its sister cell, resulting in duplication of the neuronal precursor (Figure 21C,D). In this model, the effects of *apr-1* may be antagonized by a competing signal for cell death. To explore this possibility, we examined PLM defects in *apr-1; ced-3* mutants, which do not exhibit apoptosis. Unfortunately, we did not observe an enhancement of PLM duplications. This negative result neither supports nor contradicts the suggested cell fate transformations.

To determine if *apr-1* mutants disrupts division 3 (Figure 21B), future studies can probe for ALN neuronal loss; this would indicate that PLM neurons are duplicated at the

expense of the sister cell. The results of our *apr-1; ham-1* analysis do not favour this model. If APR-1 functions in a division downstream of HAM-1 in this lineage, the *apr-1* allele would not have suppressed PLM neuronal loss in *ham-1* mutants. However, interpretation of the genetic interactions between these proteins is complicated by the occasional detection of three or four PLM neurons, which suggests that APR-1 may function in more than one division.

In addition to APR-1, we also investigated the involvement of LIN-17 in the PLM lineage. As reported by a recent publication, we observed PLM duplications in *lin-17* mutants (Hilliard and Bargmann, 2006). The authors attribute this defect to a potential cell fate transformation at division 3 (Figure 21B), since they detected a concurrent loss of the sister cell ALN. This model is consistent with the results of our *lin-17; ham-1* analysis, which can be explained by independent disruptions of division 1 or 2 by *ham-1* and division 3 by *lin-17* (described in Results section).

Currently, experimental support for interactions between HAM-1 and the Wnt pathway remains tenuous. From the preliminary studies in the PHB and PLM lineages, mutations in *ham-1* and various Wnt signalling components appear to produce antagonistic effects. However, these opposing phenotypes are not necessarily indicative of direct functional interactions, as demonstrated by the *ham-1* and *lin-17* analyses.

4.7 Summary

HAM-1 is an asymmetrically localized protein involved in the division of many neuroblasts during *C. elegans* embryogenesis (Frank et al., 2005; Guenther and Garriga, 1996). Although several models were previously proposed for HAM-1 function, the

molecular mechanisms are not well understood. In this study, we used a serial deletion analysis to determine sequences required for protein localization and function. Our results indicate that both N- and C-terminal truncations disrupt HAM-1 activity; however, the C-terminus is not essential for cortical association. Unexpectedly, our experiments revealed a potential nuclear role of HAM-1. Aside from peripheral localization, we also detected various levels of HAM-1 in the nucleus. Nuclear targeting was partially dependent on an NLS sequence at residues 321-327. Deletion of these amino acids moderately reduced protein activity, suggesting this localization may be biologically significant. Moreover, we identified a putative DNA binding domain by sequence homology, which is also consistent with potential nuclear functions. Future studies are still required to provide further evidence for this hypothesis. If the nuclear role becomes established, it will be very interesting to determine how this integrates with the current models of HAM-1 regulation of ACDs.

APPENDICES

Appendix 1 Backcrossing integrated array

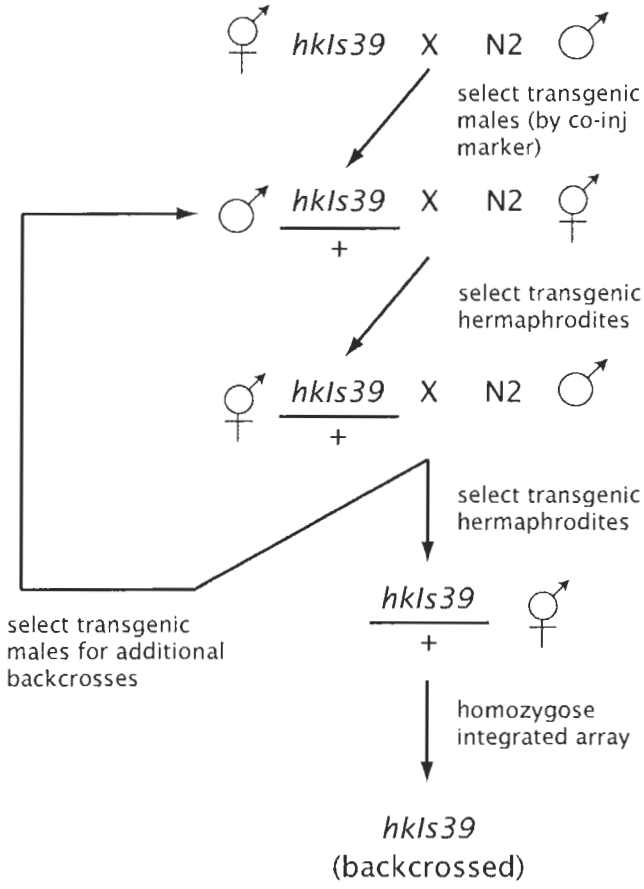

Appendix 2 Crossing transgenic arrays into reporter strains

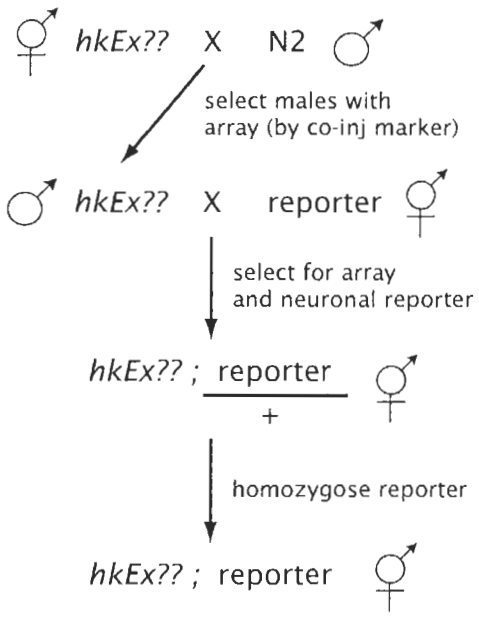

Note: for integrated concatemers, an extra final step is required to homozygose the array

Appendix 3 Crossing transgenic arrays into *ham-1* mutants with neuronal reporters

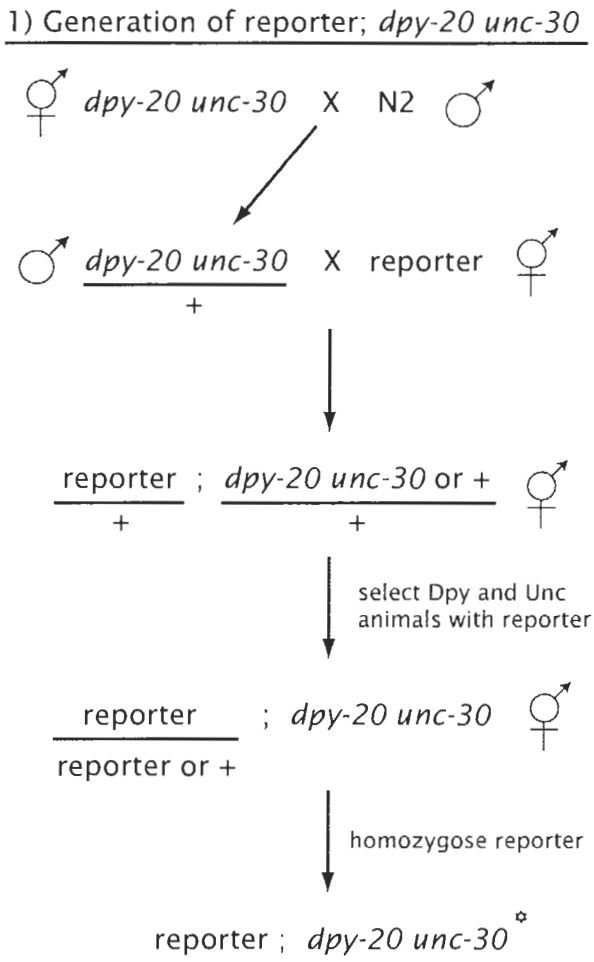

✡ This strain will be used in the second part of the crossing scheme (next page). *dpy-20* and *unc-30* maps to the left and right of *ham-1*, respectively. These mutants can be used *in trans* to track *ham-1(gm279)* throughout the genetic crosses.

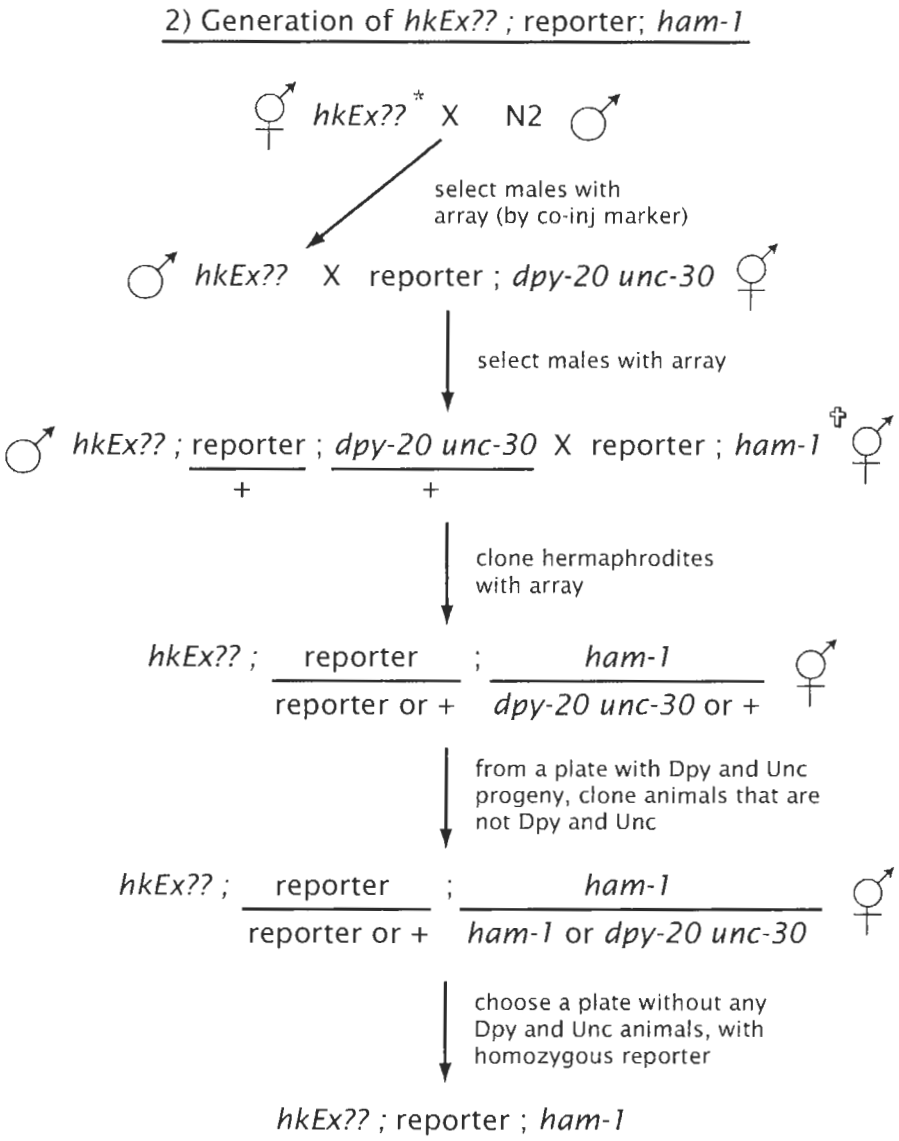

* For all constructs aside from full-length GFP::HAM-1, plasmid DNA was injected directly into *zdIs5[mec-4::gfp]*. Thus, this reporter was already in the background of many starting strains.

✞ *zdIs5[mec-4::gfp]; ham-1(gm279)* and *gmIs12[srb-6::gfp]; ham-1(gm279)* were kindly provided by G. Garriga.

Note: for integrated concatemers, an extra final step is required to homozygose the array

Appendix 4 Crossing the ALN reporter into *ham-1* mutants

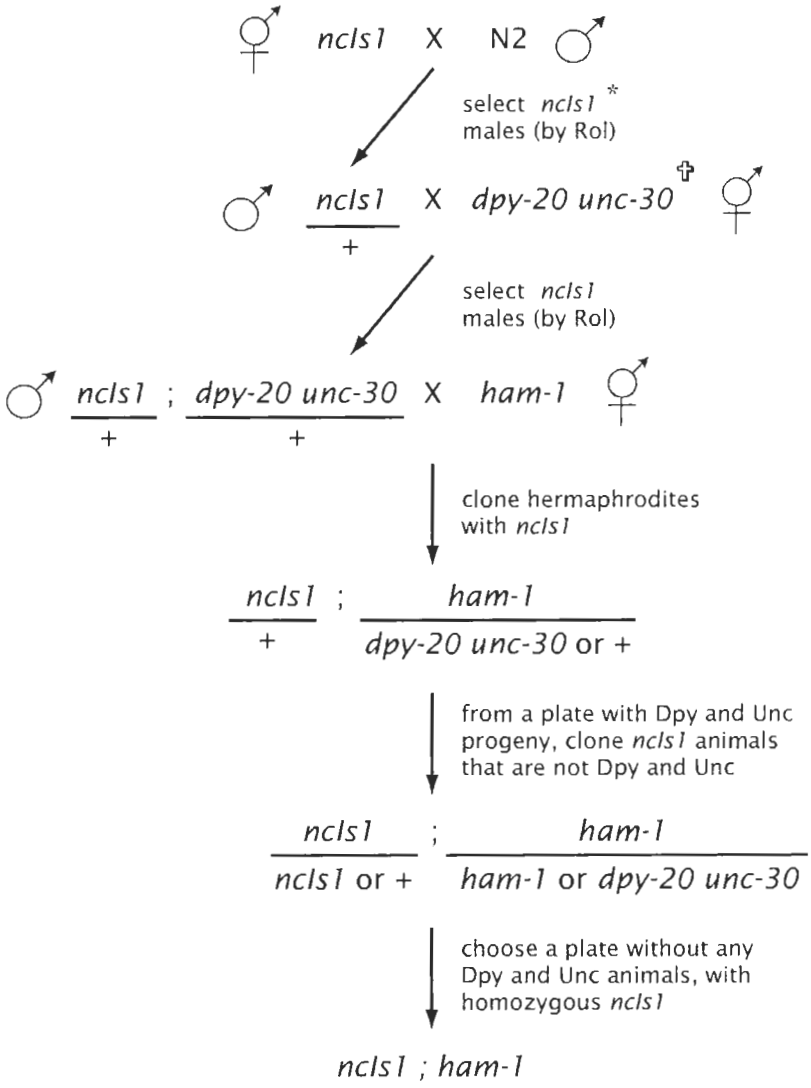

* The ALN reporter *ncIs1[eat-20::gfp pRF4]* can be followed by the dominant rolling phenotype conferred by *pRF4*.

✞ *dpy-20(e1282ts)* and *unc-30(e191)* was kindly provided by G. Garriga.

Appendix 5 Crosses to obtain *zdIs5; ced-4* and *zdIs5; ced-4; ham-1*

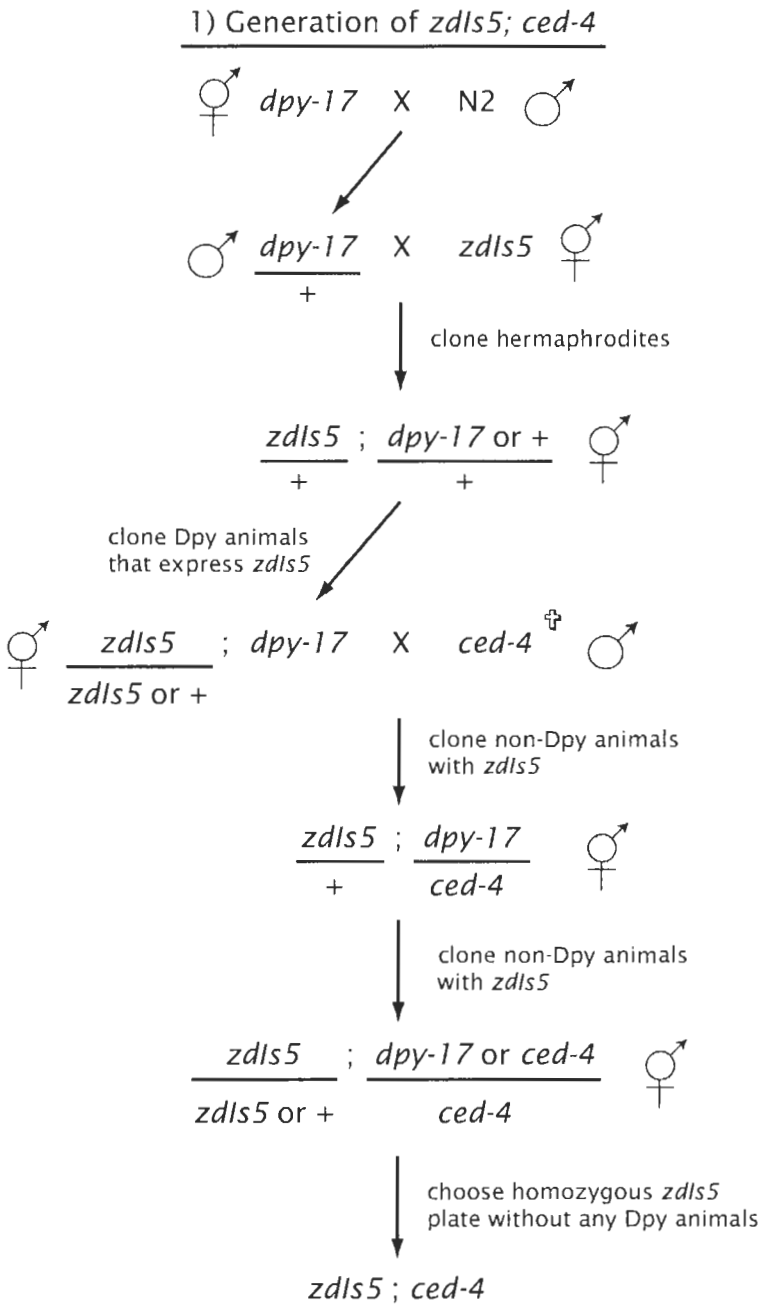

✞ *ced-4* males obtained by increasing the rate of nondisjunction (heat shocked hermaphrodites at 32°C for 6 hours)

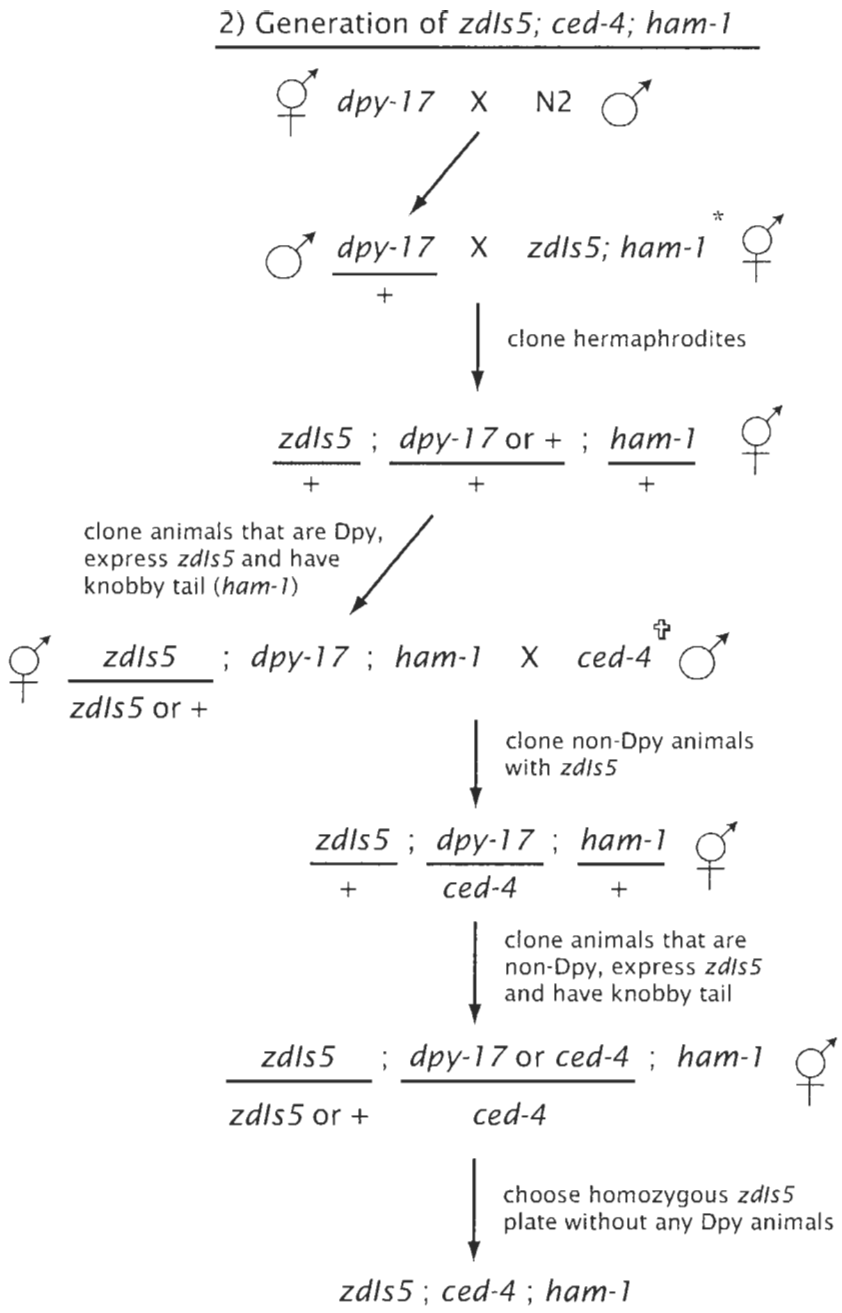

* *zdIs5[mec-4::gfp]; ham-1(gm279)* was kindly provided by G. Garriga

✞ *ced-4* males obtained by increasing the rate of nondisjunction (heat shocked hermaphrodites at 32°C for 6 hours)

Appendix 6 Crosses to obtain *apr-1 zdIs5 / hT2 zdIs5*

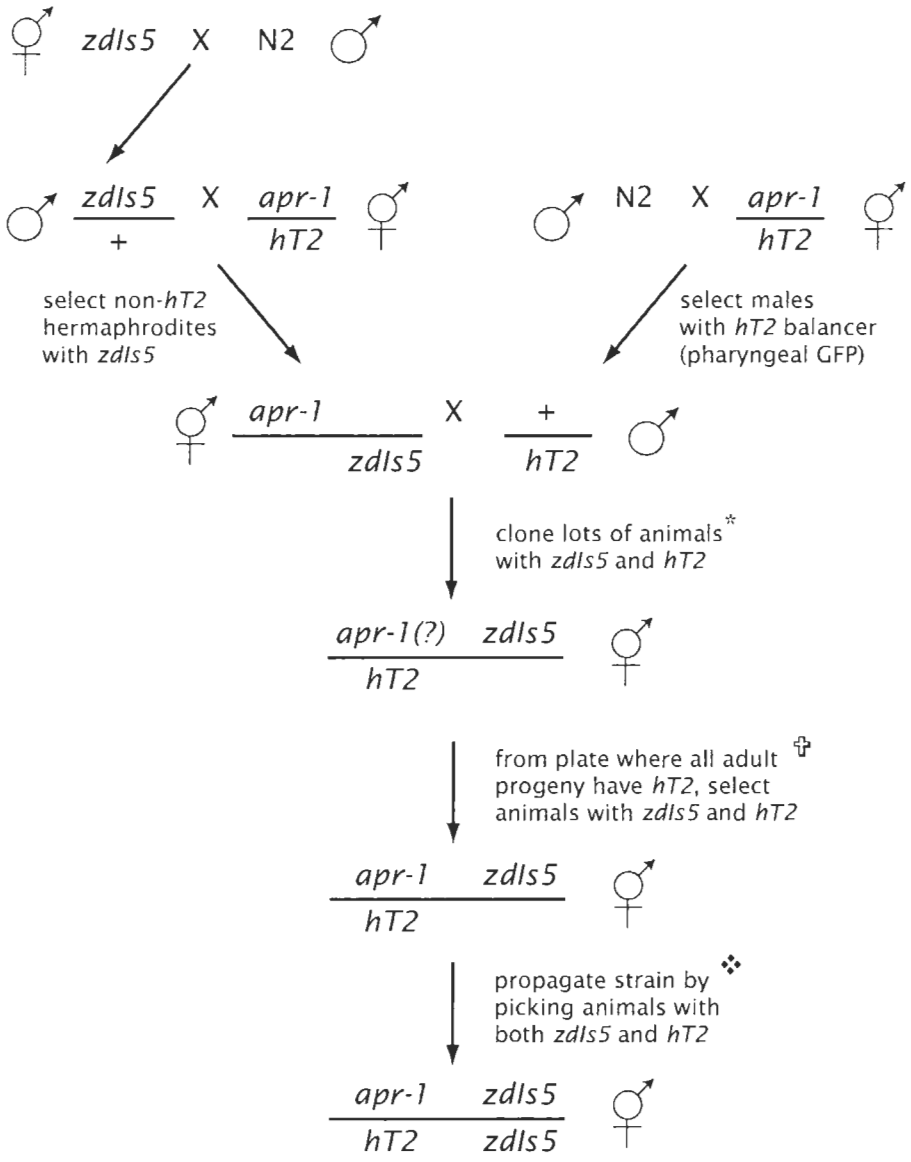

* Because *apr-1* and *zdIs5* are both on LG I, a recombinant event is required.

✞ *apr-1* causes zygotic embryonic/larval lethality. Thus, if the parent was *apr-1 zdIs5 / hT2*, all adult progeny must have received a wildtype copy of APR-1 from the *hT2* balancer. Conversely, if the parent was *zdIs5 / hT2*, some of the progeny would be homozygous *zdIs5*.

❖ *zdIs5* is not balanced by *hT2*. Continual propagation of the strain by picking animals with both *zdIs5* and *hT2* eventually homozygosed the *zdIs5* marker by recombination.

Appendix 7 Crosses to obtain *apr-1 zdIs5 / hT2 zdIs5; ham-1*

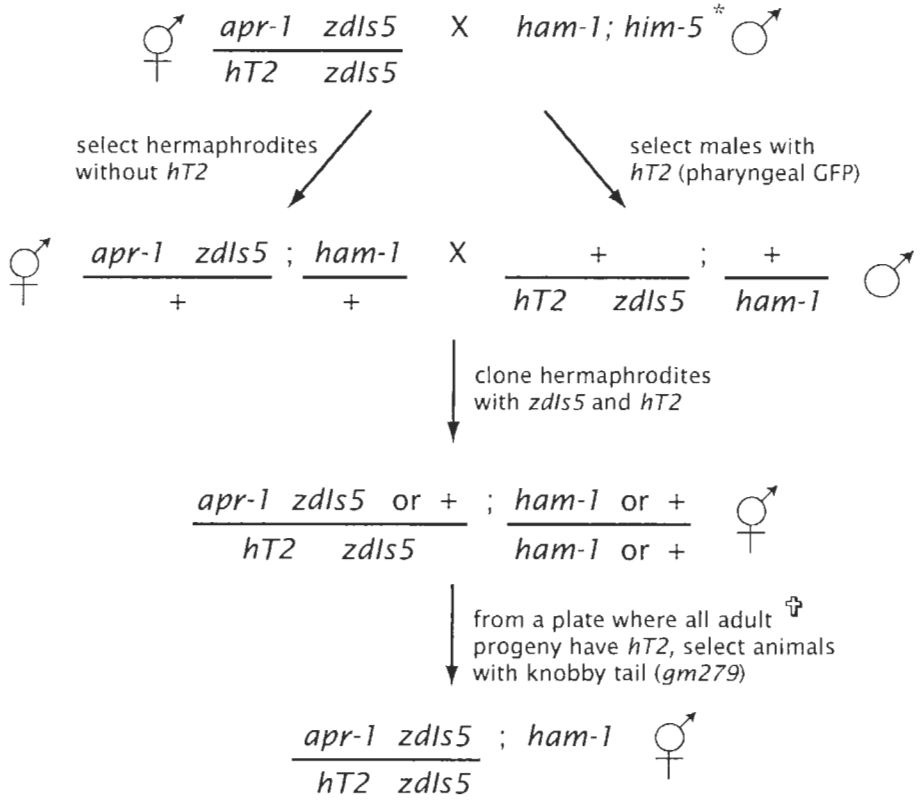

* *him-5* mutation creates a high incidence of male progeny. This allele is lost throughout these crosses, and is not shown in the schematic. *ham-1(gm279); him-5(e1490)* was kindly provided by G. Garriga.

✞ *apr-1* causes zygotic embryonic/larval lethality. Thus, if the parent was *apr-1 zdIs5 / hT2 zdIs5*, all adult progeny must have received a wildtype copy of APR-1 from the *hT2* balancer. Conversely, if the parent was + / *hT2 zdIs5*, it would segregate wildtype progeny without *hT2*.

Appendix 8 Crosses to obtain *apr-1 zdIs5 / hT2 zdIs5; ced-3*

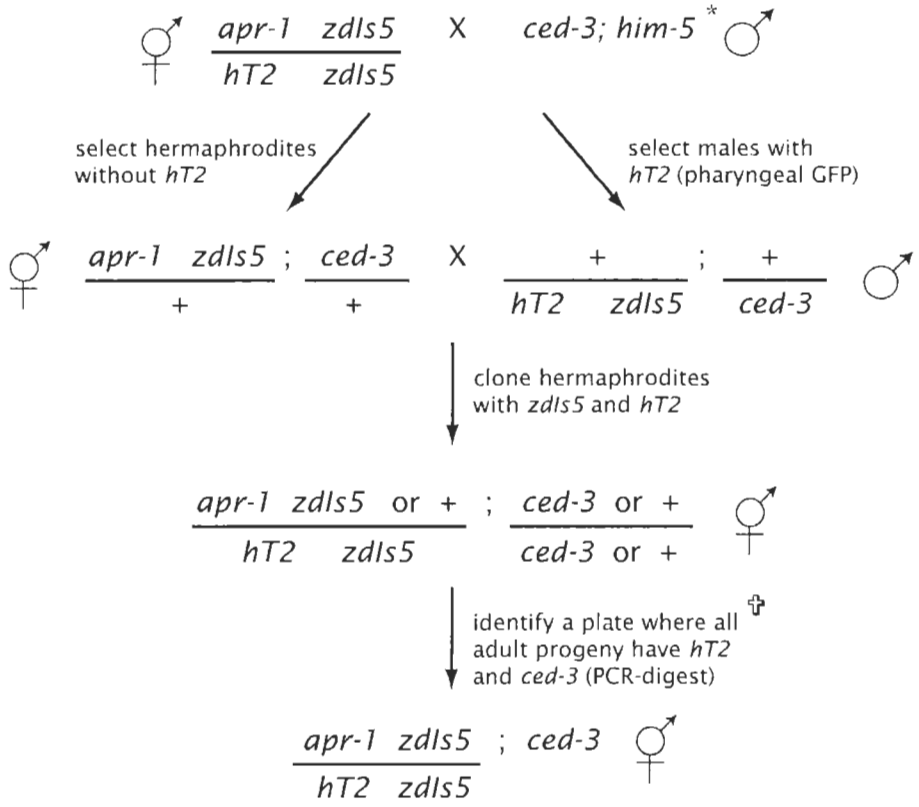

* *him-5* mutation creates a high incidence of male progeny. This allele is lost throughout these crosses, and is not shown in the schematic. *ced-3(n717); him-5(e1490)* was kindly provided by G. Garriga.

✞ *apr-1* causes zygotic embryonic/larval lethality. Thus, if the parent was *apr-1 zdIs5 / hT2 zdIs5*, all adult progeny must have received a wildtype copy of APR-1 from the *hT2* balancer. Conversely, if the parent was + / *hT2 zdIs5*, it would segregate wildtype progeny without *hT2*.

To determine whether these animals were also homozygous for *ced-3*, we used a PCR-digest method described in Section 2.2.1 (Genotyping *ced-3(n717)* mutants).

Appendix 9 Crosses to obtain *lin-17 zdIs5* and *lin-17 zdIs5; dpy-20 unc-30*

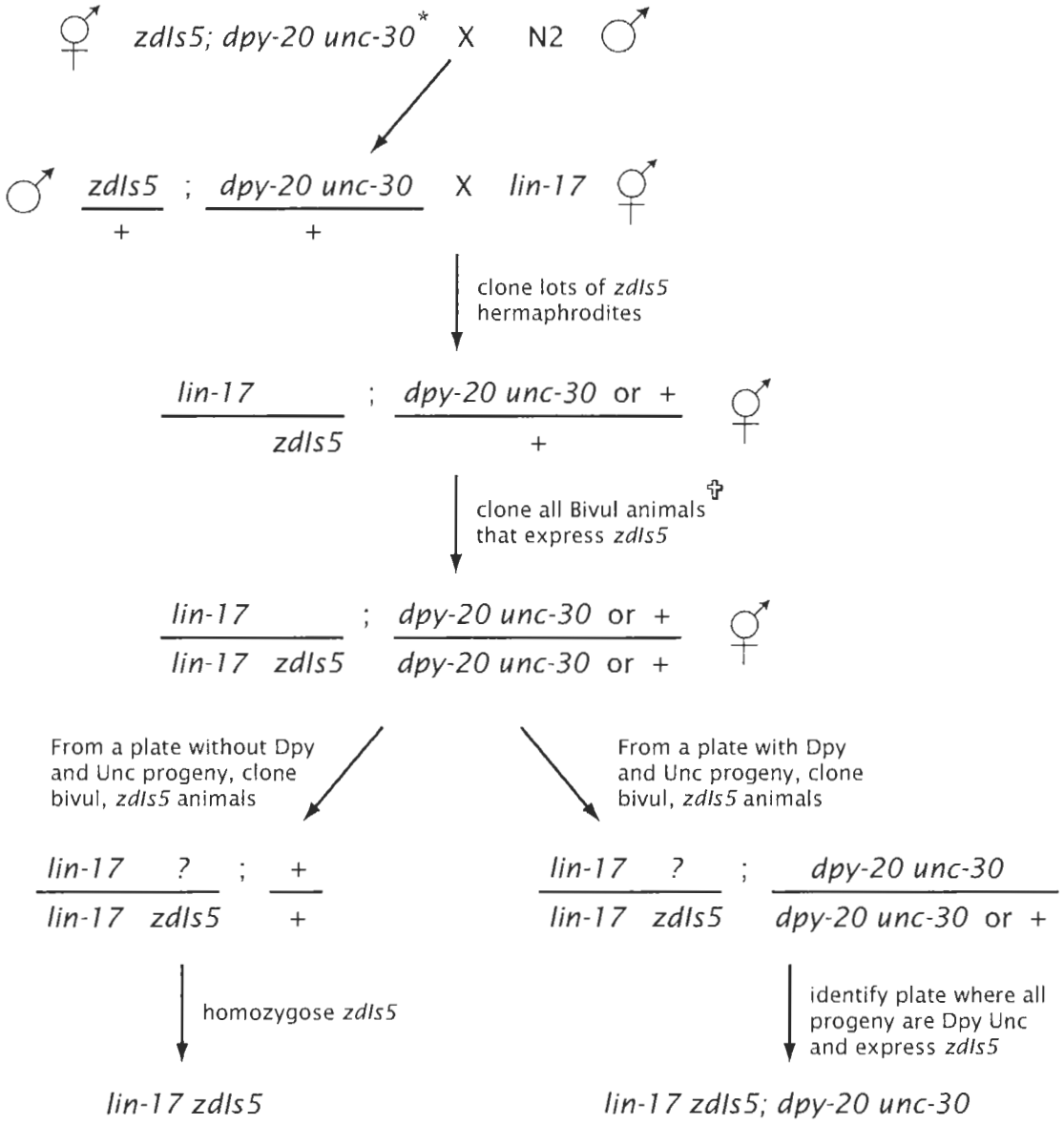

* *zdIs5; dpy-20 unc-30* was generated according to Appendix 3 (Part 1).

✞ *lin-17* mutants occasionally generate an extra pseudo-vulva (Bivul). The expression of *zdIs5* in Bivul animals is indicative of recombination between *lin-17* and *zdIs5*.

Appendix 10 Crosses to obtain *lin-17 zdIs5; ham-1*

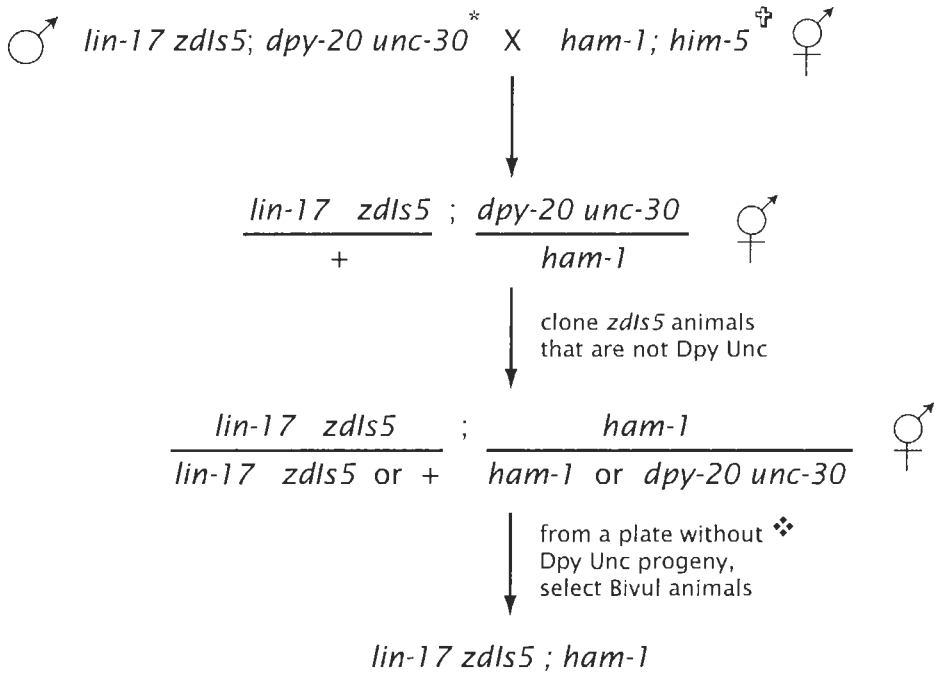

* *lin -17 zdIs5; dpy-20 unc-30* was generated according to Appendix 9.

✞ *him-5* mutation creates a high incidence of male progeny. This allele is lost throughout these crosses, and is not shown in the schematic. *ham-1(gm279); him-5(e1490)* was kindly provided by G. Garriga.

❖ Bivul phenotype is indicative of *lin-17* homozygotes. We also confirmed that *zdIs5* was expressed in all progeny.

REFERENCE LIST

Altschul, S. F., Madden, T. L., Schaffer, A. A., Zhang, J., Zhang, Z., Miller, W. and Lipman, D. J. (1997). Gapped BLAST and PSI-BLAST: a new generation of protein database search programs. *Nucleic Acids Res* **25**, 3389-402.

Aravind, L., Anantharaman, V., Balaji, S., Babu, M. M. and Iyer, L. M. (2005). The many faces of the helix-turn-helix domain: transcription regulation and beyond. *FEMS Microbiol Rev* **29**, 231-62.

Artavanis-Tsakonas, S., Rand, M. D. and Lake, R. J. (1999). Notch signaling: cell fate control and signal integration in development. *Science* **284**, 770-6.

Bashirullah, A., Cooperstock, R. L. and Lipshitz, H. D. (1998). RNA localization in development. *Annu Rev Biochem* **67**, 335-94.

Bassell, G. J., Oleynikov, Y. and Singer, R. H. (1999). The travels of mRNAs through all cells large and small. *Faseb J* **13**, 447-54.

Berdnik, D., Torok, T., Gonzalez-Gaitan, M. and Knoblich, J. A. (2002). The endocytic protein alpha-Adaptin is required for numb-mediated asymmetric cell division in Drosophila. *Dev Cell* **3**, 221-31.

Bergsten, S. E. and Gavis, E. R. (1999). Role for mRNA localization in translational activation but not spatial restriction of nanos RNA. *Development* **126**, 659-69.

Betschinger, J. and Knoblich, J. A. (2004). Dare to be different: asymmetric cell division in Drosophila, C. elegans and vertebrates. *Curr Biol* **14**, R674-85.

Boyd, L., Guo, S., Levitan, D., Stinchcomb, D. T. and Kemphues, K. J. (1996). PAR-2 is asymmetrically distributed and promotes association of P granules and PAR-1 with the cortex in C. elegans embryos. *Development* **122**, 3075-84.

Brenner, S. (1974). The genetics of Caenorhabditis elegans. *Genetics* **77**, 71-94.

Bridges, D. and Moorhead, G. B. (2005). 14-3-3 proteins: a number of functions for a numbered protein. *Sci STKE* **2005**, re10.

Broadus, J., Fuerstenberg, S. and Doe, C. Q. (1998). Staufen-dependent localization of prospero mRNA contributes to neuroblast daughter-cell fate. *Nature* **391**, 792-5.

Broverman, S. A. and Meneely, P. M. (1994). Meiotic mutants that cause a polar decrease in recombination on the X chromosome in Caenorhabditis elegans. *Genetics* **136**, 119-27.

Calvo, D., Victor, M., Gay, F., Sui, G., Luke, M. P., Dufourcq, P., Wen, G., Maduro, M., Rothman, J. and Shi, Y. (2001). A POP-1 repressor complex restricts inappropriate cell type-specific gene transcription during Caenorhabditis elegans embryogenesis. *Embo J* **20**, 7197-208.

Chiu, J., March, P. E., Lee, R. and Tillett, D. (2004). Site-directed, Ligase-Independent Mutagenesis (SLIM): a single-tube methodology approaching 100% efficiency in 4 h. *Nucleic Acids Res* **32**, e174.

Clark, S. G. and Chiu, C. (2003). C. elegans ZAG-1, a Zn-finger-homeodomain protein, regulates axonal development and neuronal differentiation. *Development* **130**, 3781-94.

Cokol, M., Nair, R. and Rost, B. (2000). Finding nuclear localization signals. *EMBO Rep* **1**, 411-5.

Cordes, S., Frank, C. A. and Garriga, G. (2006). The C. elegans MELK ortholog PIG-1 regulates cell size asymmetry and daughter cell fate in asymmetric neuroblast divisions. *Development* **133**, 2747-56.

Desai, C., Garriga, G., McIntire, S. L. and Horvitz, H. R. (1988). A genetic pathway for the development of the Caenorhabditis elegans HSN motor neurons. Nature 336, 638-46.

Doe, C. Q., Chu-LaGraff, Q., Wright, D. M. and Scott, M. P. (1991). The prospero gene specifies cell fates in the Drosophila central nervous system. *Cell* **65**, 451-64.

Dye, C. A., Lee, J. K., Atkinson, R. C., Brewster, R., Han, P. L. and Bellen, H. J. (1998). The Drosophila sanpodo gene controls sibling cell fate and encodes a tropomodulin homolog, an actin/tropomyosin-associated protein. *Development* **125**, 1845-56.

Ellis, H. M. and Horvitz, H. R. (1986). Genetic control of programmed cell death in the nematode C. elegans. *Cell* **44**, 817-29.

Esmail, M. (2006). Identification and molecular characterization of Bardet-Biedl Syndrome Protein 3. Doctoral dissertation. Molecular Biology and Biochemistry, Simon Fraser University.

Etemad-Moghadam, B., Guo, S. and Kemphues, K. J. (1995). Asymmetrically distributed PAR-3 protein contributes to cell polarity and spindle alignment in early C. elegans embryos. *Cell* **83**, 743-52.

Evans (ed.), T. C. Transformation and microinjection (April 6, 2006), *WormBook*, ed. The *C. elegans* Research Community, WormBook, http://www.wormbook.org

Ferrandon, D., Elphick, L., Nusslein-Volhard, C. and St Johnston, D. (1994). Staufen protein associates with the 3'UTR of bicoid mRNA to form particles that move in a microtubule-dependent manner. *Cell* **79**, 1221-32.

Finney, M. and Ruvkun, G. (1990). The unc-86 gene product couples cell lineage and cell identity in C. elegans. *Cell* **63**, 895-905.

Frank, C. A., Hawkins, N. C., Guenther, C., Horvitz, H. R. and Garriga, G. (2005). C. elegans HAM-1 positions the cleavage plane and regulates apoptosis in asymmetric neuroblast divisions. *Dev Biol* **284**, 301-10.

Gitai, Z., Yu, T. W., Lundquist, E. A., Tessier-Lavigne, M. and Bargmann, C. I. (2003). The netrin receptor UNC-40/DCC stimulates axon attraction and outgrowth through enabled and, in parallel, Rac and UNC-115/AbLIM. *Neuron* **37**, 53-65.

Goldstein, B. (1992). Induction of gut in Caenorhabditis elegans embryos. *Nature* **357**, 255-7.

Goldstein, B. (1993). Establishment of gut fate in the E lineage of C. elegans: the roles of lineage-dependent mechanisms and cell interactions. *Development* **118**, 1267-77.

Gouet, P., Courcelle, E., Stuart, D. I. and Metoz, F. (1999). ESPript: analysis of multiple sequence alignments in PostScript. *Bioinformatics* **15**, 305-8.

Guenther, C. and Garriga, G. (1996). Asymmetric distribution of the C. elegans HAM-1 protein in neuroblasts enables daughter cells to adopt distinct fates. *Development* **122**, 3509-18.

Guo, M., Jan, L. Y. and Jan, Y. N. (1996). Control of daughter cell fates during asymmetric division: interaction of Numb and Notch. *Neuron* **17**, 27-41.

Guo, S. and Kemphues, K. J. (1995). par-1, a gene required for establishing polarity in C. elegans embryos, encodes a putative Ser/Thr kinase that is asymmetrically distributed. *Cell* **81**, 611-20.

Hall, D. H. and Russell, R. L. (1991). The posterior nervous system of the nematode Caenorhabditis elegans: serial reconstruction of identified neurons and complete pattern of synaptic interactions. *J Neurosci* **11**, 1-22.

Hartmann, C., Landgraf, M., Bate, M. and Jackle, H. (1997). Kruppel target gene knockout participates in the proper innervation of a specific set of Drosophila larval muscles. *Embo J* **16**, 5299-309.

Hawkins, N. and Garriga, G. (1998). Asymmetric cell division: from A to Z. *Genes Dev* **12**, 3625-38.

Hawkins, N. C., Ellis, G. C., Bowerman, B. and Garriga, G. (2005). MOM-5 frizzled regulates the distribution of DSH-2 to control C. elegans asymmetric neuroblast divisions. *Dev Biol* **284**, 246-59.

Hicks, G. R. and Raikhel, N. V. (1995). Protein import into the nucleus: an integrated view. *Annu Rev Cell Dev Biol* **11**, 155-88.

Hilliard, M. A. and Bargmann, C. I. (2006). Wnt signals and frizzled activity orient anterior-posterior axon outgrowth in C. elegans. *Dev Cell* **10**, 379-90.

Hilliard, M. A., Bargmann, C. I. and Bazzicalupo, P. (2002). C. elegans responds to chemical repellents by integrating sensory inputs from the head and the tail. *Curr Biol* **12**, 730-4.

Hirata, J., Nakagoshi, H., Nabeshima, Y. and Matsuzaki, F. (1995). Asymmetric segregation of the homeodomain protein Prospero during Drosophila development. *Nature* **377**, 627-30.

Hoier, E. F., Mohler, W. A., Kim, S. K. and Hajnal, A. (2000). The Caenorhabditis elegans APC-related gene apr-1 is required for epithelial cell migration and Hox gene expression. *Genes Dev* **14**, 874-86.

Horton, P. and Nakai, K. (1997). Better prediction of protein cellular localization sites with the k nearest neighbors classifier. *Proc Int Conf Intell Syst Mol Biol* **5**, 147-52.

Horvitz, H. R. and Herskowitz, I. (1992). Mechanisms of asymmetric cell division: two Bs or not two Bs, that is the question. *Cell* **68**, 237-55.

Hosono, R., Hirahara, K., Kuno, S. and Kurihra, T. (1982). Mutants of Caenorhabditis elegans with dumpy and rounded head phenotype. *Journal of Experimental Zoology* **224**, 135-144.

Hung, T. J. and Kemphues, K. J. (1999). PAR-6 is a conserved PDZ domain-containing protein that colocalizes with PAR-3 in Caenorhabditis elegans embryos. *Development* **126**, 127-35.

Hutterer, A. and Knoblich, J. A. (2005). Numb and alpha-Adaptin regulate Sanpodo endocytosis to specify cell fate in Drosophila external sensory organs. *EMBO Rep* **6**, 836-42.

Ikeshima-Kataoka, H., Skeath, J. B., Nabeshima, Y., Doe, C. Q. and Matsuzaki, F. (1997). Miranda directs Prospero to a daughter cell during Drosophila asymmetric divisions. *Nature* **390**, 625-9.

Joseph, E. M. and Melton, D. A. (1998). Mutant Vg1 ligands disrupt endoderm and mesoderm formation in Xenopus embryos. *Development* **125**, 2677-85.

Kalderon, D., Roberts, B. L., Richardson, W. D. and Smith, A. E. (1984). A short amino acid sequence able to specify nuclear location. *Cell* **39**, 499-509.

Kemphues, K. J., Priess, J. R., Morton, D. G. and Cheng, N. S. (1988). Identification of genes required for cytoplasmic localization in early C. elegans embryos. *Cell* **52**, 311-20.

Knoblich, J. A. (2001). Asymmetric cell division during animal development. *Nat Rev Mol Cell Biol* **2**, 11-20.

Korswagen, H. C. (2002). Canonical and non-canonical Wnt signaling pathways in Caenorhabditis elegans: variations on a common signaling theme. *Bioessays* **24**, 801-10.

Kraut, R., Chia, W., Jan, L. Y., Jan, Y. N. and Knoblich, J. A. (1996). Role of inscuteable in orienting asymmetric cell divisions in Drosophila. *Nature* **383**, 50-5.

Kuchinke, U., Grawe, F. and Knust, E. (1998). Control of spindle orientation in Drosophila by the Par-3-related PDZ-domain protein Bazooka. *Curr Biol* **8**, 1357-65.

Kuersten, S. and Goodwin, E. B. (2003). The power of the 3' UTR: translational control and development. *Nat Rev Genet* **4**, 626-37.

Lee, S. (2005). Characterizing the role of *C. elegans* DSH-2 in asymmetric cell division and embryonic development. Master's dissertation. Molecular Biology and Biochemistry, Simon Fraser University.

Li, J., Tewari, M., Vidal, M. and Sylvia Lee, S. (2006). The 14-3-3 protein FTT-2 regulates DAF-16 in Caenorhabditis elegans. *Dev Biol.*

Li, P., Yang, X., Wasser, M., Cai, Y. and Chia, W. (1997). Inscuteable and Staufen mediate asymmetric localization and segregation of prospero RNA during Drosophila neuroblast cell divisions. *Cell* **90**, 437-47.

Lin, K., Hsin, H., Libina, N. and Kenyon, C. (2001). Regulation of the Caenorhabditis elegans longevity protein DAF-16 by insulin/IGF-1 and germline signaling. *Nat Genet* **28**, 139-45.

Lin, R., Thompson, S. and Priess, J. R. (1995). pop-1 encodes an HMG box protein required for the specification of a mesoderm precursor in early C. elegans embryos. *Cell* **83**, 599-609.

Liu, Q. A. and Hengartner, M. O. (1999). The molecular mechanism of programmed cell death in C. elegans. *Ann N Y Acad Sci* **887**, 92-104.

Lo, M. C., Gay, F., Odom, R., Shi, Y. and Lin, R. (2004). Phosphorylation by the beta-catenin/MAPK complex promotes 14-3-3-mediated nuclear export of TCF/POP-1 in signal-responsive cells in C. elegans. *Cell* **117**, 95-106.

Logan, C. Y. and Nusse, R. (2004). The Wnt signaling pathway in development and disease. *Annu Rev Cell Dev Biol* **20**, 781-810.

Maduro, M. and Pilgrim, D. (1995). Identification and cloning of unc-119, a gene expressed in the Caenorhabditis elegans nervous system. *Genetics* **141**, 977-88.

McKim, K. S., Peters, K. and Rose, A. M. (1993). Two types of sites required for meiotic chromosome pairing in Caenorhabditis elegans. *Genetics* **134**, 749-68.

Mello, C. C., Kramer, J. M., Stinchcomb, D. and Ambros, V. (1991). Efficient gene transfer in C.elegans: extrachromosomal maintenance and integration of transforming sequences. *Embo J* **10**, 3959-70.

Melton, D. A. (1987). Translocation of a localized maternal mRNA to the vegetal pole of Xenopus oocytes. *Nature* **328**, 80-2.

Moore, S. P., Rinckel, L. A. and Garfinkel, D. J. (1998). A Ty1 integrase nuclear localization signal required for retrotransposition. *Mol Cell Biol* **18**, 1105-14.

Morton, D. G., Shakes, D. C., Nugent, S., Dichoso, D., Wang, W., Golden, A. and Kemphues, K. J. (2002). The Caenorhabditis elegans par-5 gene encodes a 14-3-3 protein required for cellular asymmetry in the early embryo. *Dev Biol* **241**, 47-58.

Mowry, K. L. and Melton, D. A. (1992). Vegetal messenger RNA localization directed by a 340-nt RNA sequence element in Xenopus oocytes. *Science* **255**, 991-4.

Mulder, N. J., Apweiler, R., Attwood, T. K., Bairoch, A., Bateman, A., Binns, D., Bradley, P., Bork, P., Bucher, P., Cerutti, L. et al. (2005). InterPro, progress and status in 2005. *Nucleic Acids Res* **33**, D201-5.

Muslin, A. J. and Xing, H. (2000). 14-3-3 proteins: regulation of subcellular localization by molecular interference. *Cell Signal* **12**, 703-9.

Nance, J. (2005). PAR proteins and the establishment of cell polarity during C. elegans development. *Bioessays* **27**, 126-35.

Obsil, T., Ghirlando, R., Anderson, D. E., Hickman, A. B. and Dyda, F. (2003). Two 14-3-3 binding motifs are required for stable association of Forkhead transcription factor FOXO4 with 14-3-3 proteins and inhibition of DNA binding. *Biochemistry* **42**, 15264-72.

Petronczki, M. and Knoblich, J. A. (2001). DmPAR-6 directs epithelial polarity and asymmetric cell division of neuroblasts in Drosophila. *Nat Cell Biol* **3**, 43-9.

Puntervoll, P., Linding, R., Gemund, C., Chabanis-Davidson, S., Mattingsdal, M., Cameron, S., Martin, D. M., Ausiello, G., Brannetti, B., Costantini, A. et al. (2003). ELM server: A new resource for investigating short functional sites in modular eukaryotic proteins. *Nucleic Acids Res* **31**, 3625-30.

Resh, M. D. (1999). Fatty acylation of proteins: new insights into membrane targeting of myristoylated and palmitoylated proteins. *Biochim Biophys Acta* **1451**, 1-16.

Rhyu, M. S., Jan, L. Y. and Jan, Y. N. (1994). Asymmetric distribution of numb protein during division of the sensory organ precursor cell confers distinct fates to daughter cells. *Cell* **76**, 477-91.

Rocheleau, C. E., Downs, W. D., Lin, R., Wittmann, C., Bei, Y., Cha, Y. H., Ali, M., Priess, J. R. and Mello, C. C. (1997). Wnt signaling and an APC-related gene specify endoderm in early C. elegans embryos. *Cell* **90**, 707-16.

Rocheleau, C. E., Yasuda, J., Shin, T. H., Lin, R., Sawa, H., Okano, H., Priess, J. R., Davis, R. J. and Mello, C. C. (1999). WRM-1 activates the LIT-1 protein kinase to transduce anterior/posterior polarity signals in C. elegans. *Cell* **97**, 717-26.

Roh, M. (2004). Requirement fo Wnt and Planar Cell Polarity pathway genes in asymmetric neuroblast division in *Caenorhabditis elegans*. Master's dissertation. Molecular Biology and Biochemistry, Simon Fraser University.

Sambrook, J., Fritsch, E. F. and Maniatis, T. (1989). Molecular cloning : a laboratory manual, 2nd edition. Cold Spring Harbor, NY: Cold Spring Harbor Laboratory Press.

Santolini, E., Puri, C., Salcini, A. E., Gagliani, M. C., Pelicci, P. G., Tacchetti, C. and Di Fiore, P. P. (2000). Numb is an endocytic protein. *J Cell Biol* **151**, 1345-52.

Sawa, H., Lobel, L. and Horvitz, H. R. (1996). The Caenorhabditis elegans gene lin-17, which is required for certain asymmetric cell divisions, encodes a putative seven-transmembrane protein similar to the Drosophila frizzled protein. *Genes Dev* **10**, 2189-97.

Schaefer, M., Shevchenko, A., Shevchenko, A. and Knoblich, J. A. (2000). A protein complex containing Inscuteable and the Galpha-binding protein Pins orients asymmetric cell divisions in Drosophila. *Curr Biol* **10**, 353-62.

Schlesinger, A., Shelton, C. A., Maloof, J. N., Meneghini, M. and Bowerman, B. (1999). Wnt pathway components orient a mitotic spindle in the early Caenorhabditis elegans embryo without requiring gene transcription in the responding cell. *Genes Dev* **13**, 2028-38.

Schober, M., Schaefer, M. and Knoblich, J. A. (1999). Bazooka recruits Inscuteable to orient asymmetric cell divisions in Drosophila neuroblasts. *Nature* **402**, 548-51.

Schroeter, E. H., Kisslinger, J. A. and Kopan, R. (1998). Notch-1 signalling requires ligand-induced proteolytic release of intracellular domain. *Nature* **393**, 382-6.

Schuldt, A. J., Adams, J. H., Davidson, C. M., Micklem, D. R., Haseloff, J., St Johnston, D. and Brand, A. H. (1998). Miranda mediates asymmetric protein and RNA localization in the developing nervous system. *Genes Dev* **12**, 1847-57.

Schweisguth, F. (2004). Notch signaling activity. *Curr Biol* **14**, R129-38.

Shav-Tal, Y. and Singer, R. H. (2005). RNA localization. *J Cell Sci* **118**, 4077-81.

Shibata, Y., Fujii, T., Dent, J. A., Fujisawa, H. and Takagi, S. (2000). EAT-20, a novel transmembrane protein with EGF motifs, is required for efficient feeding in Caenorhabditis elegans. *Genetics* **154**, 635-46.

Shin, T. H., Yasuda, J., Rocheleau, C. E., Lin, R., Soto, M., Bei, Y., Davis, R. J. and Mello, C. C. (1999). MOM-4, a MAP kinase kinase kinase-related protein, activates WRM-1/LIT-1 kinase to transduce anterior/posterior polarity signals in C. elegans. *Mol Cell* **4**, 275-80.

Skeath, J. B. and Doe, C. Q. (1998). Sanpodo and Notch act in opposition to Numb to distinguish sibling neuron fates in the Drosophila CNS. *Development* **125**, 1857-65.

Spana, E. P. and Doe, C. Q. (1995). The prospero transcription factor is asymmetrically localized to the cell cortex during neuroblast mitosis in Drosophila. *Development* **121**, 3187-95.

St Johnston, D., Driever, W., Berleth, T., Richstein, S. and Nusslein-Volhard, C. (1989). Multiple steps in the localization of bicoid RNA to the anterior pole of the Drosophila oocyte. *Development* **107 Suppl**, 13-9.

Sternberg, P. W. Vulval development (June 25, 2005), *WormBook*, ed. The *C. elegans* Research Community, WormBook, doi/10.1895/wormbook.1.6.1, http://www.wormbook.org

Stinchcomb, D. T., Shaw, J. E., Carr, S. H. and Hirsh, D. (1985). Extrachromosomal DNA transformation of Caenorhabditis elegans. *Mol Cell Biol* **5**, 3484-96.

Struhl, G. and Adachi, A. (1998). Nuclear access and action of notch in vivo. *Cell* **93**, 649-60.

Strutt, D. (2003). Frizzled signalling and cell polarisation in Drosophila and vertebrates. *Development* **130**, 4501-13.

Sulston, J. E., Schierenberg, E., White, J. G. and Thomson, J. N. (1983). The embryonic cell lineage of the nematode Caenorhabditis elegans. *Dev Biol* **100**, 64-119.

Tabuse, Y., Izumi, Y., Piano, F., Kemphues, K. J., Miwa, J. and Ohno, S. (1998). Atypical protein kinase C cooperates with PAR-3 to establish embryonic polarity in Caenorhabditis elegans. *Development* **125**, 3607-14.

Thompson, J. D., Higgins, D. G. and Gibson, T. J. (1994). CLUSTAL W: improving the sensitivity of progressive multiple sequence alignment through sequence weighting, position-specific gap penalties and weight matrix choice. *Nucleic Acids Res* **22**, 4673-80.

Thorpe, C. J., Schlesinger, A., Carter, J. C. and Bowerman, B. (1997). Wnt signaling polarizes an early C. elegans blastomere to distinguish endoderm from mesoderm. *Cell* **90**, 695-705.

Troemel, E. R., Chou, J. H., Dwyer, N. D., Colbert, H. A. and Bargmann, C. I. (1995). Divergent seven transmembrane receptors are candidate chemosensory receptors in C. elegans. *Cell* **83**, 207-18.

Vaessin, H., Grell, E., Wolff, E., Bier, E., Jan, L. Y. and Jan, Y. N. (1991). prospero is expressed in neuronal precursors and encodes a nuclear protein that is involved in the control of axonal outgrowth in Drosophila. *Cell* **67**, 941-53.

Van Der Heide, L. P., Hoekman, M. F. and Smidt, M. P. (2004). The ins and outs of FoxO shuttling: mechanisms of FoxO translocation and transcriptional regulation. *Biochem J* **380**, 297-309.

van Dijk, M., Mulders, J., Poutsma, A., Konst, A. A., Lachmeijer, A. M., Dekker, G. A., Blankenstein, M. A. and Oudejans, C. B. (2005). Maternal segregation of the Dutch preeclampsia locus at 10q22 with a new member of the winged helix gene family. *Nat Genet* **37**, 514-9.

van Ham, M. and Hendriks, W. (2003). PDZ domains-glue and guide. *Mol Biol Rep* **30**, 69-82.

van Heusden, G. P. (2005). 14-3-3 proteins: regulators of numerous eukaryotic proteins. *IUBMB Life* **57**, 623-9.

Wang, W. and Shakes, D. C. (1997). Expression patterns and transcript processing of ftt-1 and ftt-2, two C. elegans 14-3-3 homologues. *J Mol Biol* **268**, 619-30.

Watts, J. L., Etemad-Moghadam, B., Guo, S., Boyd, L., Draper, B. W., Mello, C. C., Priess, J. R. and Kemphues, K. J. (1996). par-6, a gene involved in the establishment of asymmetry in early C. elegans embryos, mediates the asymmetric localization of PAR-3. *Development* **122**, 3133-40.

Watts, J. L., Morton, D. G., Bestman, J. and Kemphues, K. J. (2000). The C. elegans par-4 gene encodes a putative serine-threonine kinase required for establishing embryonic asymmetry. *Development* **127**, 1467-75.

Weinmaster, G. (2000). Notch signal transduction: a real rip and more. *Curr Opin Genet Dev* **10**, 363-9.

Wilhelm, J. E., Vale, R. D. and Hegde, R. S. (2000). Coordinate control of translation and localization of Vg1 mRNA in Xenopus oocytes. *Proc Natl Acad Sci U S A* **97**, 13132-7.

Wodarz, A., Ramrath, A., Grimm, A. and Knust, E. (2000). Drosophila atypical protein kinase C associates with Bazooka and controls polarity of epithelia and neuroblasts. *J Cell Biol* **150**, 1361-74.